permafrost
cci

CCI+ PHASE 2 – NEW ECVS
PERMAFROST

D4.1 PRODUCT VALIDATION AND INTERCOMPARISON REPORT (PVIR)

VERSION 4.0

15 FEBRUARY 2024

PREPARED BY

b·geos
GAMMA REMOTE SENSING
UiO : University of Oslo
AWI
UNI FR
UNIVERSITÉ DE FRIBOURG
UNIVERSITÄT FREIBURG
Stockholm University
West University of Timisoara
TERRASIGNA

Document Status Sheet

Issue	Date	Details	Authors
1.0	30.09.2019	CRDPv0 evaluation	B. Heim, M. Wieczorek (AWI), A. Bartsch, C. Kroisleitner (B.GEOS) Cécile Pellet, Reynald Delaloye, Chloé Barboux (UNIFR)
2.0	30.09.2020	Update of all evaluation results based on CRDPv1	A. Bartsch (B.GEOS), B. Heim, M. Wieczorek (AWI), Cécile Pellet, Reynald Delaloye (UNIFR)
2.1	14.01.2020	Inclusion of temporal stability	M. Wieczorek, B. Heim (AWI)
3.0	30.09.2021	Update of evaluation results based on CRDPv2	B. Heim, S. Lisovski (AWI), Cécile Pellet, Reynald Delaloye (UNIFR), A. Bartsch (B.GEOS)
4.0	15.02.2024	Update of evaluation results based on CRDPv3	B. Heim, M. Wieczorek (AWI), Cécile Pellet, Reynald Delaloye (UNIFR), A. Bartsch (B.GEOS)

Author team

Birgit Heim, AWI

Mareike Wieczorek, AWI

Cécile Pellet, UNIFR

Reynald Delaloye, UNIFR

Annett Bartsch, B.GEOS

Tazio Strozzi, GAMMA

ESA Technical Officer: Frank Martin Seifert

EUROPEAN SPACE AGENCY CONTRACT REPORT

The work described in this report was done under ESA contract. Responsibility for the contents resides in the authors or organizations that prepared it.

TABLE OF CONTENTS

EXECUTIVE SUMMARY

This document presents the Product Validation and Intercomparison Report (PVIR) version 4 of the European Space Agency (ESA) Climate Change Initiative (CCI) Permafrost project (Permafrost_cci). CCI is ESA's global monitoring program whose main objective is to provide Earth Observation (EO)-based Essential Climate Variable (ECV) time series to the climate modelling and climate user communities. Permafrost_cci was part of phase I of CCI+ (2018–2021) and has been selected for phase II (2022–2025) with the production of ECVs for permafrost, set by the Global Climate Observing System (GCOS)/World Meteorological Organisation (WMO). The PVIR describes the assessments of the three Permafrost_cci products: i) permafrost temperature expressed as Ground Temperature per Depth (GTD) [°C] ii) Active Layer Thickness (ALT) [cm] and iii) permafrost extent expressed as Permafrost FRaction (PFR) [%] derived from GTD at 2 m depth.

The Committee on EO Satellites (CEOS) Working Group on Calibration and Validation (WGCV) defines validation as 'the process of assessing, by independent means, the quality of the data products derived from the system outputs' (lpvs.gsfc.nasa.gov). According to the CEOS Quality Assurance framework for Earth Observation (QA4EO) and ESA CCI guidelines, the validation data need to be independent from the product generation. In the QA4EO sense, suitable reference data are characterised by protocols and community-wide management practices and published openly. In Permafrost_cci accordingly, assessments of the Permafrost_cci products are carried out independently from the algorithm development team using in situ data from the WMO/GCOS Global Terrestrial Network for Permafrost (GTN-P) managed by the International Permafrost Association (IPA). Within the GTN-P/IPA framework, the Thermal State of Permafrost Monitoring (TSP) program is managing the temperature monitoring via borehole temperature profiles and shallow ground temperature profiles, whereas the Circumpolar Active Layer Monitoring program (CALM) is providing global monitoring for ALT via standardised measurement grids. Both GTN-P monitoring programs, TSP and CALM, fulfil QA4EO criteria by their standards for measurements, data collection and open data publication practices. Permafrost_cci also specifically involves the mountain permafrost monitoring program GTN-P/PERMOS in Switzerland to cope with the challenge of validation of the Permafrost_cci products in mountainous regions, providing PERMOS permafrost monitoring data at highest quality levels. In addition, we incorporated in situ data collections from individual Principal Investigators (PIs) and additional national ground monitoring programs in the Permafrost_cci reference dataset.

Standard statistical summaries and binary match-up analyses comparing in situ measurements with the Permafrost_cci products are used. Permafrost_cci is also innovatively undertaking assessments in comparing Permafrost_cci GTD with EO-derived Freeze-Thaw to Temperature (FT2T) and for mountain permafrost areas using EO-derived inventories on rock glacier occurrence, which was developed by SA Data User Element (DUE) GlobPermafrost since 2016 and which was continued in Permafrost_cci phase I and worldwide in 12 mountain regions in Permafrost_cci phase II.

Permafrost_cci GTD match-up evaluation shows a median bias of -0.89 °C (mean bias -0.73 °C) for the circum-arctic for the bulk ground temperature data collection spanning depths from the surface down to 10 m and permafrost temperature regimes as well as warmer non-permafrost temperature. In summary, the Permafrost_cci permafrost temperature (that we define as GTD < 1°C) shows a high performance with a median bias of 0.35 °C for all depth layers and is well usable by the climate research

community. Users of Permafrost_cci GTD products should consider that Permafrost_cci GTD > 1 °C outside of the permafrost zones is characterised by a cold median bias of -1.17 °C (mean bias -1.11 °C). This leads in turn to an overestimation of the areal extent of permafrost (especially in the Permafrost_cci PFR = 29 % class) at the southern boundaries of Permafrost in discontinuous, and sporadic permafrost regions. We consider Permafrost_cci GTD and PFR products for the Northern hemisphere to be most reliable in the permafrost temperature range with GTD < 1 °C and in PFR > 50 % as well as PFR <= 29 % is reliable as non-permafrost.

Permafrost_cci ALT performance with match-up pairs from China and Mongolia excluded is characterised by a median bias of -13 cm (95 % CI: -90 to 48 cm) with a robust temporal stability around 60 %. A large bias > 1 m occurs only in a few match-up pairs in Alaska, Canada and Russia and Permafrost_cci bias < -1.5 m mainly occurs in Svalbard and Scandinavia for rocky and pebble terrain.

PERMOS investigations in the Swiss Alps shows that the performance of Permafrost_cci GTD and Permafrost_cci PFR highly improved for mountain regions. Permafrost_cci GTD shows a slight cold bias of -0.265 °C only. At larger depth, Permafrost_cci GTD shows a slight warm bias of +0.275 °C at 10 m depth. Due to the major improvement in Permafrost_cci GTD, also the Permafrost_cci PFR product now matches the majority of inventoried ESA GlobPermafrost slope movement products and Permafrost_cci rock glacier products that were located outside of the Permafrost_cci PFR before.

1 INTRODUCTION

1.1 PURPOSE OF THE DOCUMENT

This document is the Product Validation and Intercomparison Report (PVIR) version 4 (update of [RD-1]) of the ESA CCI+ project Permafrost_cci. The PVIR describes the quality assessments of the Permafrost_cci Climate Research Data Packages (CRDP), following CCI and CEOS Quality Assurance framework for Earth Observation (QA4EO) guidelines [AD-1, RD-2].

Besides the required WMO/GCOS Permafrost ECVs i) permafrost temperature, and ii) active layer thickness, Permafrost_cci provides iii) permafrost extent (permafrost fraction within a pixel), as an additional variable derived from permafrost temperature: the areal fraction within the grid cell that fulfils the definition for the existence of permafrost (ground temperature <0 ºC for two consecutive years).

The generation of the Permafrost_cci CRDP i) Ground Temperature per Depth (GTD) per year, Active Layer Thickness (ALT) per year, and Permafrost FRaction (PFR) per year time series relies on the ground thermal model Permafrost_cci CryoGrid, that is forced by EO time series of Land Surface Temperature (LST) and Snow Water Equivalent (SWE) with boundary conditions of EO-derived Land Cover [RD-3].

The Permafrost_cci CRDPv3 [RD-3] released in 2023, is an update of CRDPv2 and includes three time series covering the Northern Hemisphere north of 30° N:

• simulated EO-forced **mean annual Ground Temperature per Depth (GTD) in five discrete depths** (0, 1.0, 2.0, 5.0, 10.0 m) from 1997 to 2021

• simulated EO-forced **annual Active Layer Thickness (ALT)** from 1997 to 2021

• **annual Permafrost FRaction (PFR)** derived from GTD from 1997 to 2021

The CCI project team shall ensure independence for the validation, implying that the assessment of the Permafrost_cci product, as well as its uncertainties, is established with independent datasets and suitable statistical approaches [AD-1,2,3]: the validation needs to be carried out by team members not involved in the final algorithm selection [AD-1,2].

In Permafrost_cci phase II we will continue validation experiments for mountain permafrost areas using rock glacier abundance and binary-based validation on permafrost abundance similar to validation of mountain permafrost in phase I [RD-1,2].

1.2 STRUCTURE OF THE DOCUMENT

The PVIR is organised in six chapters. Chapter 1 provides the introduction and the overview on Permafrost_cci including applicable documents and the community glossary for Permafrost. Chapter 2 and its subsections describe the reference datasets and methods for the assessment of the Permafrost_cci products and their temporal stability. Chapters 3,4,5 present the results of the quality assessment for the Permafrost_cci products for Permafrost_cci permafrost Ground Temperature per Depth (GTD), Permafrost_cci Active Layer Thickness (ALT), and Permafrost_cci Permafrost FRaction (PFR), respectively. Chapter 6 provides a summary and recommendations.

1.3 APPLICABLE DOCUMENTS

[AD-1] GEO/CEOS Quality Assurance framework for Earth Observation (QA4EO) protocols 3-4

[AD-2] ESA 2017: Climate Change Initiative Extension (CCI+) Phase 1 – New Essential Climate Variables – Statement of Work. ESA-CCI-PRGM-EOPS-SW-17-0032

[AD-3] ESA Climate Change Initiative. CCI Project Guidelines. EOP-DTEX-EOPS-SW-10-0002

[AD-4] ECV 9 Permafrost: Assessment report on available methodological standards and guides, 1 Nov 2009, GTOS-62

[AD-5] Requirements for monitoring of permafrost in polar regions - A community white paper in response to the WMO Polar Space Task Group (PSTG), Version 4, 2014-10-09. Austrian Polar Research Institute, Vienna, Austria, 20 pp.

1.4 REFERENCE DOCUMENTS

[RD-1] Heim, B., Wieczorek, M., Pellet, C., Delaloye, R., Barboux, C., Westermann, S., Strozzi, T. (2020): ESA CCI+ Product Validation Plan, v3.0

[RD-2] Heim, B., Lisovski, S., Wieczorek, M., Pellet, C., Delaloye, R., Bartsch, A., Jakober, D., Pointner, G., Strozzi, T. (2020): ESA CCI+ Product Validation and Intercomparison Report, v3.0

[RD-3] Bartsch, A., Westermann, Strozzi, T., Wiesmann, A., Kroisleitner, C., Wieczorek, M., Heim, B. (2023): ESA CCI+ Permafrost Product Specifications Document, v4.0

[RD-4] van Everdingen, Robert, ed. 1998 revised May 2005. Multi-language glossary of permafrost and related ground-ice terms. Boulder, CO: National Snow and Ice Data Center/World Data Center for Glaciology. (http://nsidc.org/fgdc/glossary/; accessed 23.09.2009)

[RD-5] Bartsch, A., Westermann, S., Heim, B., Wieczorek, M., Pellet, C., Barboux, C., Delaloye, R., Kroisleitner, C., Strozzi, T. (2020): ESA CCI+ Permafrost Data Access Requirements Document, v2.0

[RD-6] Nitze, I., Grosse, G., Heim, B., Wieczorek, M., Matthes, H., Bartsch, A., Strozzi, T. (2019): ESA CCI+ Climate Assessment Report, v1.0

[RD-7] Bartsch, A., Matthes, H., Westermann, S., Heim, B., Pellet, C., Onacu, A., Kroisleitner, C., Strozzi, T. (2019): ESA CCI+ Permafrost User Requirements Document, v1.0

[RD-8] Heim, B., Wieczorek, M., Pellet, C., Barboux, C., Delaloye, R., Bartsch, A., B. Kroisleitner, C., Strozzi, T. (2019): ESA CCI+ Product Validation and Intercomparison Report, v1.0

[RD-9] Heim, B., Wieczorek, M., Pellet, C., Delaloye, R., Bartsch, A., Jakober, D., Pointner, G., Strozzi, T. (2020): ESA CCI+ Product Validation and Intercomparison Report, v2.0

[RD-10] Rouyet, L., Schmid, L., Pellet, C., Delaloye, R., Onaca, A., Sirbu, F., Poncos, V., Kääb, A., Strozzi, T., Jones, N., Bartsch, A. (2023): CCN4 Mountain Permafrost: Rock Glacier Inventories (ROGI) and Rock Glacier Velocity (RGV) products Product Specification Document v1.0

[RD-11] IPA Action Group 'Specification of a Permafrost Reference Product in Succession of the IPA Map' (2016): Final report.
https://ipa.arcticportal.org/images/stories/AG_reports/IPA_AG_SucessorMap_Final_2016.pdf

1.5 BIBLIOGRAPHY

A complete bibliographic list that supports arguments or statements made within the current document is provided in Section 6.1.

1.6 ACRONYMS

A list of acronyms is provided in section 6.2.

1.7 GLOSSARY

The glossary below based on [RD-4] provides a selection of terms relevant for Permafrost_cci [AD-2]. A comprehensive glossary is available as part of the Product Specifications Document [RD-3,4].

active-layer thickness

The thickness of the ground layer that is subject to annual thawing and freezing above permafrost. The thickness of the active layer depends on factors such as the ambient air temperature, vegetation, drainage, soil or rock type and total water content, snowcover, and degree and orientation of slope. As a rule, the active layer is thin in the High Arctic (it can be less than 15 cm) and becomes thicker farther south (1 m or more). The thickness of the active layer can vary from year to year, primarily due to variations in the mean annual air temperature, distribution of soil moisture, and snowcover. The thickness of the active layer includes the uppermost part of the permafrost wherever either the salinity or clay content of the permafrost allows it to thaw and refreeze annually, even though the material remains cryotic (T <0 °C).

Use of the term "depth to permafrost" as a synonym for the thickness of the active layer is misleading, especially in areas where the active layer is separated from the permafrost by a residual thaw layer, that is, by a thawed or noncryotic (T >0 °C) layer of ground.

REFERENCES: Muller, 1943; Williams, 1965; van Everdingen, 1985

continuous permafrost

Permafrost occurring everywhere beneath the exposed land surface throughout a geographic region with the exception of widely scattered sites, such as newly deposited unconsolidated sediments, where the climate has just begun to impose its influence on the thermal regime of the ground, causing the development of continuous permafrost. For practical purposes, the existence of small taliks within continuous permafrost has to be recognized. The term, therefore, generally refers to areas where more than 90 percent of the ground surface is underlain by permafrost.

REFERENCE: Brown, 1970.

discontinuous permafrost

Permafrost occurring in some areas beneath the exposed land surface throughout a geographic region where other areas are free of permafrost. Discontinuous permafrost occurs between the continuous permafrost zone and the southern latitudinal limit of permafrost in lowlands. Depending on the scale of mapping, several subzones can often be distinguished, based on the percentage (or fraction) of the land surface underlain by permafrost, as shown in the following table.

Permafrost	English usage	Russian Usage
Extensive	65-90%	Massive Island
Intermediate	35-65%	Island
Sporadic	10-35%	Sporadic
Isolated Patches	0-10%	-

SYNONYMS: (not recommended) insular permafrost; island permafrost; scattered permafrost.

REFERENCES: Brown, 1970; Kudryavtsev, 1978; Heginbottom, 1984; Heginbottom and Radburn, 1992; Brown et al., 1997.

mean annual ground temperature (MAGT)

Mean annual temperature of the ground at a particular depth. The mean annual temperature of the ground usually increases with depth below the surface. In some northern areas, however, it is not uncommon to find that the mean annual ground temperature decreases in the upper 50 to 100 metres below the ground surface as a result of past changes in surface and climate conditions. Below that depth, it will increase as a result of the geothermal heat flux from the interior of the earth. The mean annual ground temperature at the depth of zero annual amplitude is often used to assess the thermal regime of the ground at various locations.

permafrost

Ground (soil or rock and included ice and organic material) that remains at or below 0 °C for at least two consecutive years. Permafrost is synonymous with perennially cryotic ground: it is defined on the basis of temperature. It is not necessarily frozen, because the freezing point of the included water may be depressed several degrees below 0°C; moisture in the form of water or ice may or may not be present. In other words, whereas all perennially frozen ground is permafrost, not all permafrost is perennially frozen. Permafrost should not be regarded as permanent, because natural or man-made changes in the climate or terrain may cause the temperature of the ground to rise above 0 °C. Permafrost includes perennial ground ice, but not glacier ice or icings, or bodies of surface water with temperatures perennially below 0 °C; it does include man-made perennially frozen ground around or below chilled pipe-lines, hockey arenas, etc.

Russian usage requires the continuous existence of temperatures below 0 °C for at least three years, and also the presence of at least some ice.

SYNONYMS: perennially frozen ground, perennially cryotic ground and (not recommended) biennially frozen ground, climafrost, cryic layer, permanently frozen ground.

REFERENCES: Muller, 1943; van Everdingen, 1976; Kudryavtsev, 1978.

2 METHODS FOR QUALITY ASSESSMENT

This chapter provides an overview of methods used to evaluate the performance of the Permafrost_cci products analysed and discussed in the following order: Permafrost_cci Ground Temperature per Depth (GTD), Active Layer Thickness (ALT) and Permafrost Fraction (PFR).

2.1. OVERVIEW ON THE QUALITY ASSESSMENT METHODS

2.1.1 Unbiased Validation

The CCI project team shall ensure independence for the validation, implying that the assessment of the Permafrost_cci products is established with independent datasets and suitable statistical approaches [AD-1,2,3]: this implies that the validation needs to be carried out by team members not involved in the final algorithm selection [AD-1,2]. The validation in Permafrost_cci is fully independent as the validation team is independent of the algorithm development team and uses fully independent validation datasets from the global GCOS Global Terrestrial Network for Permafrost (GTN-P) program and additional national measurement networks such as PERMOS in Switzerland and national monitoring programs in Russia, Canada and United States, as well as datasets from individual PIs [AD-4, RD-1,2,5]. WMO/GCOS GTN-P managed by the International Permafrost Association (IPA) provides in situ measurements for the Permafrost ECVs from the Thermal State of Monitoring (TSP) and the Circumpolar Active Layer Monitoring program (CALM), including community standards for measurements and data collection (Brown et al., 2000, Clow, 2014, Biskaborn et al. 2015) [RD-5]. Specifically initiated by the International Polar Year (IPY 2007-2008), GTN-P established a temperature reference baseline for permafrost. Using this extended monitoring, the permafrost community could demonstrate that during the IPY reference decade (2007 to 2016/2017) permafrost temperature at depths of the Zero Annual Amplitude (ZAA) increased globally by 0.29 °C (Biskaborn et al., 2019, GTN-P, 2018, 2021).

In addition to the community ground temperature data collection at depths of ZAA (GTN-P, 2018, 2021), there is an obvious need for a standardised ground temperature benchmark dataset across all different depths, specifically also standardising data for shallow depths, as has been stressed by user communities of climate and biosciences, as it does not yet exist [AD-5, RD-5,6,7]. Profoundly, land surface and climate models lack standardised data on ground temperature in shallow depths for a scientific evaluation of simulated ground thermal conditions and permafrost states. Land surface and climate models are parameterized down to depths of 3 m or 5 m depths only, not reaching the deeper ZAA depths in continuous permafrost.

To validate the Permafrost_cci products, the team in Permafrost_cci responsible for validation has been thus compiling, checking and standardising all available communities' ground temperature (GT) and ALT data [RD1,2,5]. The majority of the in situ data collection is contributed from GTN-P/IPA and its individual Principal Investigators (PIs) and for the Eurasian Permafrost region from the Russian meteorological monitoring network ROSHYDROMET (RHM) program, in addition with contributions from GTN-P PIs, and datasets from Nordicana-D for Canada, and NASA Arctic-Boreal Vulnerability Experiment ABoVE datasets and United States Geological Survey (USGS) for Alaska (United States) were additionally collected. GTN-P and RHM time series and the data collections from additional networks and PIs provide a large data collection of in situ measured reference datasets [RD1,2,5].

All these data are no easy-to-use or readily available time series data that are data-fit for validation and round robin exercises. For example, the ground temperature data collection includes variable timeframes from hourly over annually to sporadic measurements, in different depths and not consistent over time. In addition, the in situ datasets, despite being produced according to community standards and published, contain a large number of caveats, including erroneous or imprecise coordinate locations and non-corrected measurement errors, depending on region and PI [RD-1,2,5,8.9]. Within Permafrost_cci, these pre-existing community in situ data collections have been for the first time all together error-checked, homogenised, filtered and standardised. The newly compiled, harmonised Permafrost_cci GTD time series provides the first consistent reference dataset covering all measurement depths for the circum-Arctic: it covers all permafrost zones from continuous to discontinuous, sporadic and isolated of the Northern Hemisphere with all available measurement depths down to 20 m [RD-1,2,8,9].

The validation and evaluation efforts also consider high-mountain permafrost regions, using in situ observations of surface and ground temperatures provided by GTN-P PERMOS in Switzerland. In addition, the EO-derived inventories on rock glacier occurrence, which was developed by the ESA Data User Element (DUE) GlobPermafrost team since 2016 and which is continued in Permafrost_cci phase I and II, are innovatively used for assessments of the Permafrost_cci products. The PERMOS monitoring data and the rock glacier inventories compiled in 12 regions around the globe in the framework of Permafrost_cci [RD-10] supports the validation in mountain areas, where the Permafrost_cci products contain the highest uncertainties [RD-1,2,8,9].

The IPA Permafrost mapping action group contributed in its active action group phase as an important collaborator for validation in Permafrost_cci phase I [RD-7]. Dr. Isabelle Gärtner-Roer, University of Zurich, CH, former vice president of IPA and former leader of the IPA Permafrost mapping action group [RD-11], and Science Officer of the World Glacier Monitoring Service (WGMS), was stating that a very profound validation is being performed in Permafrost_cci by using the in situ data from GTN-P and from PERMOS [RD-6]. IPA agrees on the fact that in situ data are clustered in regions with active permafrost monitoring programs/projects, and that therefore some regions are underrepresented. For the validation in Permafrost_cci, IPA further provides the recommendation that the validation of the Permafrost_cci ground temperature product is the most important as it builds the base for the other products, such as active layer thickness and permafrost extent [RD-6].

Permafrost_cci entirely acknowledges the efforts of the international permafrost community in this impressive realisation of circumpolar measurements, and all national initiatives from Russia, US, Canada, Switzerland and Norway for making the measurement data publicly available. The Permafrost_cci match-up dataset and its characteristics as well as data sources and availability are described in detail in [RD-5]. The previous product quality assessments are described in [RD-2,8,9].

2.1.2 Validation Process

The required Permafrost ECVs by WMO/GCOS for Permafrost are [AD-2,3,4] i) **permafrost temperature** and ii) **active layer thickness**. Permafrost_cci added iii) **permafrost extent** (permafrost fraction) as a mapped permafrost variable, which is the fraction within an area (pixel) at which the definition for the existence of permafrost (ground temperature < 0 ºC for two consecutive years) is fulfilled. The main focus of Permafrost_cci lies on the ECV permafrost temperature as its derivation also forms the base for the derivation of active layer thickness and permafrost fraction.

The Permafrost_cci products are evaluated using pixel-based match-up analyses between Permafrost_cci GTD, ALT and PFR and the compiled in situ data at individual stations, relying on statistical metrics for its common usage. On one hand, the Permafrost_cci in situ reference data collections of ground temperature are characterised by spatial and temporal biases related to regions, time covered and measurement depths due to the high variety in national measurement programs, PIs and funding sources. On the other hand, we are facing a spatial-scale mismatch between in situ measurements, i.e., the borehole locations or the 100 m×100 m CALM grid ALT measurements versus the ~1 km^2 Permafrost-cci grid cells. Already with the native MODIS-derived sinusoidal geometry, each location of an in situ measurement is moved further away from its original location to a nearby location on the grid. In addition, the WGS84 geographic projection that is finally applied requires pixel infilling and further smooths out landscape heterogeneity. The comparison of shallow depths further compromises the precision, as permafrost landscapes may contain heterogeneous micro-topography, leading to an inconsistent depth extrapolation for shallow depths. Despite these challenges, the Permafrost_cci match-up analyses do provide a robust estimation of the accuracy and usability of the Permafrost_cci products.

For a cross-product assessment we applied the Freeze-Thaw to Temperature (FT2T) product, a spaceborne radar-derived ground temperature product, for comparison with Permafrost_cci GTD.

For the mountain permafrost use case, GTN-P PERMOS in Switzerland assessed the Permafrost_cci GTD and PFR products, using expert knowledge, in situ surface temperature, borehole ground temperature and the EO-derived inventories on rock glacier occurrence, which was developed by the ESA Data User Element (DUE) GlobPermafrost team since 2016 and which is continued in Permafrost_cci phase I and worldwide in 12 mountain regions in phase II.

2.1.3 Statistical Assessments

The pixel-based pairwise Permafrost_cci match-up data collection consists of

- Permafrost_cci GTD matched with in situ mean annual ground temperature (MAGT) in discrete and interpolated depths (0, 0.1, 0.2, 0.25, 0.4, 0.5, 0.6, 0.75, 0.8, 1.0, 1.2, 1.5, 1.6, 2.0, 2.4, 2.5, 3.0, 3.2, 4.0, 5.0, 10.0 m), in annual resolution from 1997 to 2021.
- Permafrost_cci ALT matched with in situ ALT, in annual resolution from 1997 to 2021.
- Permafrost_cci PFR matched with a combination of in situ MAGT integrated over 3 m depth and in situ ALT, in annual resolution from 1997 to 2021.

We used common statistical approaches: the characterization of errors and uncertainties is carried out using evaluation measures of bias, median absolute deviation and root mean square error.

In addition, we assessed the temporal stability of the Permafrost_cci product time series using two approaches: a g-score approach and a bias stability approach.

The *bias* is the mean deviation of the product to the in situ data and calculated by

$$bias = \frac{\sum_{i=1}^{n}(Permafrost_{cci} - in\ situ)}{n}$$

This results in a positive bias in case the product is too warm and vice versa. Given that large deviations in positive and negative direction can result in a bias ~0, we additionally use the absolute bias (*abs_bias*), calculated by

$$abs\_bias = \frac{\sum_{i=1}^{n}|(Permafrost_{cci} - in\ situ)|}{n}$$

The *root mean square error* (*RMSE*) is calculated by

$$RMSE = \sqrt{\frac{\sum_{i=1}^{n}(Permafrost_{cci} - in\ situ)^2}{n}}$$

The *median absolute deviation* (*MAD*) is calculated by

$$MAD = median(|x_i\text{-}median|)$$

'Gleichläufigkeit' (g-score) approach

First, we checked how many cases of Permafrost_cci GTD and ALT respectively, follow the same year-to-year trend like the in situ reference measurements. This means, if within both, the Permafrost_cci product time series and the in situ measurement time series, the slope values decrease/increase simultaneously in the same direction (positive or negative), the value of 1 is assigned. If the two slopes develop in different directions, the value 0 is assigned, and if one slope changes direction while the other slope is constant, the value of 0.5 is assigned. The mean value of these year-to-year trend-values then gives the fraction of synchronised curve development. This approach, in dendrochronology called 'Gleichläufigkeit' or g-score, gives an impression on how well the Permafrost_cci variable follows the actual temperature and ALT trend, respectively. This method does not provide any information on the bias.

Bias Stability approach

Additionally, we checked for the magnitude of the interannual variability of the bias. We assume that physically based, the bias should not largely change in magnitude from one year to the next. We thus calculated temporal stability

$$ts = \frac{bias_j - bias_i}{year_j - year_i}$$

with i being the current year/bias and j being the previous year/bias. The difference was only calculated on a year-to-year basis and rejected, for every missing year at a specific site/depth.

2.2 ASSESSMENT OF PERMAFROST TEMPERATURE

2.2.1 Ground Temperature Reference Data

A major data provider for ground temperature time series is the WMO/GCOS **Global Terrestrial Network for Permafrost GTN-P** (https://gtnp.arcticportal.org/), the global permafrost monitoring program of the International Permafrost Association IPA. Compiled GTN-P and USGS data are also published in the Arctic Data Center (US) (https://arcticdata.io/catalog/ #view/doi:10.18739/A2KG55; Wang et al. 2018). Several more important GTN-P collections and data from individual members of the Permafrost research community are published in the PANGAEA data repository for environmental research (DE) (https://doi.pangaea.de/10.1594/PANGAEA.905233; Boike et. al. 2019; https://doi.pangaea.de/10.1594/PANGAEA.884711,
GTN-P 2018), https://doi.pangaea.de/10.1594/PANGAEA.912482, Bergstedt & Bartsch 2020a). In addition, we received ground data from more individual members of the Permafrost research community (PIs V. Romanovski and A. Kholodov (GTN-P, University of Alaska Fairbanks, US), PI M. Ulrich (University of Leipzig, DE) connected to GTN-P but not yet with this data published within the GTN-P data repository frameworks). Therefore, within our reference data collection these data are also named GTN-P. Further relevant data providers are the WMO **Roshydromet RHM** national hydrometeorological monitoring program for Russia (http://meteo.ru/data/164-soil-temperature), **Nordicana-D,** the Canadian data repository for Polar research, https://nordicana.cen.ulaval.ca/index.aspx; Allard et al., 2020, CEN 2020a,b,c,d,e,f,g, Fortier et al. 2021) and the **NASA Arctic-Boreal Vulnerability Experiment ABoVE** https://above.nasa.gov/field_data_products.html.

[RD-5] describes the data sources, measurement programs and the data compilation steps in detail. We undertook coordinate corrections, outlier and error elimination. We also processed shallow and deep depth profiles with two different processing steps: For shallow Ground Temperature GT depth profiles down to 5 m depth, all discrete values were calculated. For GT depth profiles of 5 m depth and deeper, we discard all data <2 m depth of boreholes with large diameters, as there is frequently artificial material in-filling or air. If diameter is unknown, data <2 m were only kept if confirmed reliable by the PI.

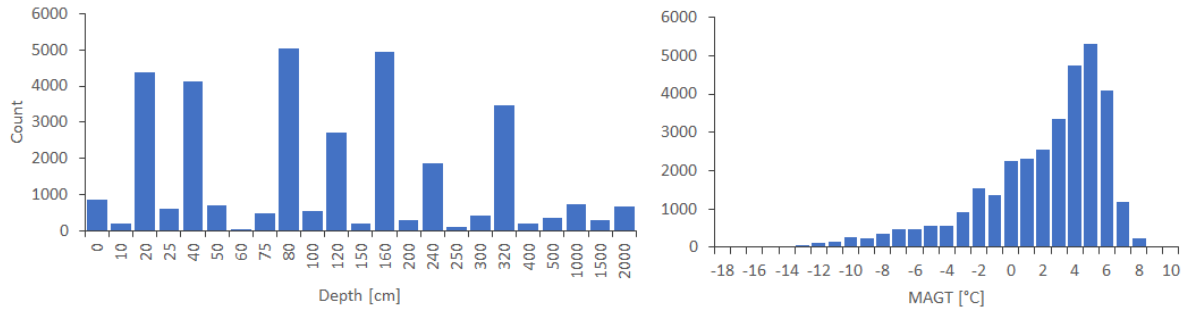

Figure 2.1: Frequency distribution of complete in situ dataset of mean annual ground temperatures (MAGT) at discrete depths for the years 1980 to 2021 (left), and across the temperature range (right). Note: not all of these data are part of the match-up, as e.g. lying outside of the simulated time or geographically covered regions.

The Permafrost_cci reference data consists of standardised mean annual Ground Temperature per Depth GTD from 1980 to 2021 (Figure 2.1), with product depths at 0, 0.1, 0.2, 0.25, 0.4, 0.5, 0.6, 0.75, 0.8, 1.0, 1.2, 1.5, 1.6, 2.0, 2.4, 2.5, 3.0, 3.2, 4.0, 5.0, 10.0, 15.0 m.

The reference data also holds metadata information, which allows assessing the quality of each temperature value (Table 2.1). These metadata comprise for yearly values the ratio of missing data per month/year (missing days per year/365) and the amount of completely missing months. Yearly means are not calculated if >20 % of yearly values are not available or if more than one complete month is missing. An exception is made for data at the depth of Zero Annual Amplitude (ZAA) that represents a valid annual value as there is zero seasonal variation in GT at this depth.

The final Permafrost_cci GT match-up data collection v4 for the time frame of 1997 to 2021 covering the Permafrost_cci model domain contains data from 477 in situ measurement locations (GTN-P, USGS n = 315, RHM n = 132, Nordicana-D n = 24, NASA ABoVE n = 6), with overall n =13,614 match-up pairs in time and depth (Figure 2.2). The Permafrost_cci GT match-up data collection v4 < 1 °C contains data from 254 in situ measurement locations (Figure 2.3; (GTN-P, USGS n = 222, RHM n = 20, Nordicana-D n = 7, NASA ABoVE n = 5)) with overall n =4,173 match-up pairs in time and depth.

Table 2.1. Example of how the compiled dataset provides metadata information of yearly values across depths. Mxx = ratio of missing values per month/year at depth xx m. mMxx = number of completely missing months per year at depth xx m.

Site	Year	Type	M0	M0.2	M0.25	M0.4	M0.5	M0.75	M0.8	M1	mM0	mM0.2	mM0.2	mM0.4	mM0.5	mM0.7	mM0.8	mM1	0	0.2	0.25	0.4	0.5	0.75	0.8	1
FB_dry_l	2006	Mean	1	1	1	1	1	1	1	1	12	12	12	12	12	12	12	12	NA	NA	NA	NA	NA	NA	NA	NA
FB_dry_l	2006	Max	1	1	1	1	1	1	1	1	12	12	12	12	12	12	12	12	NA	NA	NA	NA	NA	NA	NA	NA
FB_dry_l	2006	Min	1	1	1	1	1	1	1	1	12	12	12	12	12	12	12	12	NA	NA	NA	NA	NA	NA	NA	NA
FB_wet_	2006	Mean	0.414	0.414	0.414	0.416	0.414	NA	NA	NA	5	5	5	5	0	NA	NA	NA	1.33	1.64	1.56	1.35	1.12	NA	NA	NA
FB_wet_	2006	Max	0.414	0.414	0.414	0.416	0.414	NA	NA	NA	5	5	5	5	0	NA	NA	NA	18.9	12.7	12	10.4	8.07	NA	NA	NA
FB_wet_	2006	Min	0.414	0.414	0.414	0.416	0.414	NA	NA	NA	5	5	5	5	0	NA	NA	NA	-19.1	-12	-11.5	-10.2	-8.95	NA	NA	NA
FB_dry_l	2007	Mean	0.581	0.581	0.581	0.581	0.581	1	0.586	0.699	7	7	7	7	7	12	7	8	-3.58	-2.65	-2.53	-2.38	-2.44	NA	-2.4	-2.59
FB_dry_l	2007	Max	0.581	0.581	0.581	0.581	0.581	1	0.586	0.699	7	7	7	7	7	12	7	8	13.6	10.4	9.31	8.01	4.87	NA	1.73	0.63
FB_dry_l	2007	Min	0.581	0.581	0.581	0.581	0.581	1	0.586	0.699	7	7	7	7	7	12	7	8	-21.9	-17.5	-16.9	-16	-14.6	NA	-11.9	-8.83
FB_wet_	2007	Mean	0	0	0	0	0	NA	NA	NA	0	0	0	0	0	NA	NA	NA	-5.99	-5.41	-5.62	-5.48	-5.63	NA	NA	NA
FB_wet_	2007	Max	0	0	0	0	0	NA	NA	NA	0	0	0	0	0	NA	NA	NA	17.8	15.2	11.7	10.6	7.49	NA	NA	NA
FB_wet_	2007	Min	0	0	0	0	0	NA	NA	NA	0	0	0	0	0	NA	NA	NA	-30.2	-23.3	-22.7	-21.3	-20.3	NA	NA	NA
FB_dry_l	2008	Mean	0.18	0.18	0.18	0.18	0.18	1	0.183	0.183	2	2	2	2	2	12	2	2	-7.37	-6.62	-6.63	-6.63	-6.44	NA	-6.26	-5.82
FB_dry_l	2008	Max	0.18	0.18	0.18	0.18	0.18	1	0.183	0.183	2	2	2	2	2	12	2	2	18.7	13.2	11.8	9.48	8.1	NA	3.79	1.35
FB_dry_l	2008	Min	0.18	0.18	0.18	0.18	0.18	1	0.183	0.183	2	2	2	2	2	12	2	2	-28.7	-23.9	-23.2	-22.4	-20.7	NA	-18.2	-15.1
FB_wet_	2008	Mean	0.372	0.372	0.372	0.426	0.372	NA	NA	NA	4	4	5	4	0	NA	NA	NA	-6.62	-7.34	-7.43	-9.01	-7.73	NA	NA	NA
FB_wet_	2008	Max	0.372	0.372	0.372	0.426	0.372	NA	NA	NA	4	4	5	4	0	NA	NA	NA	18.2	12.4	11.8	9.71	9.12	NA	NA	NA
FB_wet_	2008	Min	0.372	0.372	0.372	0.426	0.372	NA	NA	NA	4	4	5	4	0	NA	NA	NA	-24.9	-22	-21.7	-20.7	-20.2	NA	NA	NA
FB_dry_l	2009	Mean	0.586	0.003	0	0.586	0	0.414	0.586	0.586	7	0	0	7	0	5	7	7	-13.2	-3.73	-3.9	-11.5	-3.92	0.11	-9.42	-7.8
FB_dry_l	2009	Max	0.586	0.003	0	0.586	0	0.414	0.586	0.586	7	0	0	7	0	5	7	7	-1.34	13.5	11.5	-3.74	7.1	3.58	-2	-1.09
FB_dry_l	2009	Min	0.586	0.003	0	0.586	0	0.414	0.586	0.586	7	0	0	7	0	5	7	7	-19.9	-18	-17.7	-17.3	-16.2	-5.97	-14.3	-11.9
FB_wet_	2009	Mean	0.414	0.416	0.416	1	0.414	NA	NA	NA	5	5	12	5	0	NA	NA	NA	1.95	1.65	1.65	NA	1.46	NA	NA	NA

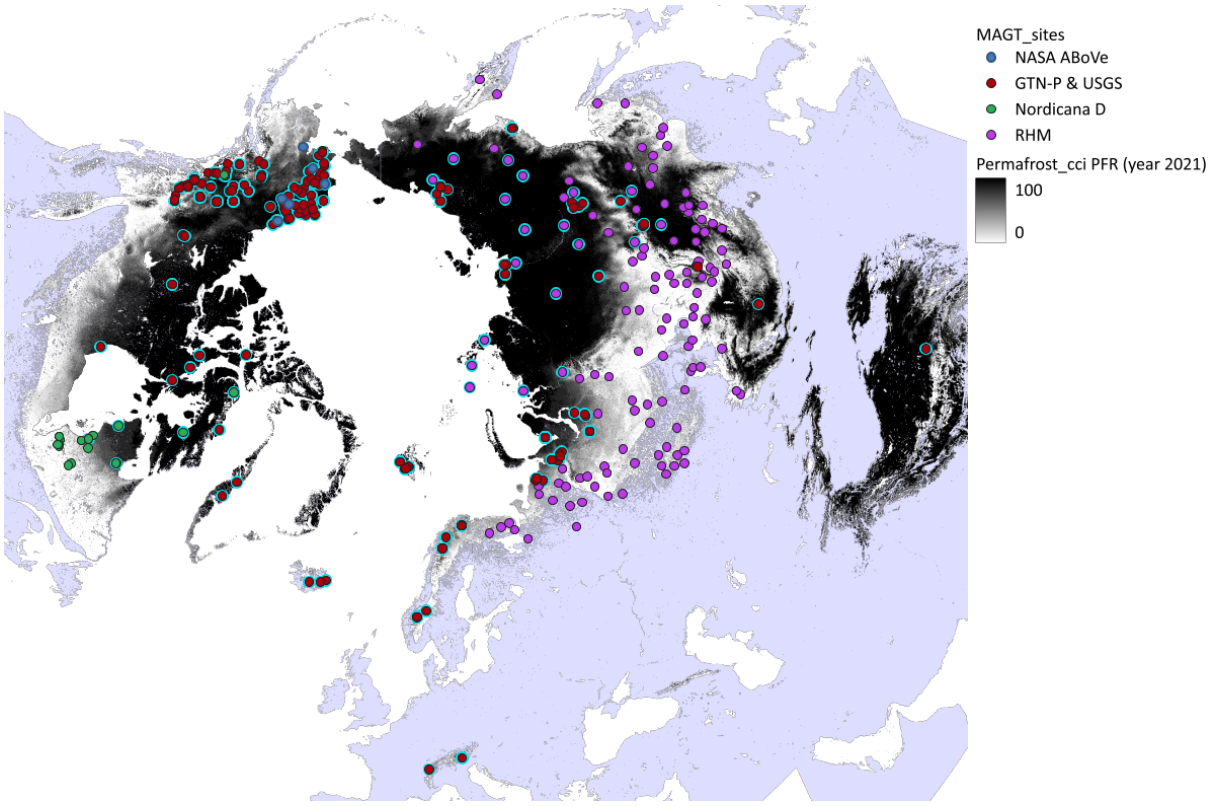

Figure 2.2. Northern hemisphere Permafrost_cci PFR permafrost probability and in situ ground temperature stations of the match-up dataset v4 (grouped by data source). Circle symbols with thick outlines represent sites with MAGT < 1 °C.

Versions of Ground Temperature Reference and Match-up Datasets

GTD match-up dataset v1 (2003 to 2017) Exclusion of non-permafrost temperature value range (Validation in phase I, CRDPv0 2019)

For straightforward match-up analyses in the first validation round v, we focused on the permafrost temperature range excluding all stations with in situ measurements of MAGT ≥ 1 °C at least once (independent of measurement depth) from the match-up analyses. This GTD match-up dataset, with all 'non-permafrost temperature' station types excluded, contained n = 3,185 pairs in time and depth. [RD-8]

GTD match-up dataset v2 (1997 to 2018) Inclusion of non-permafrost temperature value range, exclusion of sites in Yedoma regions in Siberia (Validation in phase I, CRDPv1 2020)

We conducted the validation v2 using the GTD data collection with MAGT ≥ 1 °C included (depths down to 10 m). This GTD match-up dataset for Permafrost_cci MAGT in 0, 0.2, 0.25, 0.4, 0.5, 0.6, 0.75, 0.8, 1.0, 1.2, 1.6, 2.0, 2.4, 2.5, 3.0, 3.2, 4.0, 5.0, 10.0 m depth included n = 13,695 match-up pairs in time and depth from n = 300 sites. [RD-9]

As especially the Russian sites have only few measurements at exactly 1 or 2 m depth, we interpolated temperature values fitting the Permafrost_cci product depths. To achieve this, we only use sites with at least three sensors in the shallow depth range down to 1.20 m.

Interpolation was conducted by linear regression between two single measurement depths, resulting in separate equations for each sensor-pair and year.

Please note that we excluded all sites that are not representative of the landscape-scale of in situ measurements from all three match-up data collections: these are selected mountain sites (n = 18) that are specifically assessed by PERMOS, small-scale landscape anomalies such as very local peatland patches or in situ measurements in pingos (ice hills, n = 3). Please also note that we excluded all sites within the Siberian Yedoma area (shape file from Bryant et al., 2017) due to incorrect parameterisation of Yedoma stratigraphy (n = 7) in *CRDPv1*. [RD-9]

GTD match-up dataset v3 (1997 to 2019) (Validation in phase I, CRDPv2 2021)

We conducted the validation v3 using the GTD data collection with interpolated depths down to 20 m. This GTD match-up dataset for Permafrost_cci MAGT in 0, 0.2, 0.25, 0.4, 0.5, 0.6, 0.75, 0.8, 1.0, 1.2, 1.6, 2.0, 2.4, 2.5, 3.0, 3.2, 4.0, 5.0, 10.0 m depth includes n = 14,107 match-up pairs in time and depth from 354 sites. [RD-2]

The PERMOS mountain permafrost sites and landscape anomalies excluded in v2 were also excluded in v3. All sites within the Siberian Yedoma area are included in v3 as CRDPv2 contains no artefacts in the Yedoma regions. [RD-2]

GTD match-up dataset v4 (1997 to 2021) (Validation in phase II, CRDPv3 2023)

We conduct the validation v4 using the GTD data collection with original and interpolated depths down to 10 m. This GTD match-up dataset for Permafrost_cci MAGT in 0, 0.1, 0.2, 0.25, 0.4, 0.5, 0.6, 0.75, 0.8, 1.0, 1.2, 1.5;1.6, 2.0, 2.4, 2.5, 3.0, 3.2, 4.0, 5.0, 10.0 m depth includes n = 13,614 match-up pairs in time and depth from 477 sites (27,389 pairs for the interpolated dataset). In this dataset, several sites lying directly in settlements with their coordinates were excluded from the match-ups if the bias was high (+/- 2.5 °C).

The PERMOS mountain permafrost sites and landscape anomalies excluded in v2 and v3 were also excluded in v4. We kept some mountain sites outside the PERMOS region, if they were not located in high mountain areas (e.g. > 1500 m). All sites within the Siberian Yedoma area are included in v4 as *CRDPv3* contains no artefacts in the Yedoma regions.

2.2.2 Characteristics of GTD Match-up Dataset

The GTD match-up v4 (2023) contains the cleaned and interpolated in situ MAGT at discrete depths matched with interpolated CRDPv3 Permafrost_cci MAGT at 0, 0.1, 0.2, 0.25, 0.4, 0.5, 0.6, 0.75, 0.8, 1.0, 1.2, 1.5, 1.6, 2.0, 2.4, 2.5, 3.0, 3.2, 4.0, 5.0, 10.0 m depth. The Permafrost_cci GTD map product is provided at 0, 1, 2, 5, and 10 m depths. For the accuracy assessment, the Permafrost:cci product development team produced per measurement station, GTD time series at the additional depths. Figure 2.3 shows the frequency distribution of the original, non-interpolated match-up data with n = 13,614, Figure 2.7 with in situ MAGT ≥1 °C excluded, with n =4,173.

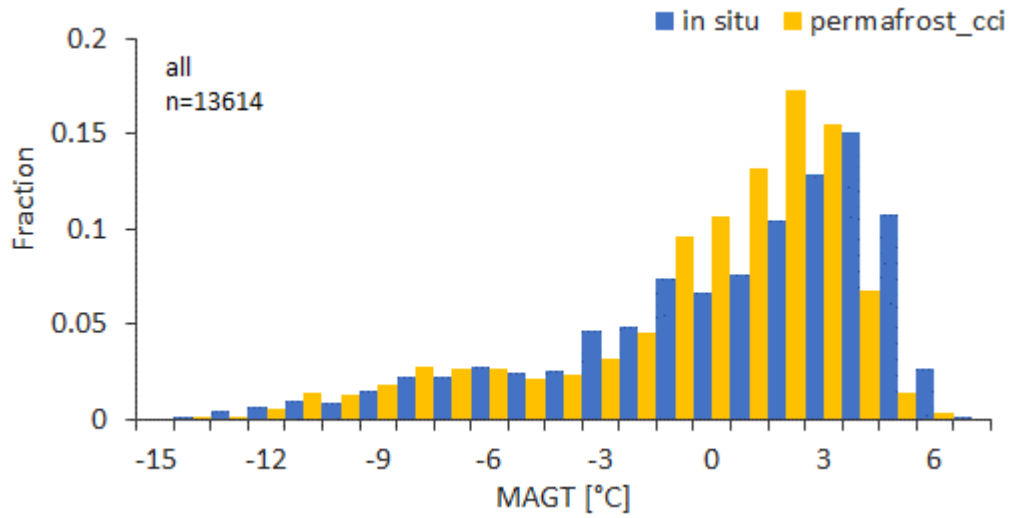

Figure 2.3. Frequency distribution of the match-up data collection v4, at all discrete depths down to 10 m in entire ranges with steps of 1 °C, n = 13,614.

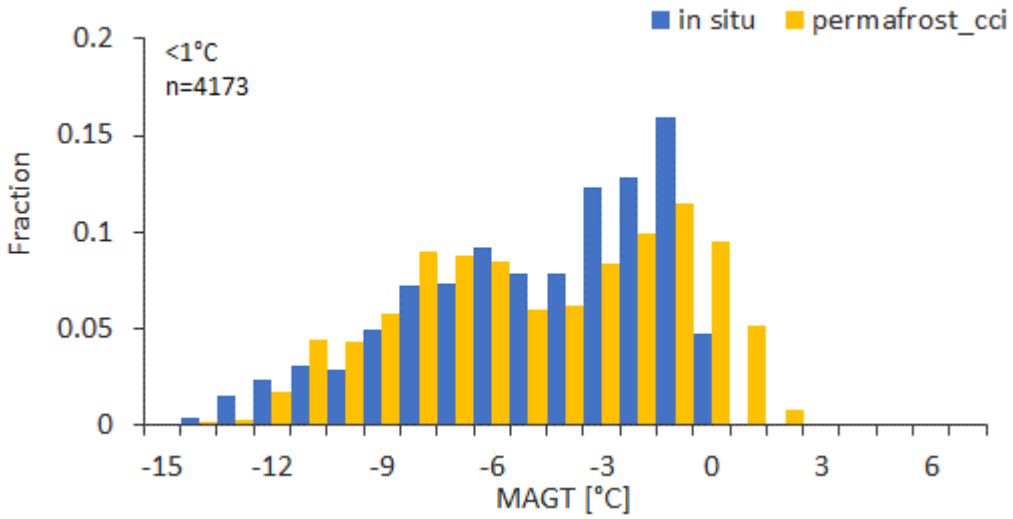

Figure 2.4. Frequency distribution of the match-up data collection v4 with sites MAGT ≥1 °C being excluded, n = 4,173 (excluded samples = 9,441).

The bulk MAGT sample size peaks between 2 °C and 4 °C for Permafrost_cci MAGT and between 3 °C and 5 °C for in situ MAGT (Figure 2.3). This data group is mainly constructed from the RHM long-term measurement network. The match-up data characteristics of MAGT < 1 °C (Figure 2.4) show a bimodal distribution with a maximum around -6 °C and another one around -1 °C. The depth-specific frequency distributions vary as they cover different latitudes and regions depending on the data provider. RHM with main contributions to depths of 0.80, 1.20, 2.40 m covers fewer measurement sites at high latitudes than GTN-P and Nordicana-D that more frequently cover the depths of 0.75, 1.00 and 2.00 m (Figure 2.5).

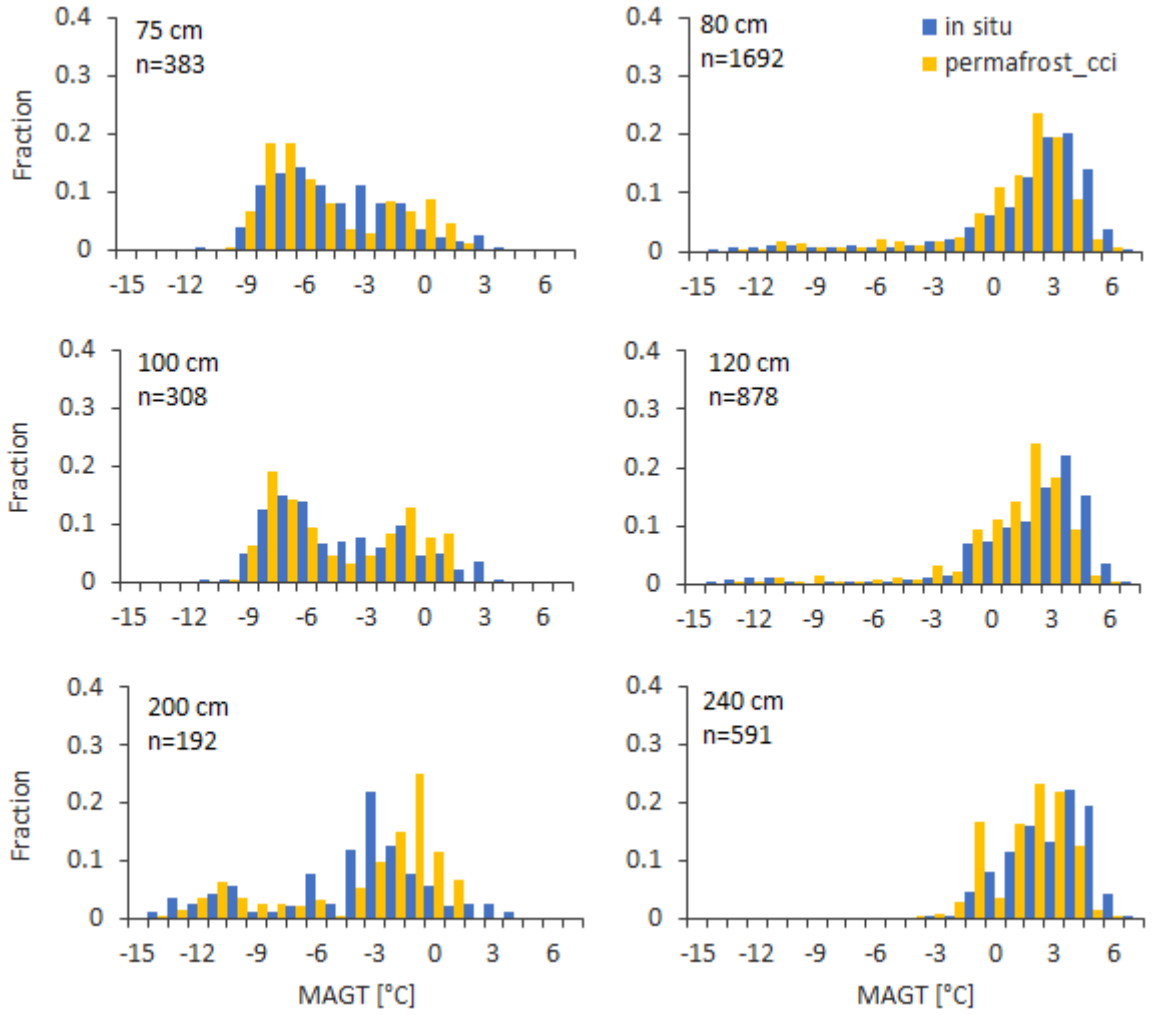

Figure 2.5. Frequency distribution of the bulk match-up data collection v4 confined to match-up pairs in specific ground temperature sensor depths (0.75, 0.80, 100, 120, 200, 240 cm).

2.2.3 PERMOS Reference GST and GTD Data Generation

The PERMOS network currently comprises 27 boreholes distributed within 16 sites (Figure 2.8) across Switzerland, which continuously measure permafrost temperatures between 0 and 100 m depth. The sites are located at elevations between 2400 m a.s.l. and 3400 m a.s.l. with boreholes drilled in bedrock, rock glaciers, talus slopes, steep rock walls or moraines ([RD-1]).

For each single borehole, PERMOS selected the thermistor closest to the depth of the Permafrost_cci GT product (0, 1, 2, 5 and 10 m) and compiled mean annual ground temperature (MAGT) over the period 1997-2021. Only data series with at least 80 % data completeness over the year were selected for computing MAGT.

The match-up of the 1 km x 1 km grid cell of the Permafrost_cci product with the in situ data functions by selecting the grid cells in which the boreholes are located. The in situ measured MAGT and Permafrost_cci GTD values are compared pairwise for each single borehole and depth. In mountainous terrains, the differences in the subsurface thermal regime due to varying climate conditions (i.e., latitudinal and regional gradients) are considered smaller than those caused by topography or surface and subsurface conditions of the different landforms. Therefore, we analysed Permafrost_cci product performance based on the landform typologies rather than based on climatic regions.

Ground surface temperature (GST) are temperatures measured between 0 and 10 cm depth by miniature loggers placed only with a small distance below the surface to avoid the influence of the direct shortwave radiation and to capture a slightly filtered temperature signal. Within the PERMOS network, GST are measured at 23 different sites, each with four to more than 20 individual loggers adding up to 247 measurement points (see also Figure 2.8). Each logger measures continuously with a temporal resolution of 1 to 3 hours.

Based on this dataset, PERMOS filtered and gap-filled the time series using the approach of Staub et al. 2017. Mean annual ground surface temperature (MAGST) has been computed for each single logger over the period 1997 to 2021. Only series with at least 80% data completeness over the year were selected for computing the annual mean. Thus, the number of MAGST available is variable from one year to the next. It ranges from 25 MAGST match-up data computed in 1997 to 160 in 2012.The MAGST data is highly variable depending on snow conditions, radiation and shading effects as well as surface and subsurface properties. The variability within one specific site (i.e., 4 to 30 loggers) was found to be in the same range as the variability in-between the different sites.

Given the high impact of topography and other (sub-)surface properties on the GST, a direct match-up between the 1 km x 1 km grid cell of the Permafrost_cci GTD product and single point locations is inapplicable. Therefore, we computed the average MAGST of all available GST logger and compared it to the average of all Permafrost_cci GT grid cells located between 2500 and 3000 m a.s.l.

2.2.4 Satellite derived Freeze/Thaw Surface Status GT Evaluation Dataset Generation

The Freeze-Thaw to Temperature (FT2T) model is an empirical model, based on a linear regression analysis between the annual sum of frozen days, measured with microwave EO sensors, and in situ ground temperature measurements (Kroisleitner et al., 2018). It was initially developed for temperature retrieval at the coldest sensor depth spanning the years 2007-2013 available from Paulik et al. (2014). The method by Naeimi et al. (2012) which forms the basis for the 2007-2013 record of Paulik et al. (2014) has been applied to further records, extending the dataset to 2018. The method and set parameters were evaluated by in situ records and C-band SAR data (Sentinel-1; Bergstedt et al. 2020b). A Metop ASCAT global gridded dataset available from EUMETSAT (SOMO12) has been used for this purpose. FT2T has been further developed for Permafrost_cci to represent the depths of the CRDPv2 and calendar years. With respect to in situ data availability for the model calibration, only 1 m depth can be considered. Further improvements have been made regarding bias correction for lake fraction using Sentinel-1 (Bergstedt et al., 2020a). These apply to lake rich regions. Records have been extracted for selected borehole locations of the match-up dataset for site comparisons and for regions in addition to the circumpolar comparison presented in [RD-8,9].

2.3 ASSESSMENT OF ACTIVE LAYER THICKNESS

2.3.1 Active Layer Thickness Reference Data

Same as for permafrost temperature, the major data provider for ALT time series is the WMO/GCOS Global Terrestrial Network for Permafrost GTN-P, the global permafrost monitoring programme of the International Permafrost Association IPA. The comprehensive, continuously updated GTN-P data collection of ALT time series is available for download under the Circum-Polar Active Layer Monitoring Network, https://www2.gwu.edu/~calm/. [RD-5] describes the CALM measurement program and our data compilation steps in detail. For an in situ estimation of ALT, it is relevant to measure active layer depths at the end of the active-layer thawing season in late summer. This maximum thaw depth measured in late summer represents the ALT of a specific year. Figure 2.6 shows an overview on the CALM measurement network of the Northern hemisphere including the measurement sites in Mongolia, central Asia and in China on the Tibetan plateau and in the Alps in Europe.

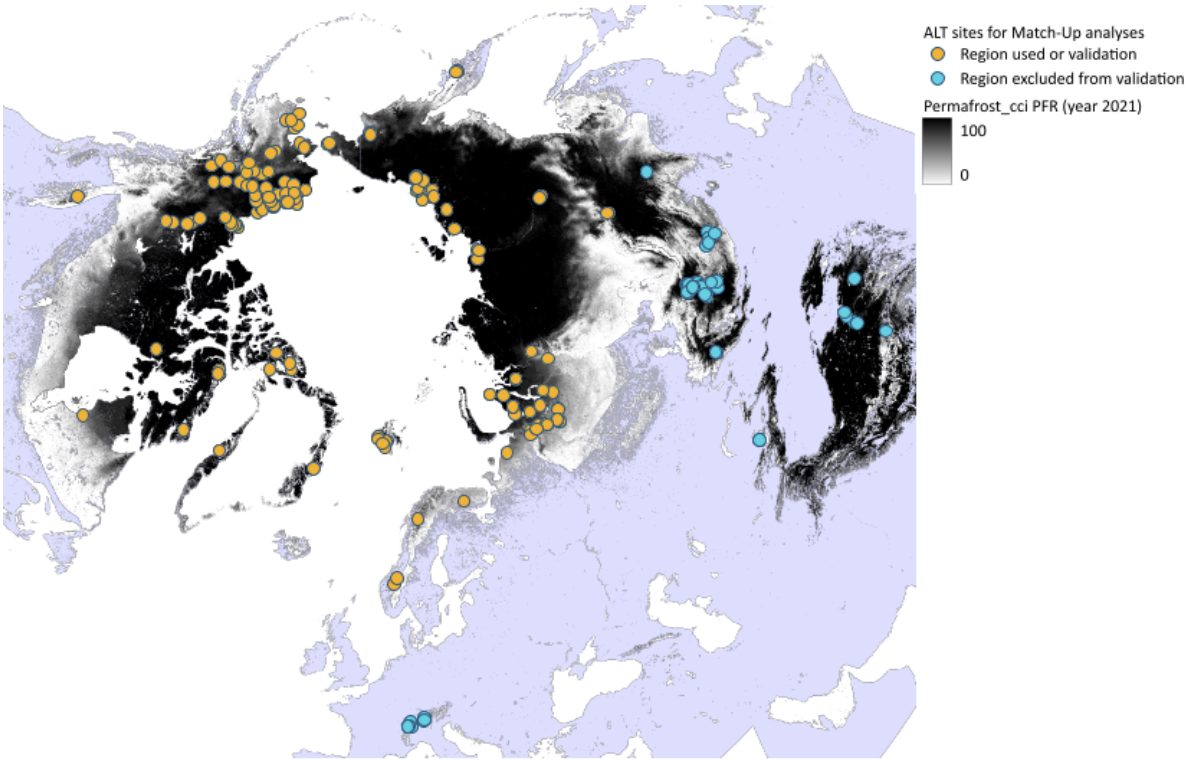

Figure 2.6. Northern hemisphere Permafrost_cci PFR permafrost probability and in situ sites (yellow symbols) of active layer thickness ALT (GTN-P CALM programme and RAS ALD data). Sites with blue dots (Central Asia, Alps) are analysed separately.

Versions of ALT and Match-up Datasets

ALT match-up dataset v1 (2003 to 2017) (Validation in phase I, CRDPv0 2019)

standardised annual ALT time series from 2003 and 2017 with a circum-Arctic geographic coverage. The collection contained data from 207 sites (China + Mongolia: 67, Greenland + Svalbard + Scandes: 11, Canada: 6, Russia: 57, USA: 207), with 1,835 match-up pairs.

ALT match-up dataset v2 (1997 to 2018) (Validation in phase I, CRDPv1 2020)

standardised annual ALT time series from 1997 and 2018 with a circum-Arctic geographic coverage. The collection was updated with ALT measurements from the GTN-P CALM program and contained data from 156 sites. Please note that we excluded all sites in Mongolia, Central Asia, and on the Tibetan Plateau (China). Please also note that we excluded in the validation v2 also all sites within the Siberian Yedoma area (Bryant et al., 2017) due to incorrect parameterisation of Permafrost_cci CryoGrid of the Yedoma stratigraphy.

ALT match-up dataset v3 (1997 to 2019) (Validation in phase I, CRDPv2 2021)

standardised annual ALT time series from 1997 to 2019 with a circum-Arctic geographic coverage. The collection was updated with ALT measurements from the GTN-P CALM program, included the Yedoma regions and therefore, contained considerably more data, from 314 sites. Please note that we still excluded all sites in Mongolia, Central Asia, and China.

ALT match-up dataset v4 (1997 to 2021) (Validation in phase II, CRDPv3 2023)

standardised annual ALT time series from 1997 and 2021 with a circum-Arctic geographic coverage. The collection was updated with ALT measurements from the GTN-P CALM program. Please note that we still exclude all sites in Mongolia, Central Asia, and China. We experimentally included Russian ALD sites (Bartsch, oral communication, 2020), which are also included for PFR analyses. As these however do not provide the maximum thaw depth, the deviations to the model are higher. The overall influence on the validation is yet not high, as these sites comprise only one year of measurements (2018).

2.3.2 Characteristics of ALT Match-up Dataset

The ALT match-up v4 dataset (2024) contains standardised in situ ALT matched with *CRDPv3* Permafrost_cci ALT. Figure 2.7 shows the frequency distribution of the match-up data. In situ ALT can, by definition, only occur within permafrost. Therefore, the characteristics of the ALT Permafrost_cci and ALT in situ data collections represent all data sampled in permafrost zones. The characteristics of Permafrost_cci ALT show an unimodal right-skewed distribution with a maximum around 40 cm ALT. Both Permafrost_cci ALT and in situ ALT show highest abundance in shallow ALT values.

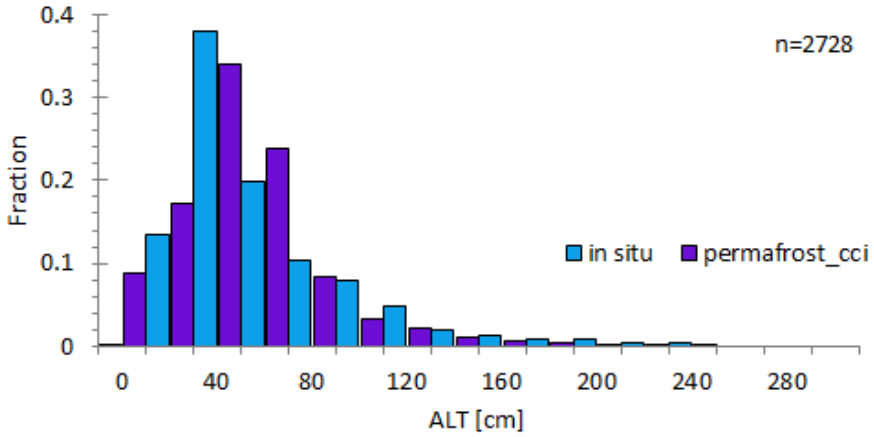

Figure 2.7. Frequency distribution of Permafrost_cci ALT and in situ ALT from GTN-P CALM and RAS (sites in China, Mongolia and the Swiss Mountains are excluded).

2.4 ASSESSMENT OF PERMAFROST EXTENT

2.4.1 Permafrost Fraction Reference Data

In Perrmafrost_cci we approximate permafrost abundance with the GTD and ALT reference datasets. Within the first validation round v1 of Permafrost_cci CRDPv0 PFR we applied a binary match-up assessment. We allowed a small variability around MAGT 0 °C not setting "permafrost" strictly as in situ MAGT < 0 °C in 2 consecutive years. This approach in [RD-8] was successful and we applied it more in depth for the assessments of Permafrost_cci CRDPv1 and CRDPv2 PFR adding the ALT time series [RD-9,2] .

PFR match-up dataset v1 (2003 to 2017) (Validation in phase I, CRDPv0 2019)

- Permafrost_cci PFR per site and year in 0, 20, 40, 60, 80 or 100 % Permafrost
- Binary PFR dataset compiled from GTDv1: Permafrost abundance:
- Yes if all measurements in depths (0 – 2 m) MAGT ≤ 0.5 °C.
- Criteria permafrost abundance yes / no

PFR match-up dataset v2 (1997 to 2018) (Validation in phase I, CRDPv1 2020)

- Permafrost_cci PFR per site and year in 0, 14, 29, 43, 57, 71 or 100 % Permafrost
- Binary PFR dataset compiled from GTDv2, ALTv2
- ALD from Russian expeditions (Bartsch, oral communication, 2020)
- Yes if any measurements in depths (0 – 2.4 m) MAGT ≤ 0.5 °C and Yes to all ALT < 300 cm
- Criteria permafrost abundance yes / no

PFR match-up dataset v3 (1997 to 2019) (Validation in phase I, CRDPv2 2021)

- Permafrost_cci PFR per site and year in 0, 14, 29, 43, 57, 71 or 100 % Permafrost
- Binary PFR dataset compiled from GTDv3, ALTv3
- ALD from Russian expeditions (Bartsch, oral communication, 2020)
- Yes if any measurements in depths (0 – 2.4 m) MAGT ≤ 0.5 °C and Yes to all ALT < 300 cm
- Criteria permafrost abundance yes / no

PFR match-up dataset v4 (1997 to 2021) (Validation in phase II, CRDPv3 2023)

- Permafrost_cci PFR per site and year in 0, 14, 29, 43, 57, 71 or 100 % Permafrost
- Binary PFR dataset compiled from GTDv4, ALTv4
- (case 1: Permafrost=No PFR <=14 %, case 2: Permafrost=No PFR 29 %)
- ALD from Russian expeditions (Bartsch, oral communication, 2020)
- Yes if any measurements in depths (0 – 3 m) MAGT ≤ 0.5 °C and Yes to all ALT < 300 cm
- Criteria permafrost abundance yes / no

2.4.2 PERMOS Reference PFR Data Generation

The best visual expression of mountain permafrost is represented by rock glaciers, which, in contrast to the sub-ground permafrost itself, can be mapped and monitored directly using remotely sensed data. Rock glaciers are debris landforms generated by the former or current creep of frozen ground (permafrost), detectable in the landscape with the following morphologies: front, lateral margins and optionally ridge-and-furrow surface topography (RGIK 2023). Their abundance can be used as validation for the high permafrost probability extent. The information on rock glacier abundance and extent was computed within the GlobPermafrost program in the Bas-Valais region (Figure 2.8) and within the CCI Permafrost phase I in 12 regions worldwide (Figure 2.9). These inventories were compared with the Permafrost_cci PFR product.

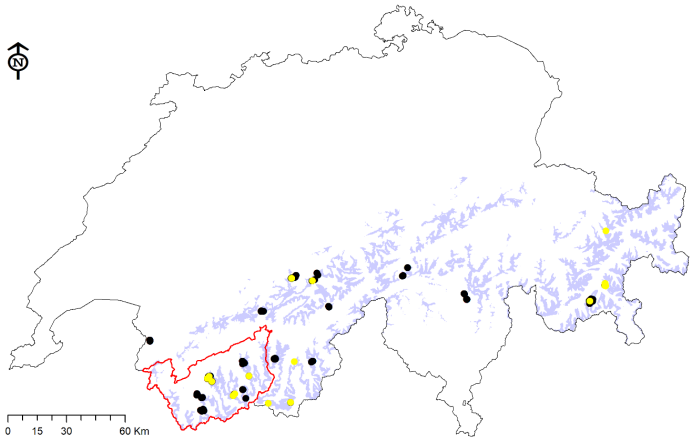

Figure 2.8. Location of the 247 GST logger (black circles), 27 GT boreholes (yellow circles) and the extent of the ESA GlobPermafrost rock glacier inventory (red outline) used for the validation of the Permafrost_cci GTD and Permafrost_cci PFR products in the Swiss Alps. The bluish color-coded zones represent the areas located between 2500 m and 3000 m a.s.l.

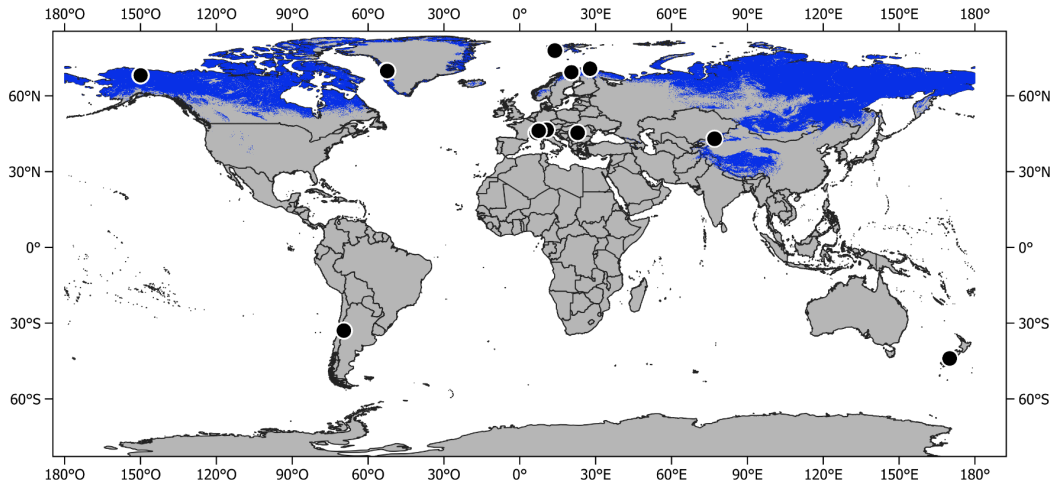

Figure 2.9. Location of the 12 rock glacier inventories compiled within Permafrost CCI phase I (black dots, see RD-10). The blue color-coded areas represent the simulated Permafrost_cci PFR in 2021.

3 ASSESSMENT RESULTS: PERMAFROST TEMPERATURE

3.1 PERMAFROST TEMPERATURE USER REQUIREMENTS

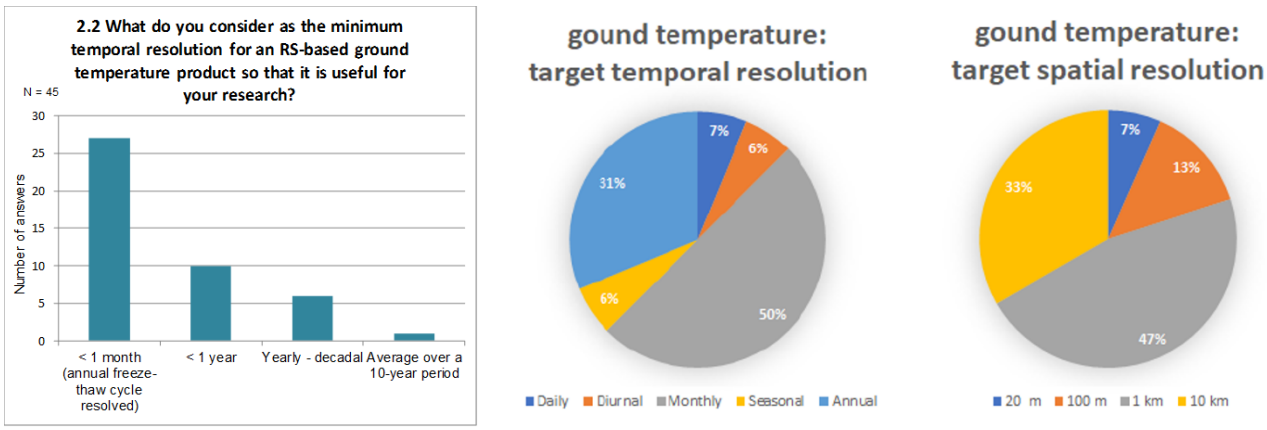

Figure 3.1a,b. User Survey results. Left: ESA DUE GlobPermafrost User Survey results, question 2.2 [RD-7]. Right: ESA CCI Permafrost User Survey results, Figure 3 [RD-7].

Users of potential products of permafrost temperature are interested in high temporal resolution: monthly or higher as documented in [RD-7]. However, 30 % of users also rated annual resolution as adequate as target temporal resolution in [RD-7]. Half of the user group are satisfied with a target spatial resolution of 1 km. The first release of the Permafrost_cci CRDPv0 GTD provided annual resolution with 1×1 km spatial resolution over a range of depths (0, 1, 2, 5, 10 m) from 2003 to 2017, Permafrost_cci CRDPv1,2,3 GTD provide annual resolution with 1×1 km spatial resolution over the same range of depths (0, 1, 2, 5, 10 m) but covering a longer time spans from 1997 to 2018, 1997 to 2019, and 1997 to 2021, respectively.

3.2 PERMAFROST_CCI GTD MATCH-UP ANALYSES WITH IN SITU DATA

The match-up was performed for Permafrost_cci GTD versus in situ MAGT and a focus on the entire data collection as well as on a subset of measurements in the cold temperature only that more closely represents the permafrost (in situ MAGT < 1 °C). For each in situ point location and year, the pixel value in the Permafrost_cci products closest to the in situ measurement was extracted to compile the match-up dataset and calculate summary statistics.

For further in depth analyses, we extracted the residuals of the match-up pairs from the bulk regression line (residual = Permafrost_cci GTD - (0.8342 x in_situ_MAGT - 0.567), see Figure 3.2) and calculate summary statistics of the bulk dataset as well as the temperature related subsets. Furthermore, we used spatial visualisations to illustrate potential geographic biases in residuals.

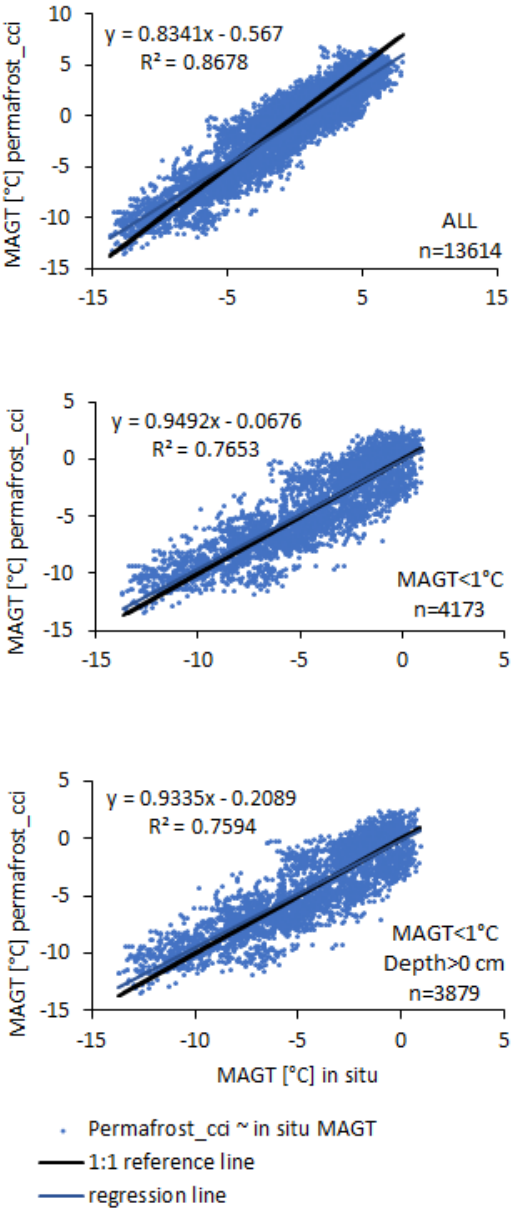

	all	<1°C	<1°C & >0 cm	≥1°C
bias				
mean±SD	-0.73 ± 1.55	0.15 ± 1.78	0.08 ± 1.77	-1.11 ± 1.25
median	-0.89	0.38	0.32	-1.17
0.05	-3.00	-2.88	-2.92	-3.05
0.95	2.05	2.84	2.75	1.01
MAD	1.03	1.23	1.23	0.80
RMSE	1.71	1.78	1.77	1.68
abs_bias				
mean±SD	1.42 ± 0.96	1.46 ± 1.02	1.45 ± 1.02	1.40 ± 0.93
median	1.28	1.27	1.26	1.28
0.05	0.14	0.15	0.15	0.14
0.95	3.16	3.38	3.36	3.08
MAD	0.68	0.69	0.69	0.67

Figure 3.2. Regression of Permafrost_cci GTD versus in situ MAGT in all discrete depths and across all years for all sites (upper panel) and for MAGT < 1 °C only (middle panel) and for MAGT < 1 °C with only depth > 0 cm (lower panel). Summary statistics of Permafrost_cci GTD versus in situ MAGT in all discrete depths are given for the entire dataset and the temperature related subsets. SD=standard deviation, MAD=median absolute deviation, RMSE=root mean square error.

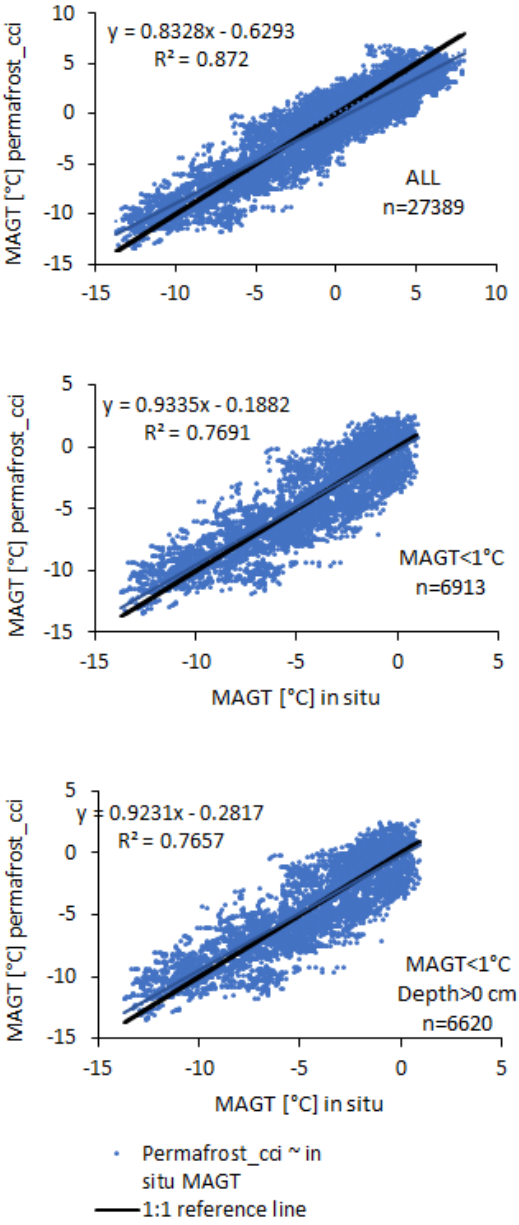

	all	<1°C	<1°C & >0 cm	≥1°C
bias				
mean±SD	-0.87 ± 1.49	0.11 ± 1.78	0.06 ± 1.78	-1.19 ± 1.22
0.05	-3.06	-2.93	-2.96	-3.10
0.95	1.86	2.77	2.71	0.87
median	-1.04	0.36	0.33	-1.25
MAD	0.95	1.28	1.28	0.78
RMSE	1.73	1.79	1.78	1.71
abs_bias				
mean±SD	1.44 ± 0.95	1.48 ± 1.00	1.47 ± 1.00	1.43 ± 0.93
0.05	0.15	0.16	0.16	0.15
0.95	3.18	3.35	3.34	3.11
median	1.32	1.31	1.31	1.32
MAD	0.68	0.69	0.69	0.67

*Figure 3.3. Regression of Permafrost_cci GTD versus in situ MAGT in all discrete depths and across all years for all sites (upper panel) and for permafrost sites only (lower panel), calculated with **in situ MAGT** data **interpolated through depth**. Summary statistics of Permafrost_cci GTD versus in situ MAGT in all discrete depths are given for the entire dataset and the temperature related subsets.*

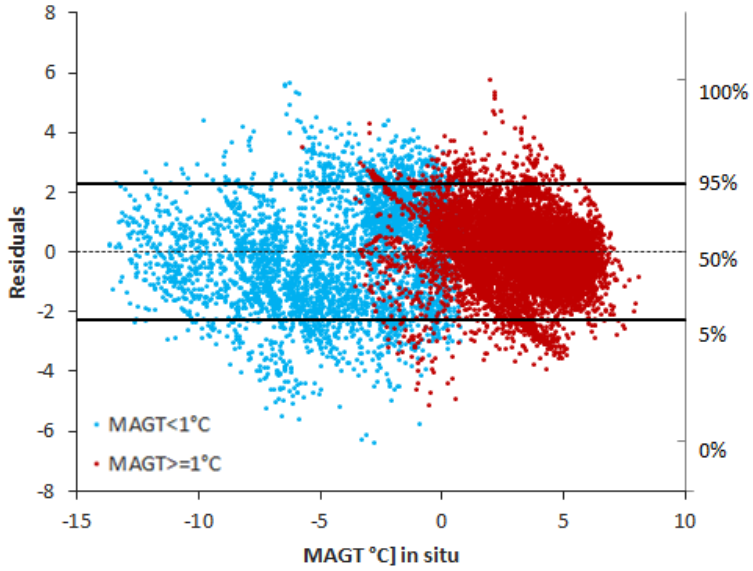

	all	<1°C	≥1°C
100%	5.78	5.68	5.78
95%	2.31	2.72	1.90
50%	0.03	0.16	0.01
5%	-2.29	-2.88	-1.85
0%	-6.34	-6.34	-5.13

Figure 3.4. Residuals of Permafrost_cci GTD and in situ MAGT match-up (blue = sites with MAGT < 1 °C, red = sites with MAGT > 1 °C,) with summary statistics for the entire dataset and the temperature related subsets.

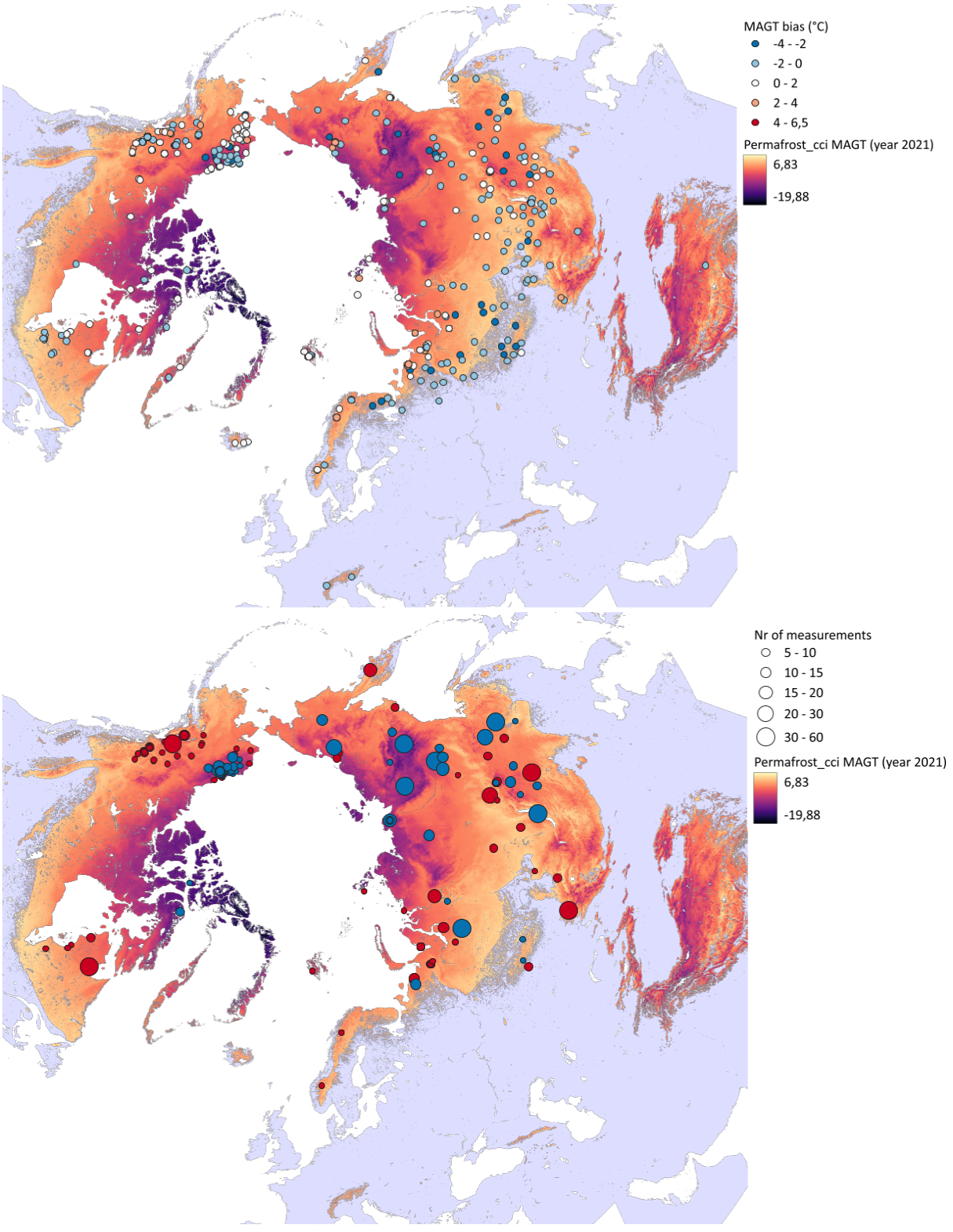

Figure 3.5a Bias (upper panel) and location of residuals > 95% quantile (red) and < 5% quantile (blue) over mapped Permafrost_cci GTD (2 m). The size of the circle represents the number of samples with specific residuals at the particular location.

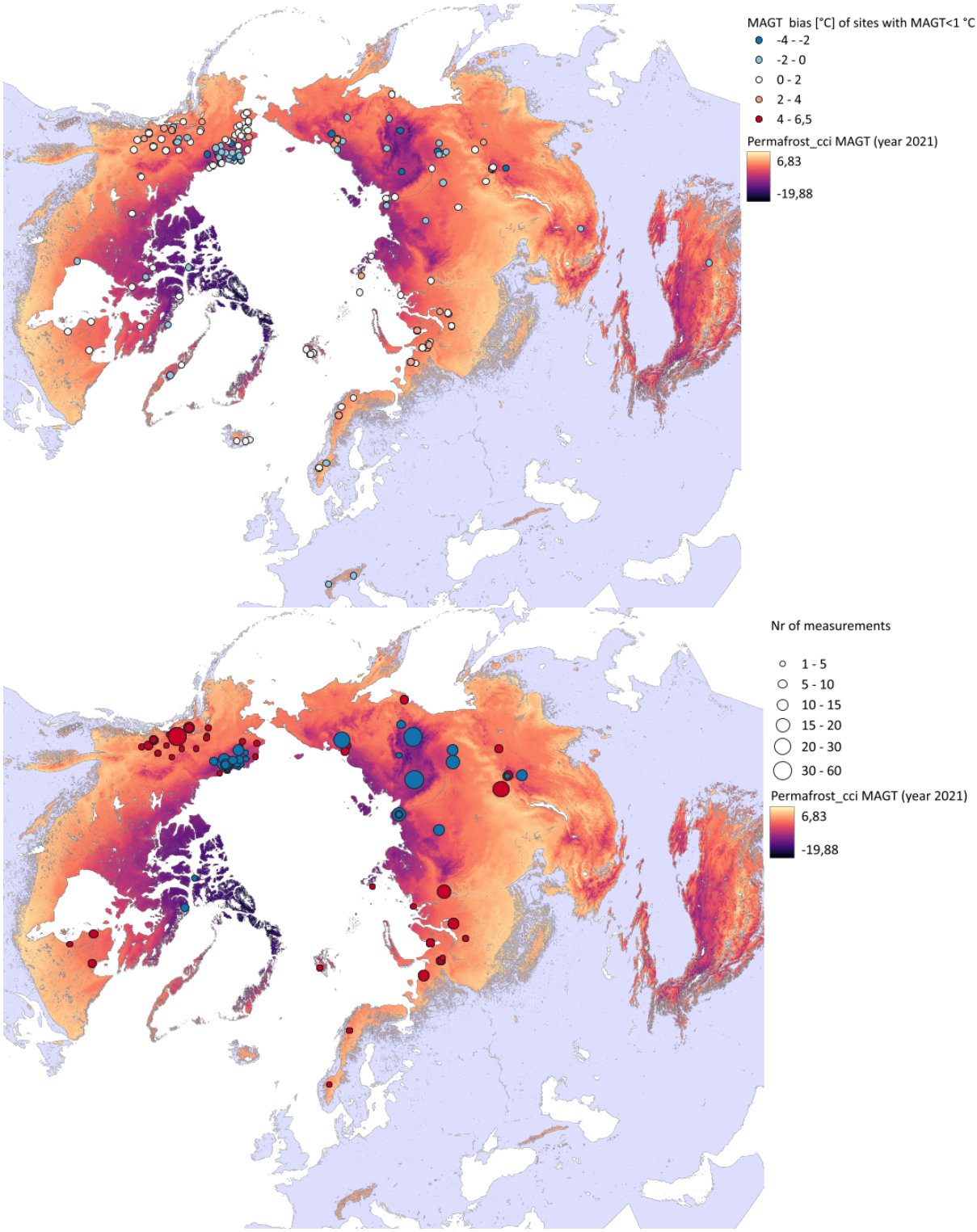

*Figure 3.5b Bias (upper panel) and location of residuals > 95% quantile (red) and < 5% quantile (blue) for the in situ **MAGT < 1 °C subset** of sites over mapped Permafrost_cci GTD (2 m). The color of circles represents the temperature subset and size of the circle represents the number of samples with specific residuals at the particular location.*

Table 3.1: GTD bias over sampling depths and temperature subsets for original depths and interpolated ground temperature across depths.

original data						
Depth	**ALL**	**#**	**<1°C**	**#**	**≥1°C**	**#**
0	0.48	709	1.04	294	0.08	415
10	-0.53	95	-0.29	52	-0.83	43
20	-0.84	1851	-0.04	278	-0.98	1573
25	-0.34	475	-0.30	399	-0.53	76
40	-0.91	1733	0.07	272	-1.09	1461
50	-0.23	483	-0.15	415	-0.67	68
60	-0.65	20	-0.77	18	0.42	2
75	-0.52	383	-0.45	332	-1.00	51
80	-1.11	1692	-0.22	229	-1.25	1463
100	-0.21	308	0.00	247	-1.08	61
120	-1.20	878	-0.46	95	-1.29	783
150	-0.32	67	0.64	35	-1.37	32
160	-1.34	1657	-1.24	148	-1.35	1509
200	0.60	192	0.75	128	0.32	64
240	-1.28	591	-1.67	13	-1.27	578
250	0.31	50	0.55	40	-0.64	10
300	0.71	282	0.68	222	0.84	60
320	-1.46	1138	-0.45	70	-1.52	1068
400	0.65	141	0.78	89	0.41	52
500	0.70	276	0.68	228	0.78	48
1000	0.81	592	0.84	569	0.18	23

interpolated data						
	ALL	**#**	**<1°C**	**#**	**≥1°C**	**#**
0	0.48	709	1.04	294	0.08	415
10	-0.06	158	0.39	98	-0.80	60
20	-0.81	1909	0.04	311	-0.98	1598
25	-0.78	2068	-0.18	622	-1.03	1446
40	-0.80	2169	-0.15	647	-1.07	1522
50	-0.84	1991	-0.14	601	-1.14	1390
60	-0.94	1891	-0.28	530	-1.19	1361
75	-1.01	1891	-0.33	518	-1.27	1373
80	-1.00	1958	-0.15	450	-1.25	1508
100	-0.95	1110	-0.08	326	-1.31	784
120	-1.20	878	-0.46	95	-1.29	783
150	-1.20	886	-0.56	104	-1.29	782
160	-1.29	1742	-0.90	181	-1.34	1561
200	-1.07	1410	0.50	176	-1.30	1234
240	-1.10	1405	0.45	174	-1.32	1231
250	-1.14	1252	0.46	184	-1.42	1068
300	-1.03	1368	0.46	284	-1.42	1084
320	-1.05	1407	0.42	271	-1.41	1136
400	0.73	287	0.81	219	0.45	68
500	0.74	308	0.73	260	0.78	48
1000	0.81	592	0.84	569	0.18	23

Permafrost_cci GTD and in situ MAGT consensus in temporal trends

Table 3.2. Gleichläufigkeit (glk) and temporal stability (ts) per year for all sites, and the subsets MAGT < 1 °C and MAGT > 1 °C.

	all			MAGT<1°C			MAGT≥1°C		
Year	**glk**	**ts**	**#**	**glk**	**ts**	**#**	**glk**	**ts**	**#**
1998	0.65	0.23	564	0.60	0.27	62	0.66	0.23	502
1999	0.69	-0.10	591	0.70	-0.23	76	0.69	-0.08	515
2000	0.63	-0.27	614	0.62	-0.19	80	0.63	-0.28	534
2001	0.73	0.12	608	0.71	-0.05	90	0.73	0.14	518
2002	0.75	0.03	628	0.77	0.28	112	0.74	-0.01	516
2003	0.76	0.09	630	0.65	-0.03	112	0.78	0.11	518
2004	0.69	-0.20	672	0.54	0.09	126	0.71	-0.25	546
2005	0.67	-0.06	679	0.59	-0.40	150	0.68	0.01	529
2006	0.70	0.00	727	0.62	-0.49	179	0.72	0.13	548
2007	0.85	0.02	853	0.70	-0.10	259	0.90	0.06	594
2008	0.64	-0.15	887	0.54	-0.15	299	0.68	-0.15	588
2009	0.65	0.11	943	0.71	0.17	332	0.62	0.08	611
2010	0.71	0.00	946	0.66	0.09	335	0.73	-0.04	611
2011	0.70	0.05	962	0.64	0.10	351	0.74	0.03	611
2012	0.74	-0.09	785	0.77	-0.18	335	0.72	-0.04	450
2013	0.63	-0.14	468	0.67	-0.33	275	0.58	0.10	193
2014	0.74	0.09	475	0.81	0.07	284	0.66	0.11	191
2015	0.62	-0.13	414	0.61	-0.10	245	0.64	-0.17	169
2016	0.74	0.31	198	0.70	0.47	128	0.81	0.00	70
2017	0.57	-0.15	189	0.41	-0.36	123	0.81	0.18	66
2018	0.58	0.29	136	0.45	0.38	83	0.79	0.13	53
2019	0.54	-0.52	42	0.53	-0.53	39	0.67	-0.42	3
2020	0.95	-0.45	26	0.94	-0.40	20	1.00	-0.70	6
2021	1.00	0.36	1	1.00	0.36	1			0
MEAN	**0.70**	**-0.01**		**0.66**	**-0.05**		**0.71**	**0.00**	0

Table 3.3. Summary statistics per site for Gleichläufigkeit (glk), temporal stability (ts) and absolute temporal stability (abs_ts)

	all		**MAGT<1°C**		**MAGT≥1°C**	
	glk	**ts**	**glk**	**ts**	**glk**	**ts**
mean±SD	0.68 ± 0.24	-0.04 ± 0.37	0.65 ± 0.34	-0.06 ± 0.43	0.72 ± 0.28	-0.01 ± 0.20
5%	0.25	-0.58	0.00	-0.73	0.00	-0.31
95%	1.00	0.41	1.00	0.45	1.00	0.21
median	0.70	-0.01	0.61	0.00	0.71	0.00

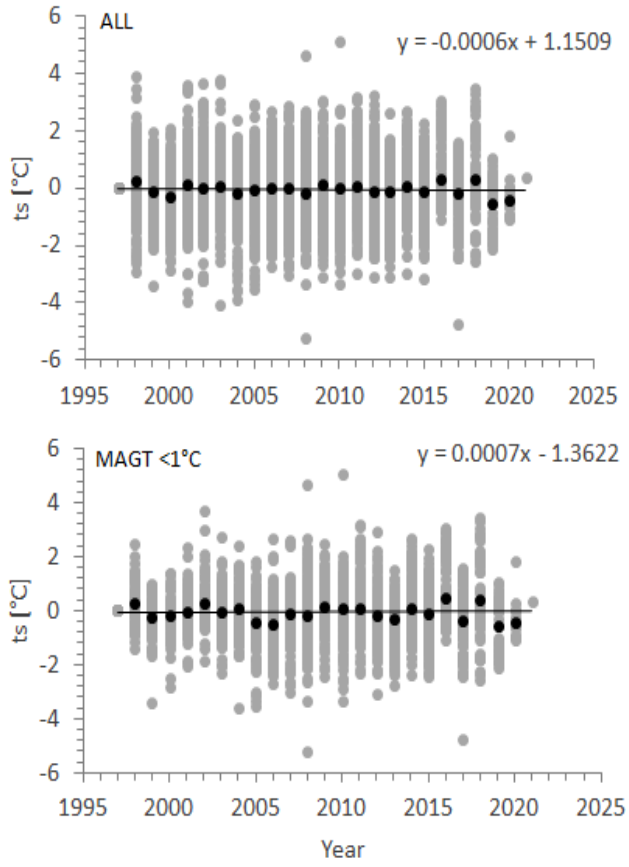

Figure 3.6. Temporal stability (ts, year-year change in magnitude of the bias) for the bulk Permafrost_cci GTD dataset. Black dots represent the mean values.

Regional Assessments

We characterise the Permafrost_cci GTD performance related to regions/countries with permafrost. These are Russia, United States of America, Canada, Greenland, Iceland, and Scandinavia.

Table 3.4. GTD match-up and summary (bias and absolute bias) and temporal statistics (glk and ts) for different countries/regions.

Region	#	bias	abs_bias	glk	ts
Russia	10347	-0.97	1.48	0.71	0.00
US	1359	-0.46	1.39	0.64	-0.12
Canada	1353	0.45	1.15	0.67	-0.01
Greenland	25	-0.29	0.85	0.83	-0.08
Iceland	25	0.81	0.81	0.63	0.01
Scandinavia (Sweden, Norway, Finland)	468	0.39	0.83	0.68	-0.01
Europe (Italy, France)	20	-0.24	0.63	0.54	0.70
China	10	-1.52	1.52	0.78	0.06
Mongolia	6	-0.04	0.10	0.50	0.04

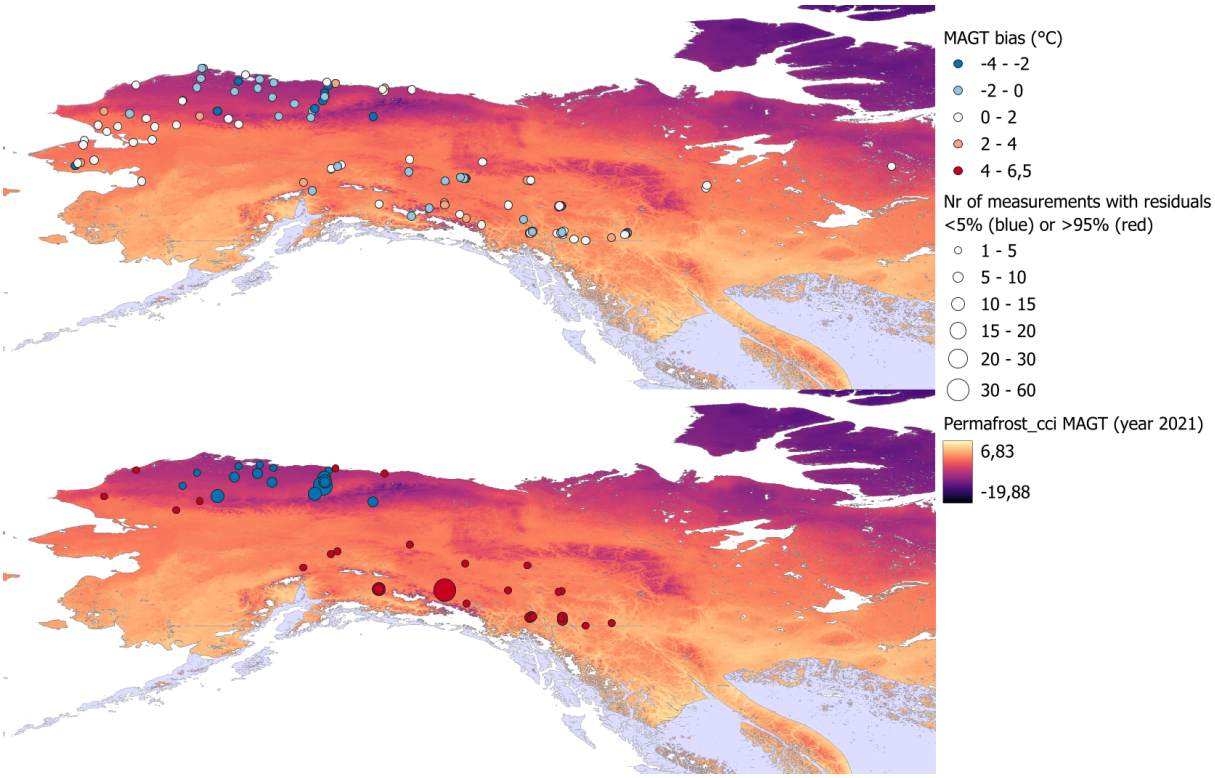

Figure 3.7. GTD Bias (upper panel) and residuals (lower panel) over mapped Permafrost_cci GTD 2021 (2 m) in North-western America.

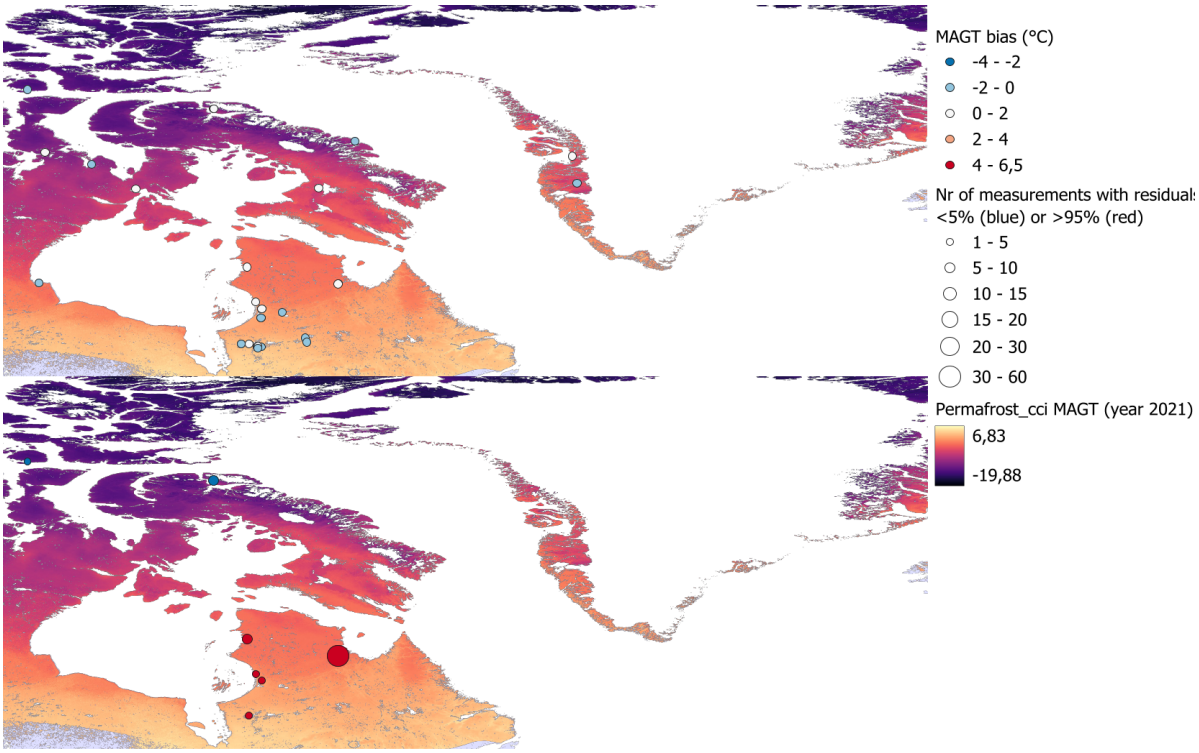

Figure 3.8. GTD Bias (upper panel) and residuals (lower panel) over mapped Permafrost_cci GTD 2021 (2 m) in north-eastern America and Greenland.

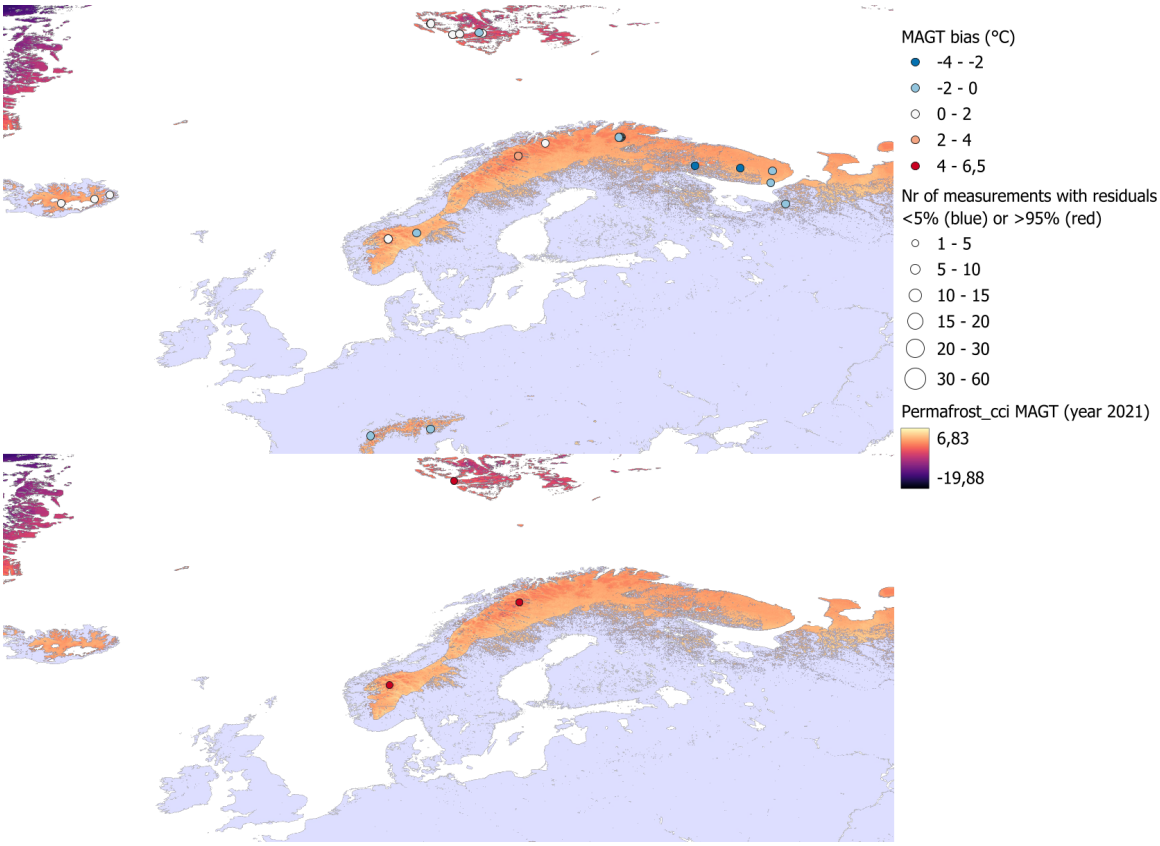

Figure 3.9. GTD Bias (upper panel) and residuals (lower panel) over mapped Permafrost_cci GTD 2021 (2 m) in northern Europe and the Alps (no high/low residuals and thus not shown in lower panel)

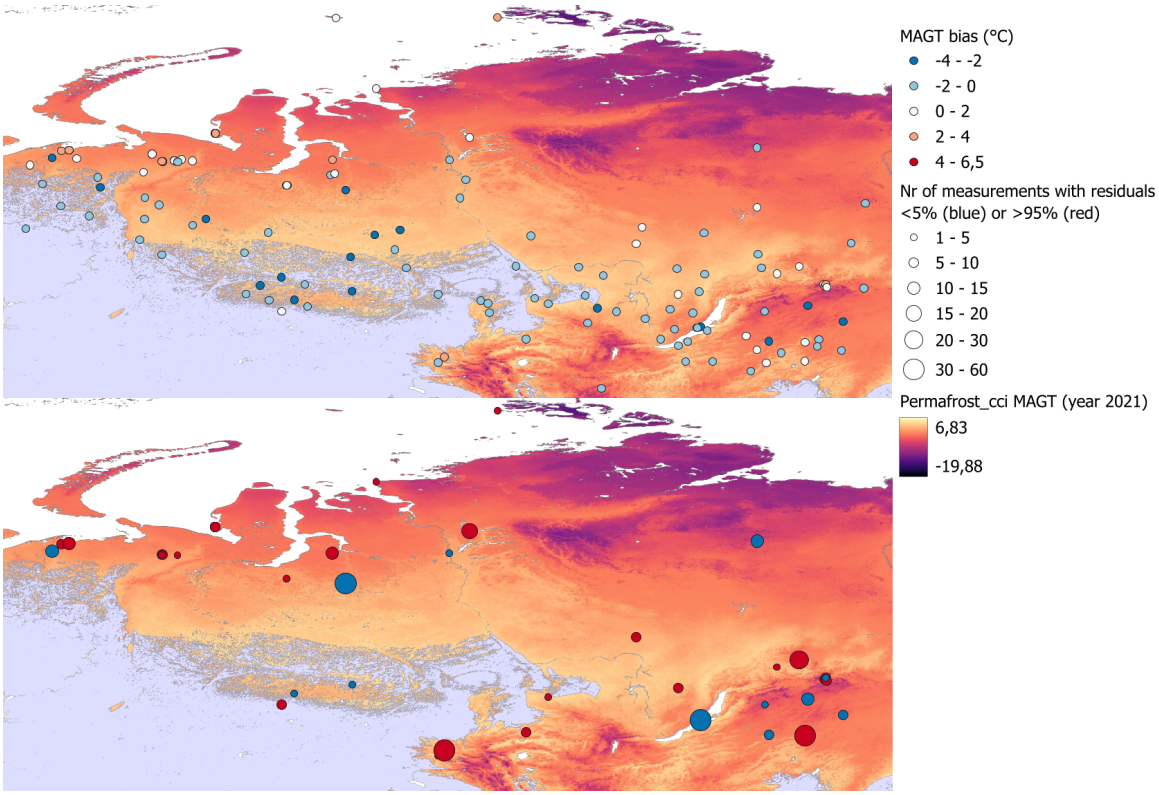

Figure 3.10. GTD Bias (upper panel) and residuals (lower panel) mapped Permafrost_cci GTD 2021 (2 m) in western Siberia.

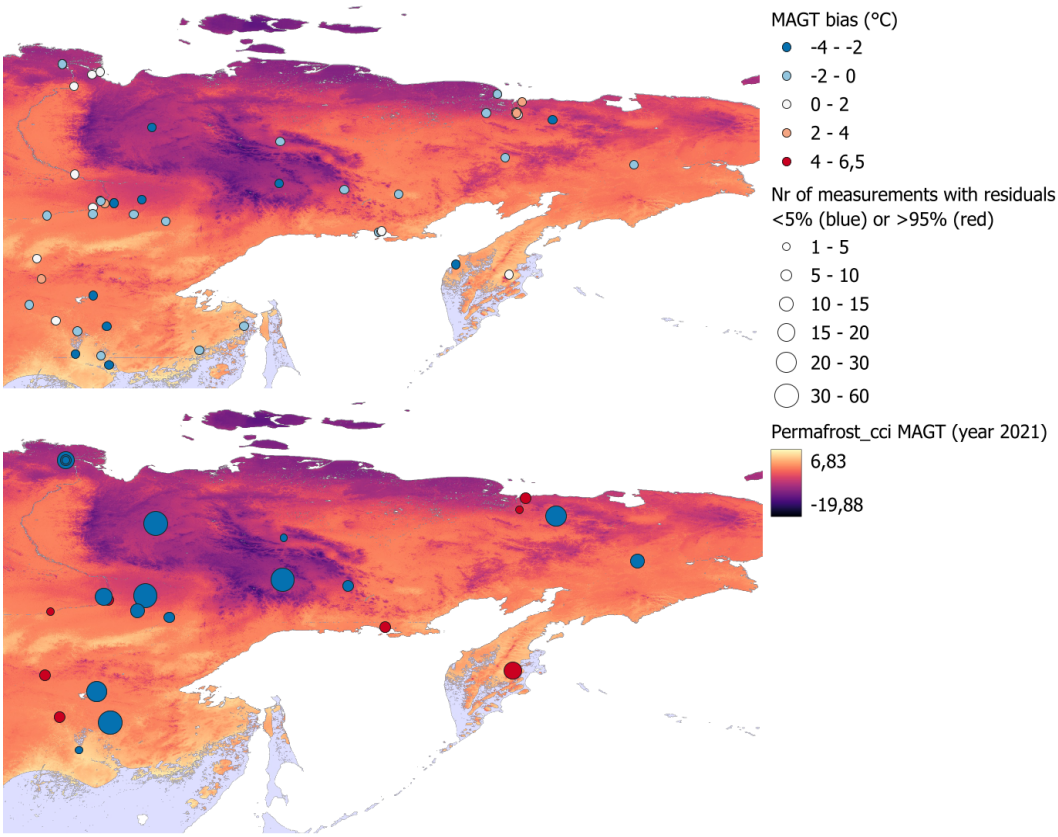

Figure 3.11 GTD Bias (upper panel) and residuals (lower panel) over mapped Permafrost_cci GTD 2021 (2 m) in eastern Siberia.

In summary, Permafrost_cci GTD (1997–2021) shows the following performance characteristics:

- overall, GTD shows a median bias of -0.89 °C (95% CI: -3.00 °C to 2.05 °C) and -1.04 °C (CI -3.06 °C to 1.86 °C) for the depth-interpolated bulk dataset.
- match-up pairs from in situ measurements with MAGT < 1 °C and thus from reliable permafrost sites show a better performance (**median bias of 0.38 °C, 95% CI: -2.88 to 2.84 °C**), compared to the bulk dataset and notably in comparison to warmer sites with MAGT >= 1 °C (median bias of -1.11 °C, 95% CI: -3.05 °C to 1.01 °C). For the depth-interpolated dataset, these account to a median of 0.36 °C (-2.93 °C to 2.77 °C) for the MAGT < 1 °C subset and -1.25 °C (-3.10 °C to 0.87 °C) for the warmer sites. For the MAGT < 1 °C subset without the surface temperature at 0 m the performance is even higher with a median bias of 0.38 °C and a mean bias of 0.08 °C only.
- GTD bias across depths is rather stable with a slightly larger negative mean bias in shallow depths (0 to- 3m), mainly caused by a negative bias in match-up pairs of the warmer sites (MAGT >= 1°C). The surface temperature GTD = 0 m shows the largest bias of the permafrost temperature subgroup, in contrast to all depths.
- the extreme residuals appear with < 5% quantile mainly in Northern Alaska and Eastern Siberia and with > 95% quantile mainly in Southern Alaska. Permafrost_cci GTD bias is mainly negative at the southern boundary zones in Siberia and Northern America. Regional assessments of GTD bias and temporal trends show a higher absolute bias in Russia, North America and in China (> 1 °C) for the bulk dataset. Temporal trends show no regional bias except for the two sites in the European Alps and one site in Mongolia.
- the trends over years generally match well between the in situ measurements and Permafrost_cci GTD, with a high gleichläufigkeit (glk>50%) and temporal stability (ts+/- 0.5 °C) in all years for the bulk dataset.

3.3 PERMAFROST_CCI GTD COMPARISON WITH PERMOS PERMAFROST TEMPERATURE

The comparison of the evolution of the mean in situ measured MAGST and Permafrost_cci GTD at 0 m over the Swiss Alps from 1997 to 2021 shows that Permafrost_cci GTD at 0 m has a slight cold bias of -0.27 °C compared to the in situ measurements. However, the warming tendency observed in the in situ measurements is well reproduced by the Permafrost_cci GTD product (Figure 3.12a) as well as the inter-annual variations. The standard deviation of the in situ measurements, although limited to 23 sites, is larger than the standard deviation of the Permafrost_cci GTD product at 0 m over the entire Swiss Alps between 2500 and 3000 m a.s.l. This is emphasised in Figure 3.12b which shows the measured MAGST for each single logger in the PERMOS network compared to the minimum and maximum Permafrost_cci GTD at 0 m depth in-between 2500 and 3000 m a.s.l. in the Swiss Alps. The measured in situ data ranges from around -4 °C to +7.5 °C, whereas Permafrost_cci GTD ranges from around -1 °C to +4.5 °C. Only few loggers exhibit MAGST values greater than the Permafrost_cci GTD, whereas many in situ measurements show lower MAGST.

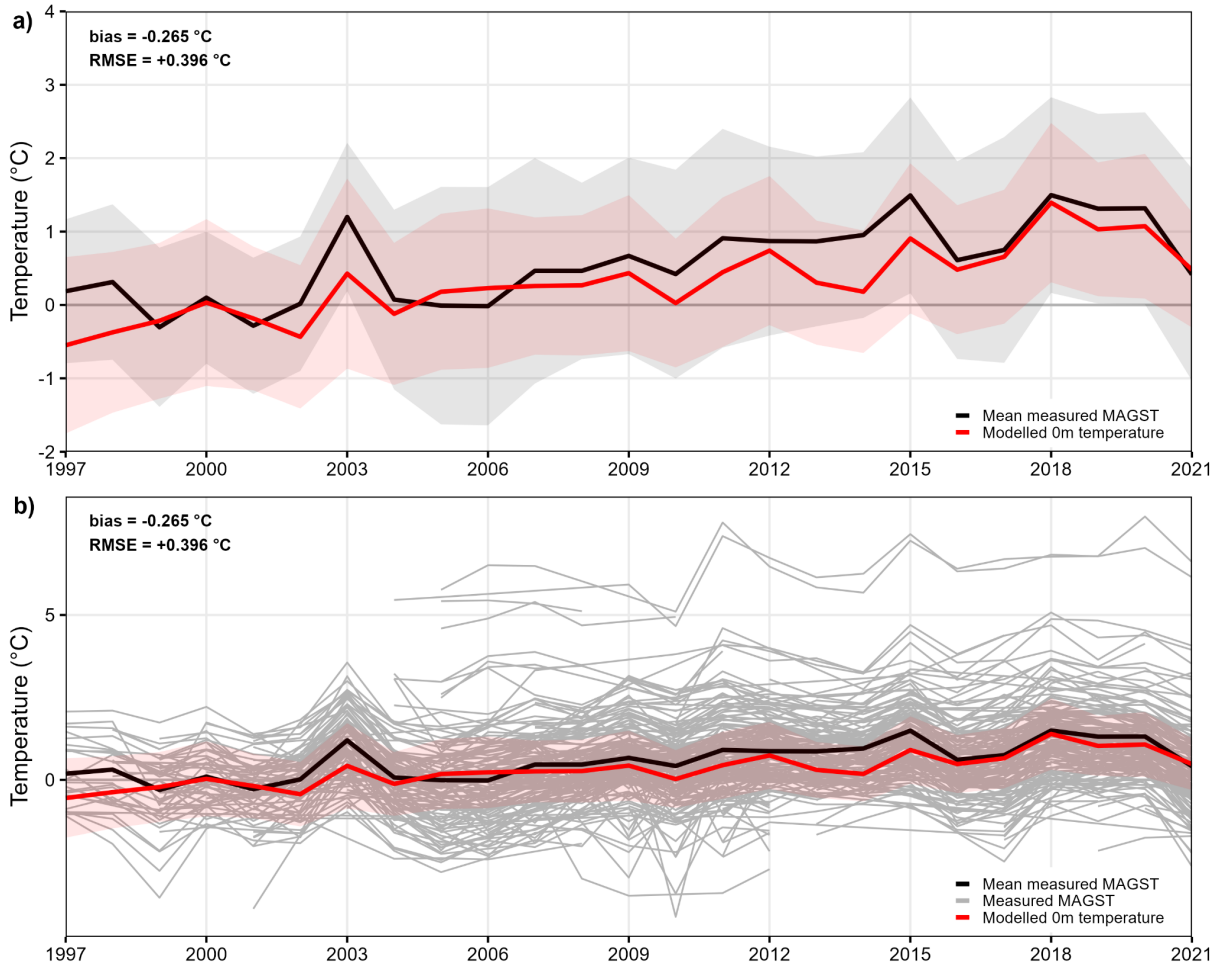

Figure 3.12. Temporal evolution of the mean in situ measured MAGST (black) in Switzerland (a) and measured MAGST at each logger (b) compared to the mean Permafrost_cci GTD at 0 m depth (red) over the entire Swiss Alps between 2500 and 3000 m a.s.l. The shaded area represents ± one standard deviation.

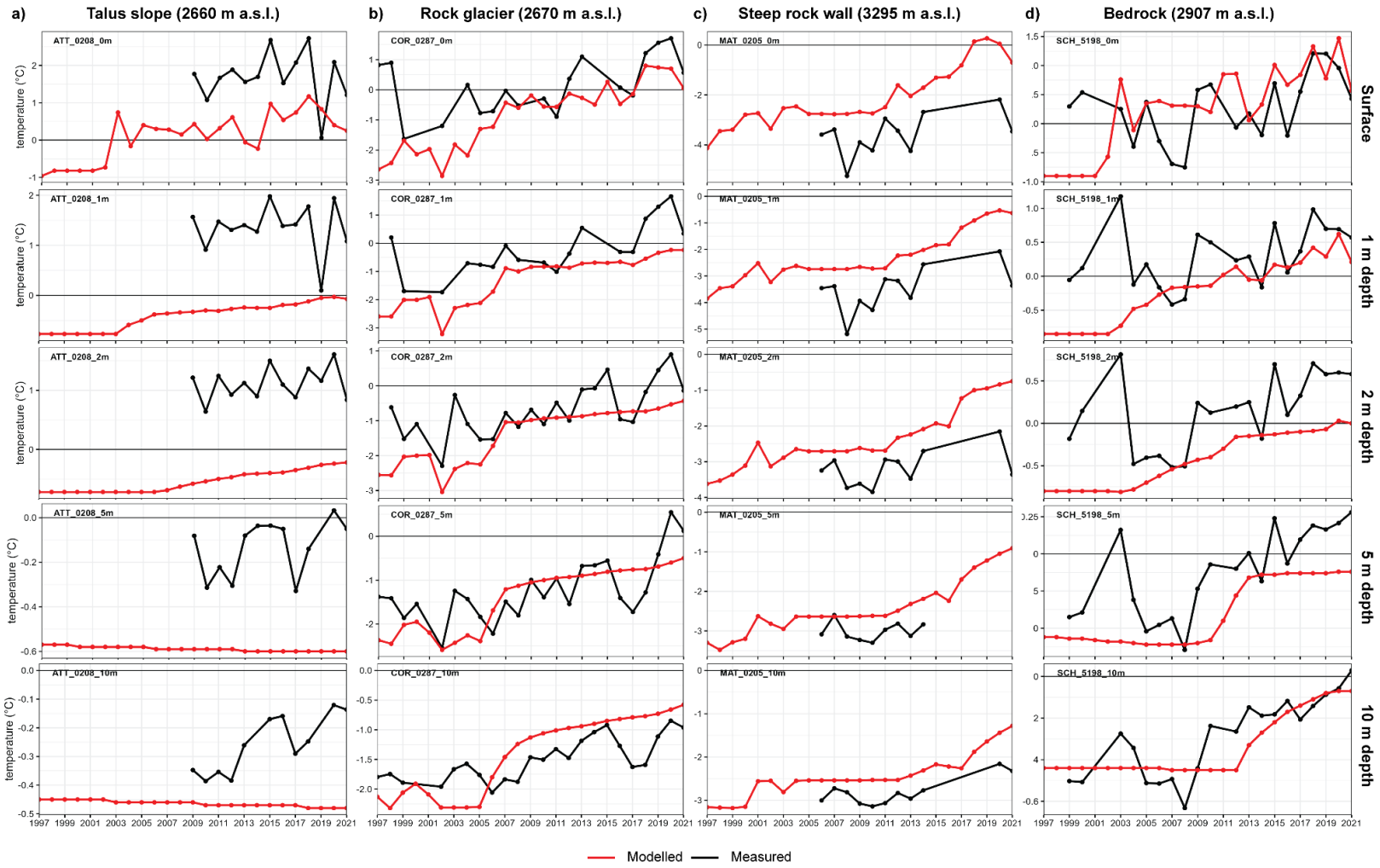

Figure 3.13. Comparison of simulated mean Permafrost_cci GTD (red) and in situ measured (black) MAGT at 0, 1, 2, 5 and 10 m depth at 4 sites in the Swiss Alps.

Comparing Permafrost_cci GTD at 0, 1, 2, 5 and 10 m depth to the in situ measured MAGT in boreholes (see Figure 3.13), there is no systematic bias of the Permafrost_cci GTD product. The best model fit is found at Murtèl and Schilthorn (Figure 3.13b and d) whereas a cold bias is found at Attelas (Figure 3.13a) and a warm bias exists at the Matterhorn (Figure 3.13c). Based on the data from the 13 PERMOS sites (not shown) Permafrost_cci GTD fit is independent from the landform type, elevation or regional site location. The simulated Permafrost_cci GTD values fit better the in situ observations near the surface (bias is +0.153°C at 0m and +0.106°C at 1m) than at depth (bias is +0.275°C at 10m, Figure 3.14).

Although the absolute values are different, both, the measured and the simulated MAGT, show a warming trend over the period 1997-2021. However, Permafrost_cci GTD fails to reproduce the inter-annual variability. At depth, all in situ measured MAGT in 2017 exhibit a more or less marked cooling effect. This is due to the extremely snow-poor winter 2016/17 in the Swiss Alps, which enabled the cold winter air temperature to cool more efficiently the ground (PERMOS 2019). This effect is not reproduced in Permafrost_cci GTD, illustrating the difficulty to include snow effects in global models.

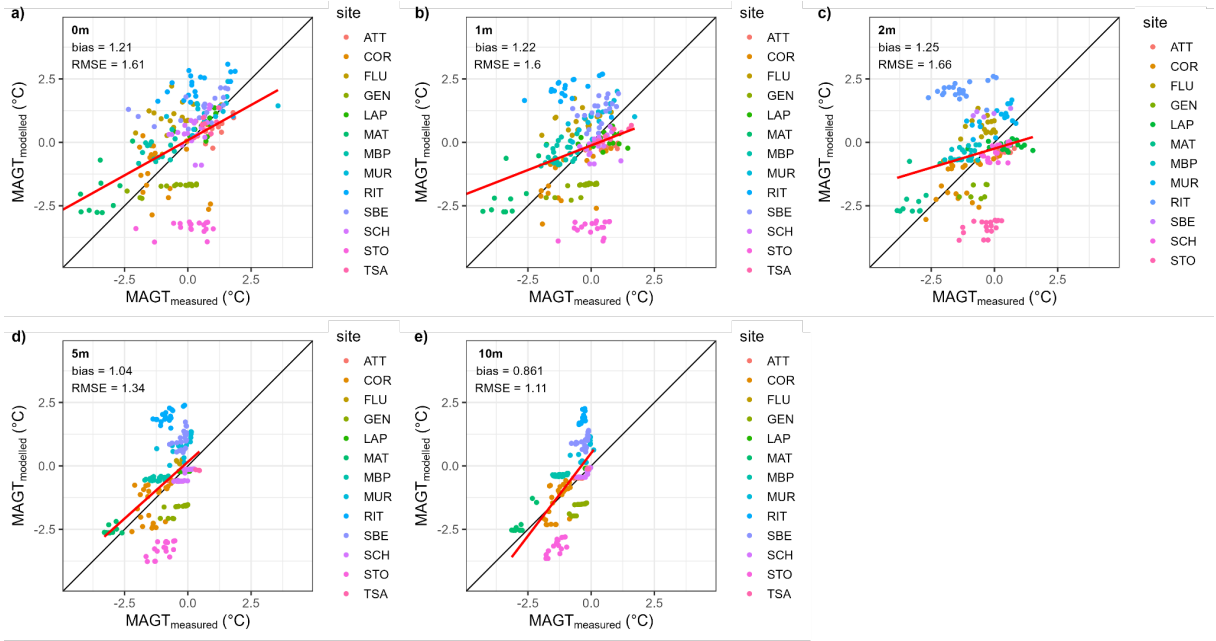

Figure 3.14. Comparison of simulated mean Permafrost_cci (y-axis) and in situ measured MAGT (x-axis) at the surface (a), 1m (b), 2m (c), 5m (d) and 10m depth (e). The black line represents the one-to-one relationship and the red one the best linear fit. Statistics are displayed for each depth.

3.4 PERMAFROST_CCI GTD COMPARISON WITH FT2T GT

A comparison of Permafrost_cci GTD at 0 and 2 m depth with FT2T derived ground temperatures for selected locations demonstrate the expected higher variability of surface state from year to year, but also agreement of the different data sources regarding temperature level (Figures 3.15 & 3.16). Deviations can be found for sites in the transition zone (temperatures around 0°C) in Alaska as well as Russia. FT2T results are closer to in situ records than CRDPv1 at Svetlyy in Central Siberia and Boza Creek, Alaska (Figures 3.17 and 3.18). Specifically, Svetlyy is an outlier location regarding permafrost extent evaluation. Results of CRDPv1 for Nadym, Western Siberia agree better with in situ then FT2T results. FT2T is too cold at this location. Here, the covered ASCAT footprint (appr. 12.5 km) contains a wide range of vegetation types (tundra shrubs to tall floodplain shrubs) and comparably wet soils. Either the Nadym borehole site is not representative for the footprint (but is for the 1km CRDv1 grid) or soil type/snow cover play an important role for heat transfer (insulation) which is not represented in the simple FT2T approach.

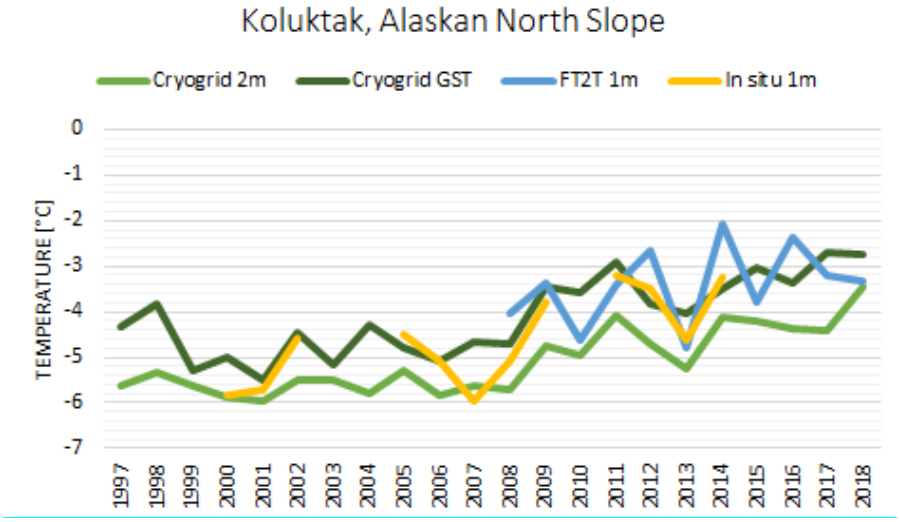

Figure 3.15. Comparison of FT2T product with CRDPv1 results and in situ data at Koluktak, Alaska.

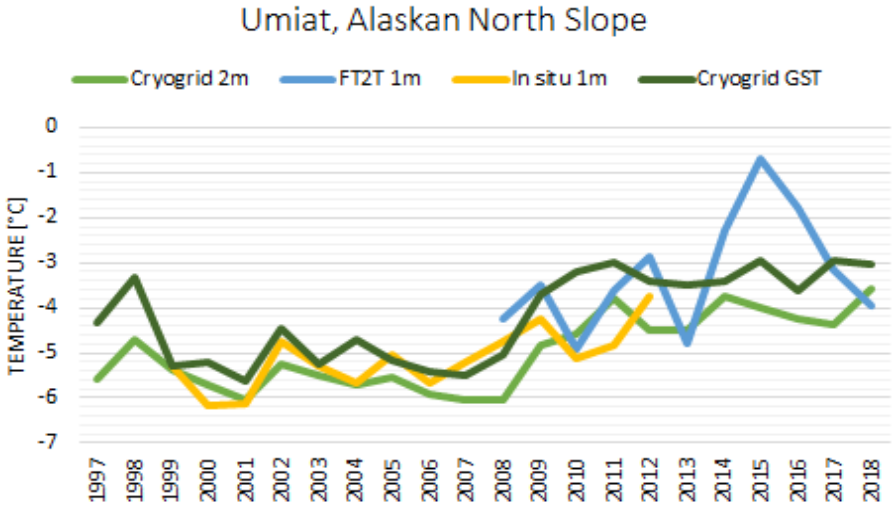

Figure 3.16. Comparison of FT2T product with CRDPv1 results and in situ data at Umiat, Alaska

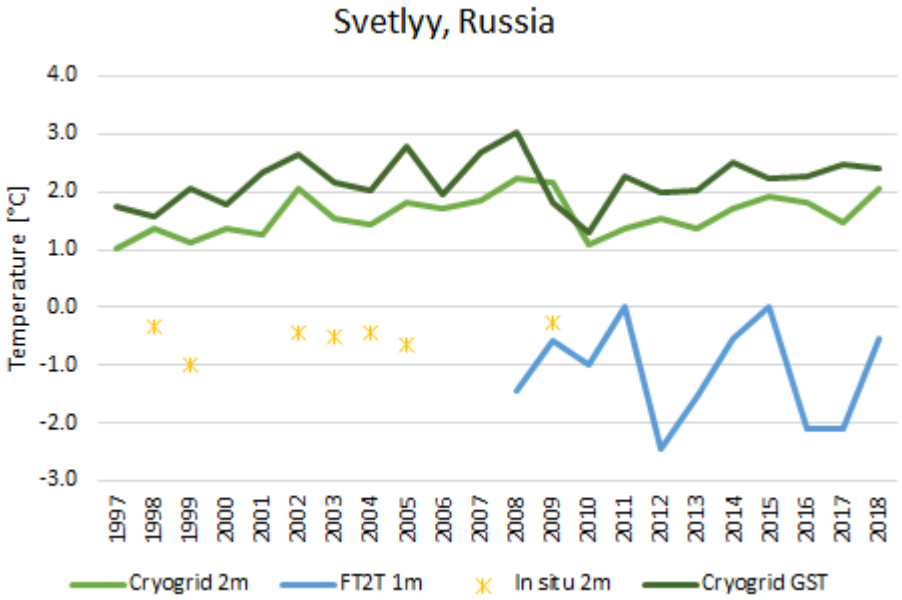

Figure 3.17. Comparison of FT2T product with CRDPv1 results and in situ data at Svetlyy, Central Siberia, Russia.

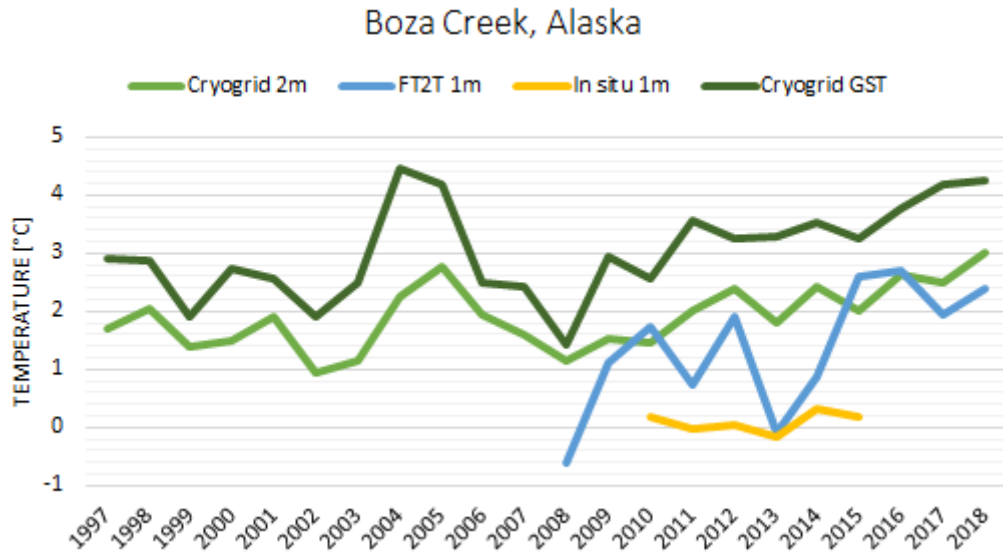

Figure 3.18. Comparison of FT2T product with CRDPv1 results and in situ data at Boza Creek, Alaska

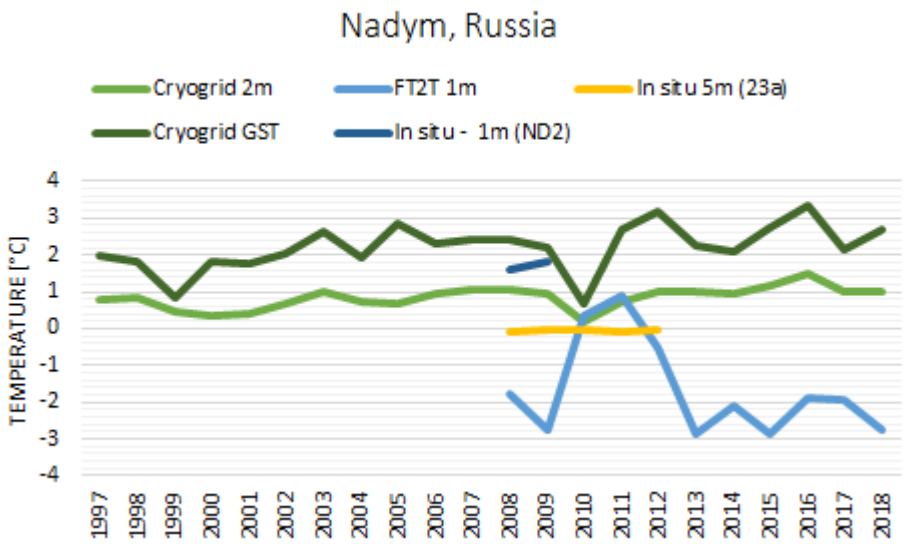

Figure 3.19. Comparison of FT2T product with CRDPv1 results and in situ data at Nadym, Western Siberia, Russia

Regional comparisons have been made for CRDPv2. This required the correction for water fraction as detailed in Bergstedt et al. (2020). The water class of Landcover_cci has been used to assign a water fraction for each original ASCAT footprint (hexagonal approximation as in Högström et al. 2018) overlapping with permafrost according to Permafrost_cci CRDPv2. The calibration of FT2T has been revised and extended to include 1m depth borehole data (North America) and 80 cm depth data (Russian Arctic) in order to avoid a regional (and temperature range) bias. Regional aggregation of results was applied to countries and administrative districts.

Temperature averages partially correlate with R^2=0.45 (Alaska) and R^2=0.35 (Canada). No correlation can be observed for Russia and Greenland. An offset can be observed in case of Greenland and Alaska. This bias is similar for both regions and is about 1.5°C (Figure 3.20). Similar temporal patterns can be however observed for Alaska (Figures 21 and 22, Bartsch et al. 2023).

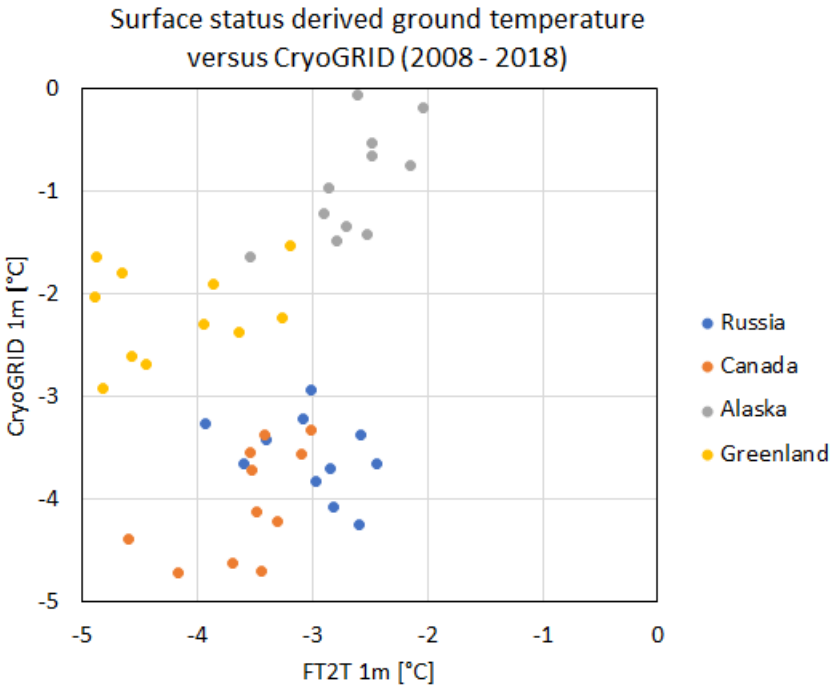

Figure 3.20: Regional average for areas with at least once <0°C. CRDPv2 versus Metop ASCAT derived ground temperature (from freeze/thaw - FT2T Model).

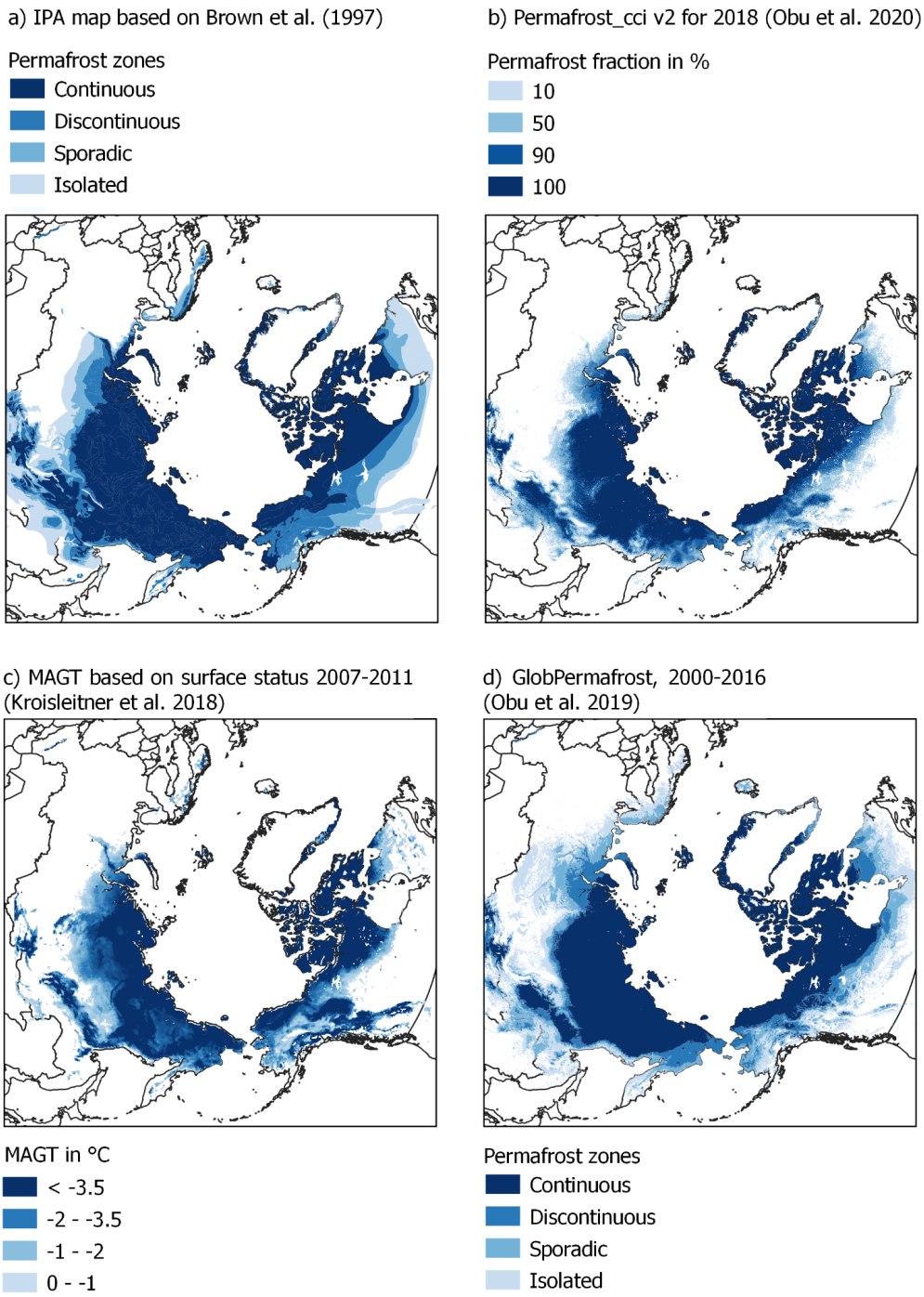

Figure 3.21. Circumpolar representation of permafrost: a permafrost zones based on traditional mapping (Brown et al. 1997), b Transient modelling of permafrost fraction using satellite-derived landsurface temperature representing a specific year (Obu et al. 2021b), c satellite radar-derived surface status converted to mean annual ground temperature (MAGT) (Kroisleitner et al. 2018) and d Equilibrium modelling of permafrost probability converted to permafrost zones using satellite-derived landsurface temperature representing an average of several years (Obu et al. 2019) (source: Bartsch et al. 2023).

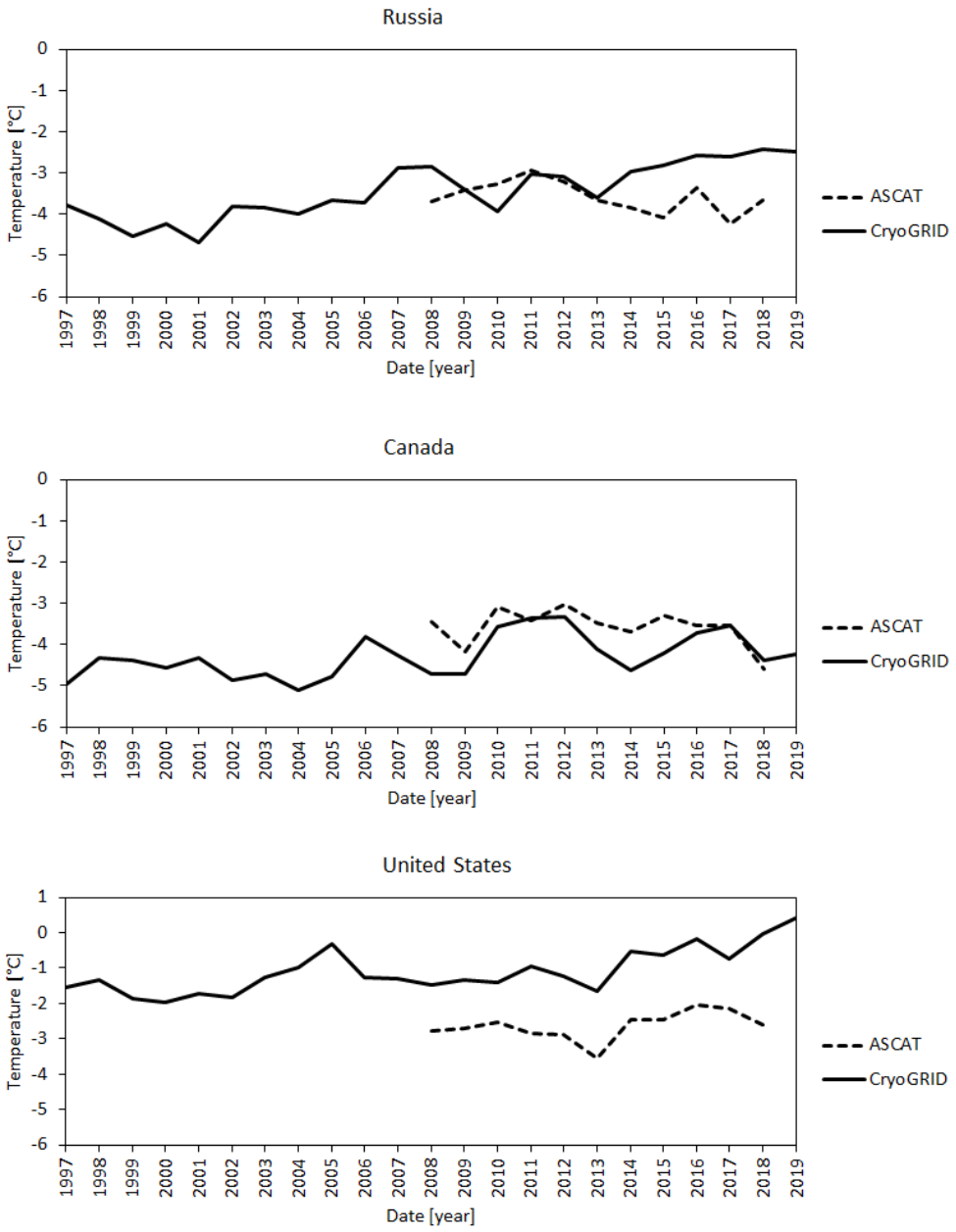

Figure 3.22. Regional ground temperature change (1 m depth) in permafrost regions of selected countries: comparison between surface status derived temperature (C-band scatterometer, Metop ASCAT; FT2T; Kroisleitner et al. (2018), corrected for water fraction according to Bergstedt et al. 2020)) and transient modelling using landsurface temperature (near infrared, MODIS, 1 km; CryoGRID; Permafrost_cci v3, (Obu et al. 2021b)) (source: Bartsch et al. 2023).

4 ASSESSMENT RESULTS: ACTIVE LAYER THICKNESS

4.1 ACTIVE LAYER THICKNESS USER REQUIREMENTS

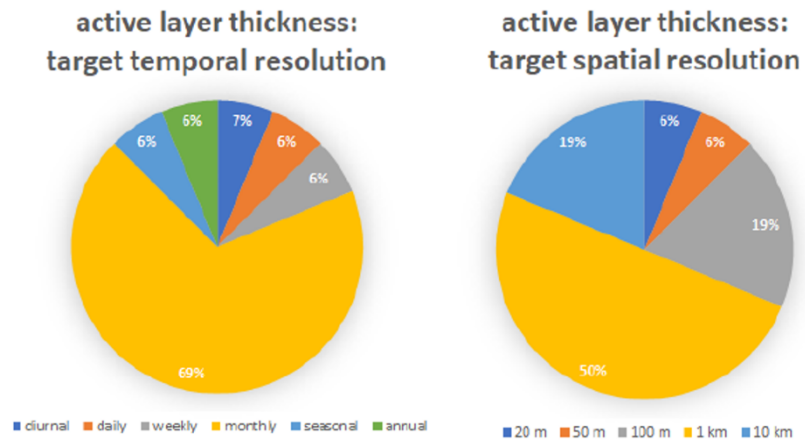

Figure 4.1. User Survey results. ESA CCI Permafrost User Survey results, Figure 4 [RD-7].

Users of potential products of active layer thickness are interested in high temporal resolution: monthly or higher in [RD-7]. Finally, less than 10% of users rated annual resolution as adequate as target temporal resolution in [RD-7]. However, the definition of the official ECV ALT is that it is the maximum thaw depth in summer and has by this the maximum temporal resolution of one year. Like this, the CRDP Permafrost_cci with ALT in annual resolution is the highest temporal resolution possible for this Permafrost ECV. Users were interested in higher temporal resolution, the representation of thaw depth that is developing deeper throughout the summer season until reaching the maximum depth in late summer, the ALT. But seasonal thaw depth evolution is not considered an ECV (see also glossary in section 1.7). Half of the user group are satisfied with a target spatial resolution of 1 km. The 1^{rst} release of the Permafrost_cci CRDPv0 ALT provided annual resolution with the required 1×1 km spatial resolution from 2003 to 2017. Permafrost_cci CRDPv1,2,3 ALT provide annual resolution with the required 1×1 km² spatial resolution with a longer time span from 1997 to 2018, 1997 to 2019 and 1997 to 2021, respectively.

4.2 PERMAFROST_CCI ALT MATCH-UP ANALYSES WITH IN SITU DATA

For each in situ measurement location, the pixel in Permafrost_cci ALT products closest to the in situ measurement was extracted to produce the match-up dataset and derive comparisons and summary statistics. Note that we assessed the fitness of Permafrost_cci ALT with focus on the Northern Hemisphere high-latitude continuous permafrost region. The midlatitude discontinuous permafrost regions on high plateaus in Mongolia, Central Asia and China (e.g., Tibetan Plateau) are characterised by very different snow regimes and subground properties requiring further model parameterisation. We therefore excluded all sites in Mongolia, Central Asia, and on the Tibetan Plateau (China) to allow an adequate assessment of mid-latitude to high-latitude permafrost regions.

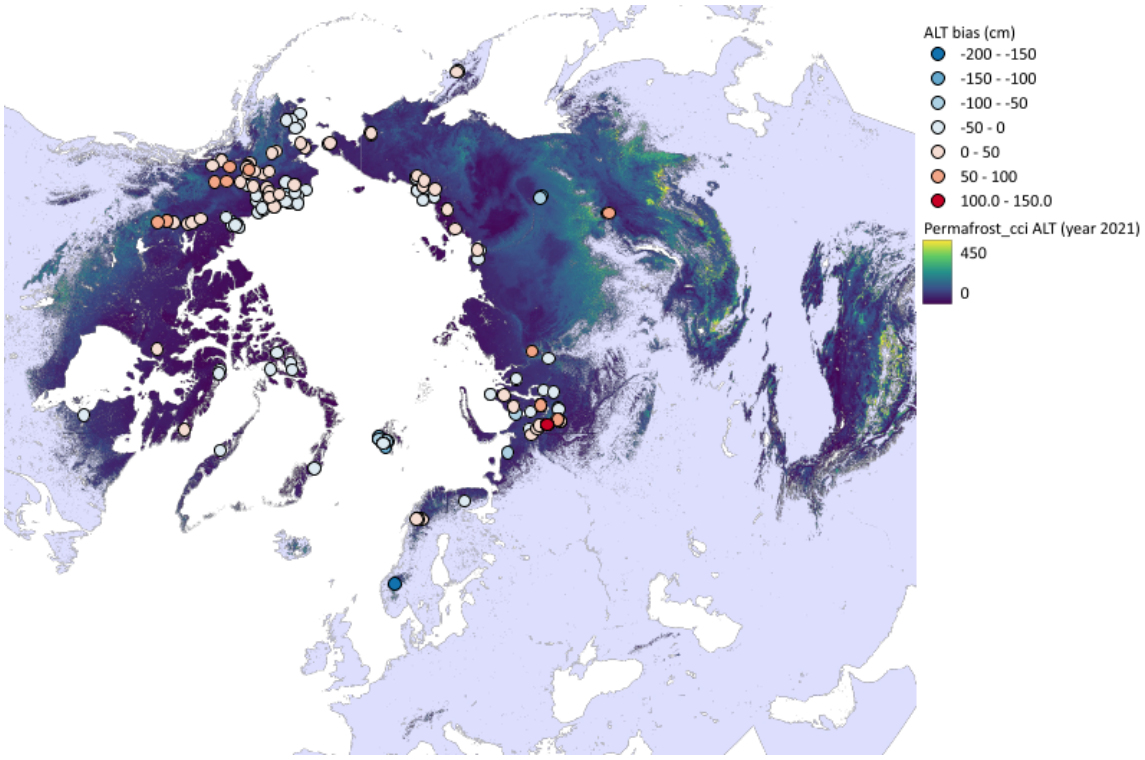

Figure 4.2. Spatial distribution of mean bias per site from Permafrost_cci ALT and in situ ALT match-up over mapped Permafrost_cci ALT in cm.

The majority of sites (Figure 4.2) and match-up pairs (Figure 4.3) ranges with a bias between -0.5 m to 0.5 m. A larger bias > 1 m (deep Permafrost_cci ALT versus shallow in situ ALT) occurs only in few match-up pairs in Alaska, Canada and Russia. Bias of -1.5 m occurs in some match-up pairs mainly on Svalbard and also in Norway (Figure 4.2) (shallow Permafrost_cci ALT versus deep in situ ALT).

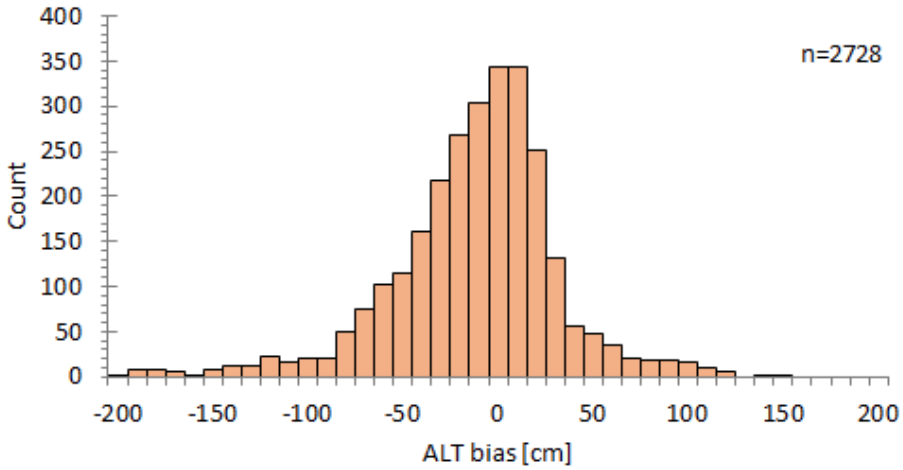

Figure 4.3. Frequency distribution of Permafrost_cci ALT minus in situ ALT. Summary statistics including all ALT match-up data pairs and with locations from Swiss Mountains, Mongolia, and China excluded (n = 497). Positive bias values are due to deeper Permafrost_cci ALT than the in situ value and vice versa.

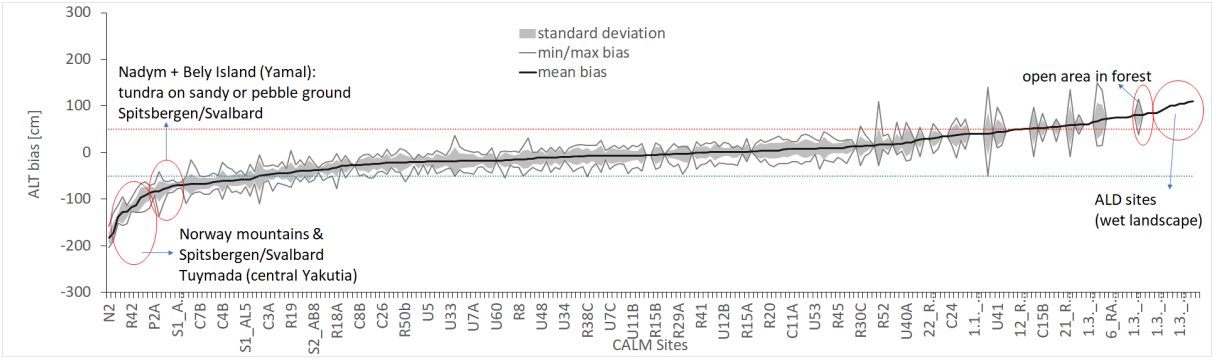

Figure 4.4. Mean bias of ALT (Mongolia, China and Swiss Mountains excluded), including SD and min/max bias. x-Axis shows the single sites, sorted by mean bias. Blue line = bias -50 cm (Permafrost cci ALTT too shallow), red line = bias +50 cm (Permafrost_cci ALT too deep).

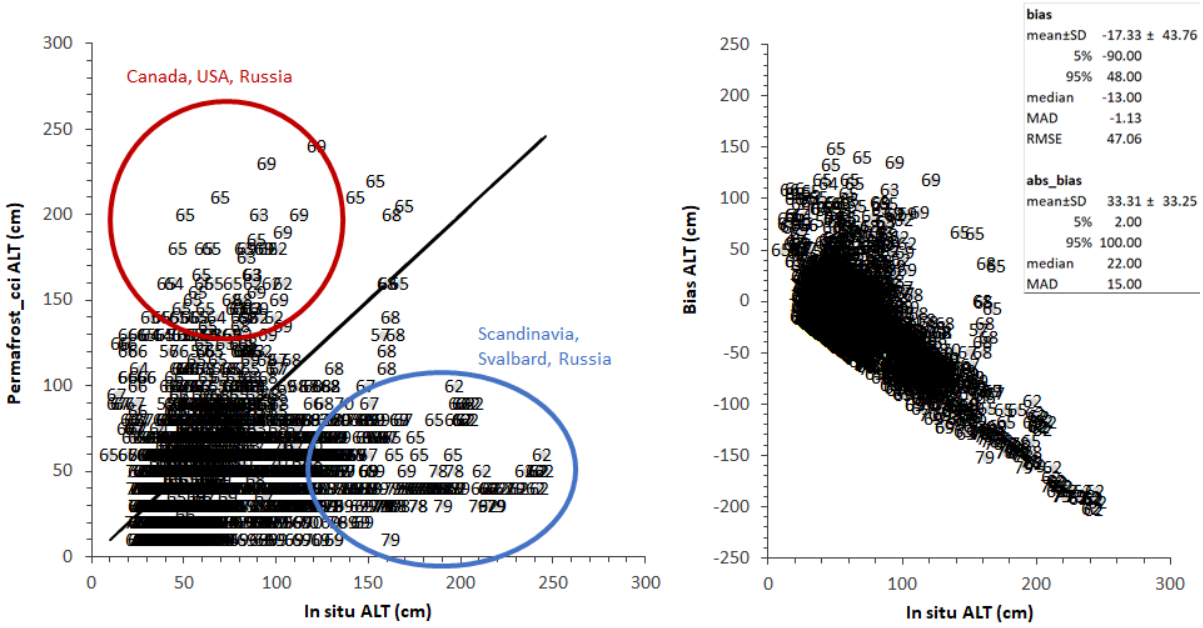

Figure 4.5. Left Panel: x=in situ ALT vs y=Permafrost_cci ALT with a black solid 1:1 reference line. Right Panel: x=in situ ALT, y=corresponding bias (Permafrost_cci ALT minus in situ ALT. Labels = Latitude. The table-insert includes summary statistics on the bias and absolute bias (SD=standard deviation, MAD=median absolute deviation, RMSE=root mean square error).

Permafrost_cci ALT and in situ ALT consensus in temporal trends

Table 4.1. Gleichläufigkeit (glk) and temporal stability (ts) per year of Permafrost_cci ALT time series.

Year	glk	ts	#
1998	0.64	-3.12	86
1999	0.73	-7.81	99
2000	0.63	0.42	100
2001	0.51	5.08	90
2002	0.67	-3.54	81
2003	0.63	-1.93	83
2004	0.72	17.51	94
2005	0.74	-4.90	108
2006	0.61	-11.89	99
2007	0.69	4.24	104
2008	0.63	-5.35	113
2009	0.59	8.79	121
2010	0.61	-3.31	129
2011	0.60	4.64	126
2012	0.69	-5.40	118
2013	0.54	-4.37	127
2014	0.63	7.29	122
2015	0.55	-2.26	111
2016	0.68	3.72	117
2017	0.66	-9.35	103
2018	0.55	9.85	149
2019	0.64	-5.11	101
2020	0.67	2.21	76
2021	0.60	0.08	90
MEAN	**0.63**	**-0.20**	**106.13**

Table 4.2. Summary statistics per site for Gleichläufigkeit (glk), temporal stability (ts) and absolute temporal stability (abs_ts) of Permafrost_cci ALT time series.

	glk	ts	abs_ts
mean±SD	0.62 ± 0.17	-0.38 ± 5.95	16.17 ± 8.38
5%	0.00	-5.80	7.08
95%	1.00	6.69	33.91
median	0.63	-0.04	14.83

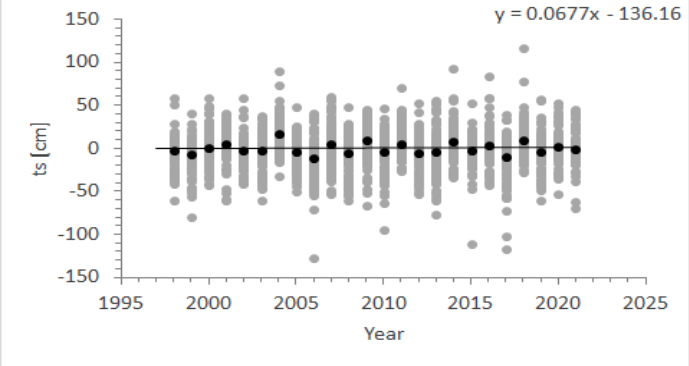

Figure 4.6: Temporal stability (ts, year-year change in magnitude of the bias) for the bulk ALT dataset (Mongolia, China and Swiss Mountains excluded). Black dots are the mean values, the thin black line is the linear regression through all points.

Regional Assessment

Table 4.3 Bias, absolute bias, Gleichläufigkeit (glk) and temporal stability (ts) of Permafrost_cci ALT time series per region. Note the high performance for the Alaska (US) domain.

Region	bias (cm)	abs_bias (cm)	glk	ts (cm)
Canada	-20.80	42.87	0.60	1.33
Greenland	-39.61	39.61	0.63	-0.10
Russia	-17.80	32.48	0.66	-0.34
Scandinavia	-51.03	60.90	0.59	-1.11
Svalbard	-111.88	111.88	0.60	-0.40
US	-2.05	20.44	0.63	-0.35
China	-121.67	127.11	0.43	-3.02
Mongolia	-207.53	210.30	0.36	-6.09
Switzerland	-425.35	425.35	0.30	-11.65

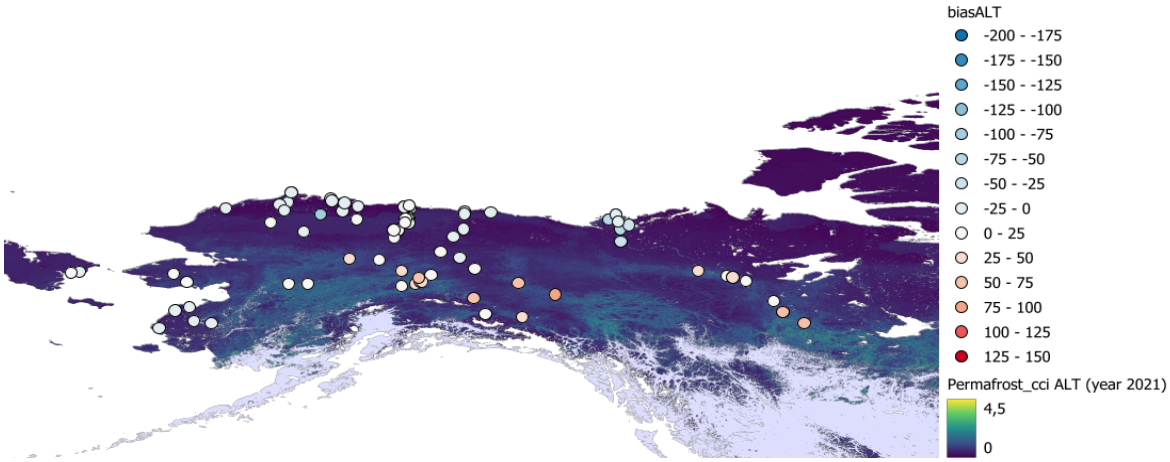

Figure 4.7. ALT bias over mapped Permafrost_cci ALT 2021 in cm in north-western America.

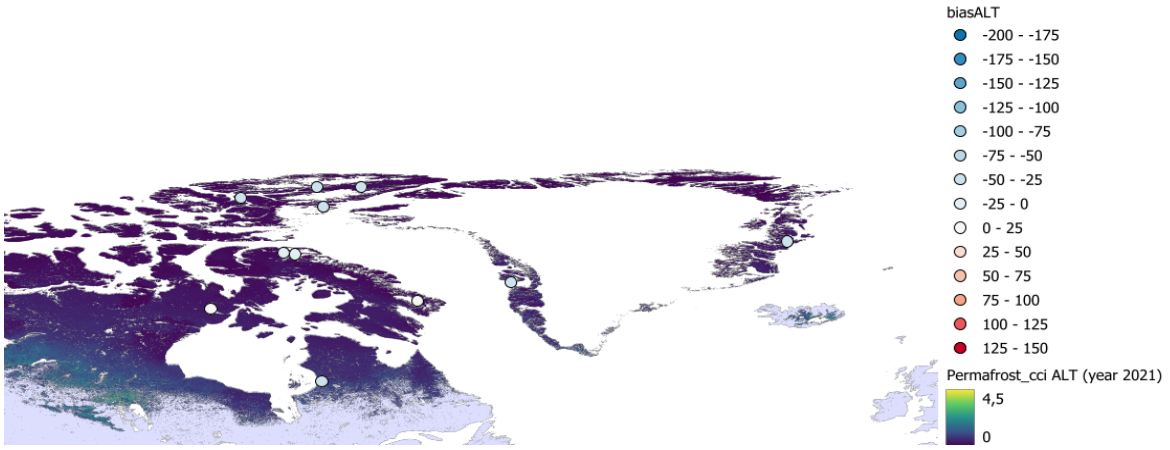

Figure 4.8. ALT bias over mapped Permafrost_cci ALT 2021 in cm in north-eastern America and Greenland.

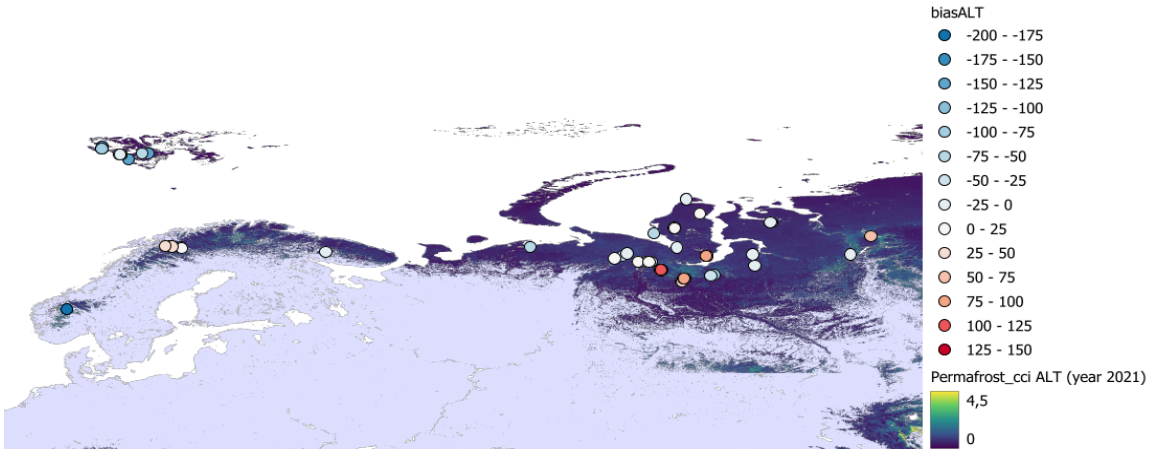

Figure 4.9 ALT bias over mapped Permafrost_cci ALT 2021 in cm in northern Europe and Western Siberia.

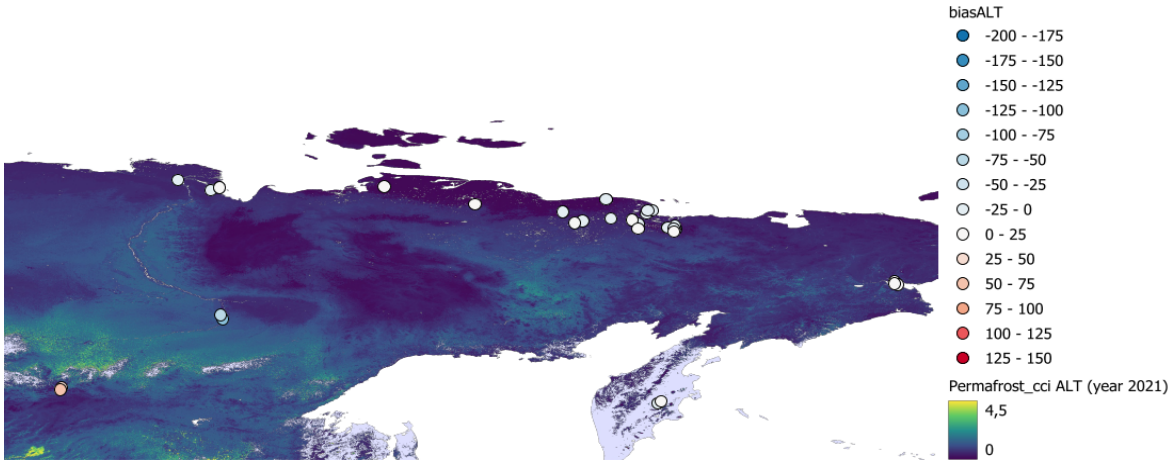

Figure 4.10 ALT bias over mapped Permafrost_cci ALT 2021 in cm in Eastern Siberia.

In summary, Permafrost_cci ALT (1997–2021) shows the following performance characteristics:

- a median bias of -13cm (95% CI: -90 to 48 cm).
- a large bias > 1 m (deep Permafrost_cci ALT versus shallow in situ ALT) occurs only in a few match-up pairs in Alaska, Canada and Russia. A large bias < -1.5 m mainly occurs in Svalbard in rocky and pebble terrain (shallow Permafrost_cci ALT versus deep in situ ALT).
- the mean temporal stability (ts, year-year change in magnitude of the bias*)* ranges around -0.2 cm, with variation mainly in the range of +/- 50 cm and gleichläufigkeit (glk, fraction of same-directional year-to-year changes) shows a robust temporal stability around 60 %.

5 ASSESSMENT RESULTS: PERMAFROST EXTENT

5.1 PERMAFROST_CCI PFR MATCH-UP ANALYSES WITH IN SITU DATA

The match-up dataset contains in situ binary information on permafrost existence (FALSE/TRUE) and Permafrost_cci PFR across different percentage groups (0, 14, 29, 43, 57, 71, 86, 100 %). Using both, ALT and MAGT in situ measurements as proxy for permafrost abundance, the match-up dataset contains n = 6,025 match-up pairs at 648 sites.

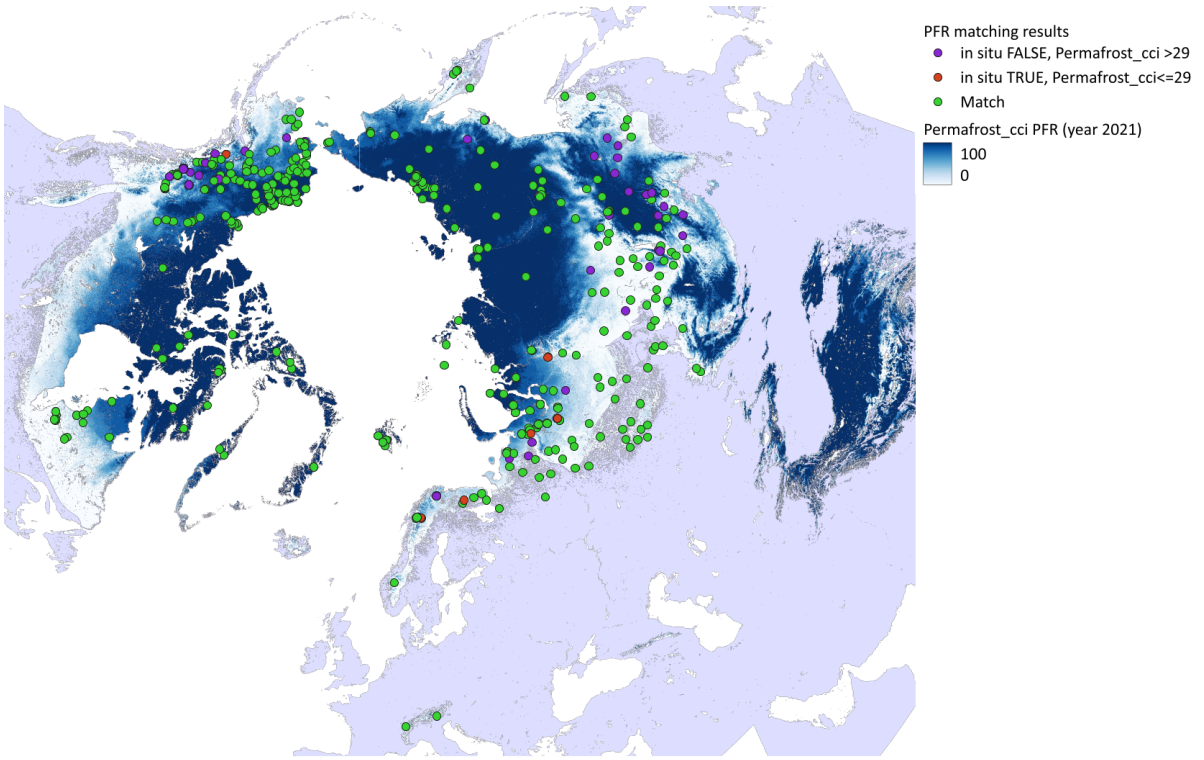

Figure 5.1. Spatial distribution of PFR 2021 match-up pairs grouped by matching characteristics over mapped Permafrost_cci PFR.

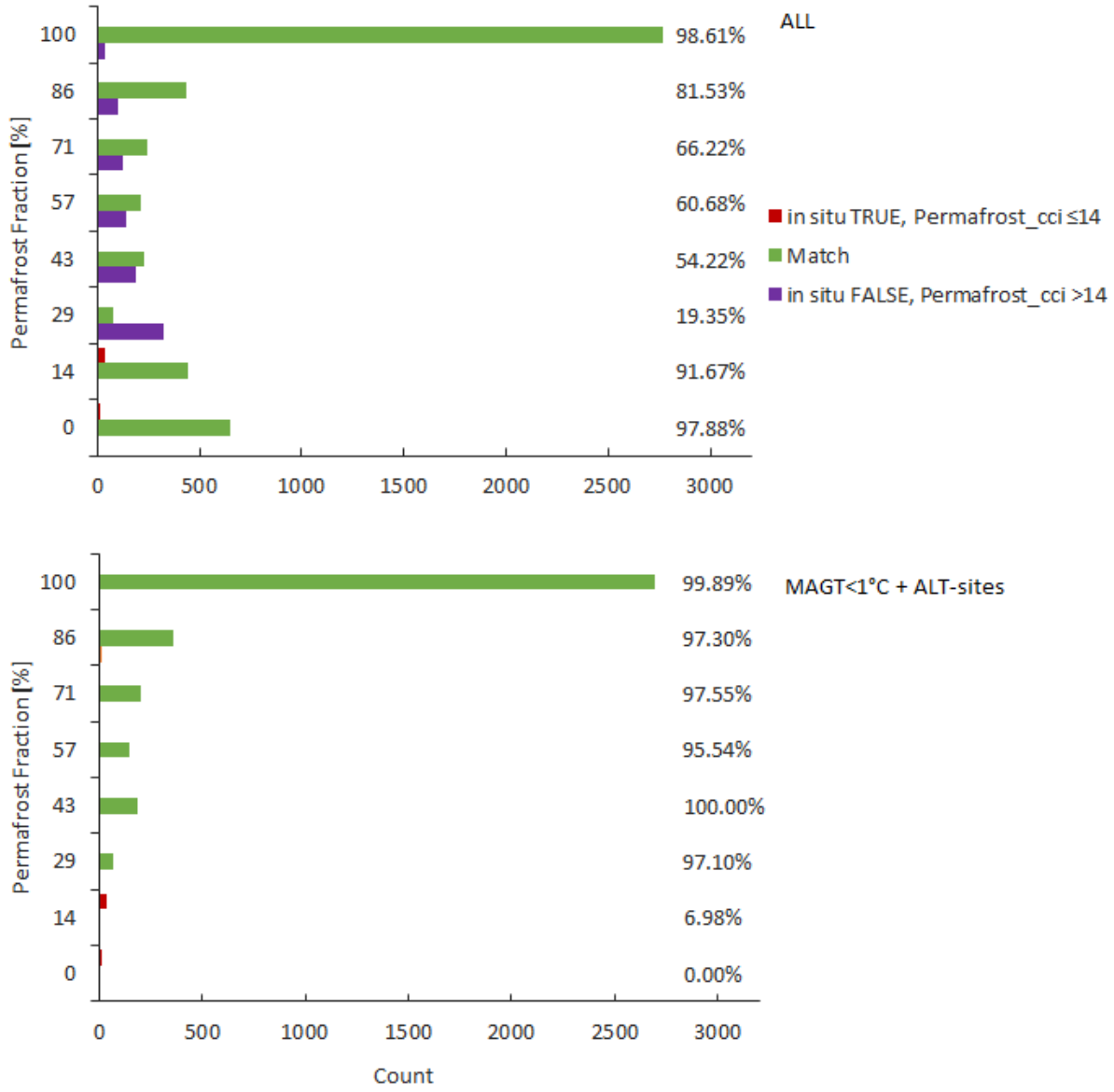

Figure 5.2a. Match-up summary of Permafrost_cci PFR vs. in situ MAGT and ALT datasets. The percentage values depict the amount of matches compared to all match-up pairs. The upper panel consists of all match-up pairs, the lower panel only cold sites with an MAGT < 1 °C (all ALT sites are classified as "cold" sites). Permafrost_cci ***PFR <= 14 %*** *is classified as "no permafrost".*

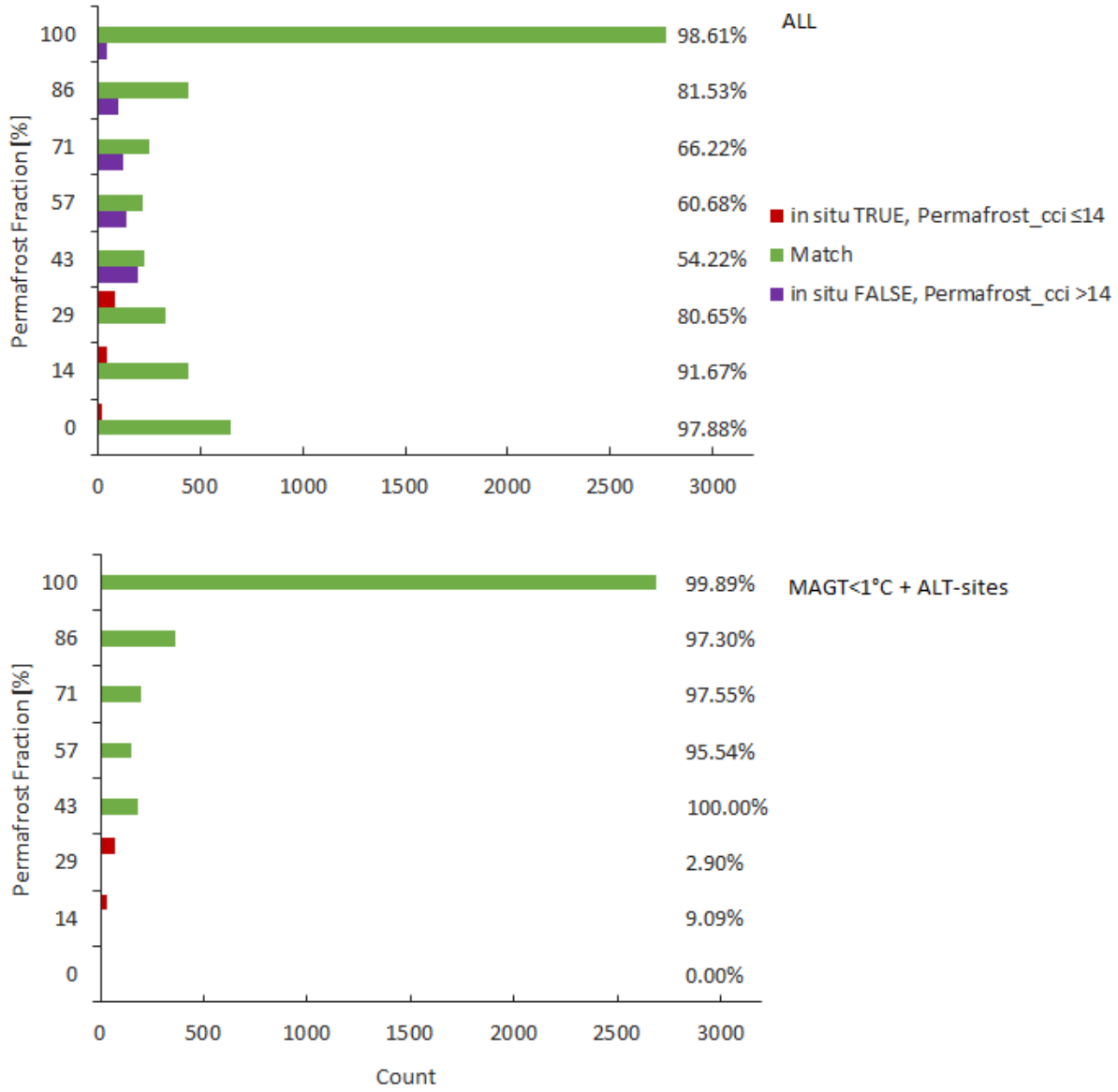

Figure 5.2b. Match-up summary of Permafrost_cci PFR vs. in situ MAGT and ALT datasets. The percentage values depict the amount of matches compared to all match-up pairs The upper panel consists of all match-up pairs, the lower panel only cold sites with an MAGT < 1 °C (all ALT sites are classified as "cold" sites). Permafrost_cci ***PFR <= 29 %*** *is classified as "no permafrost".*

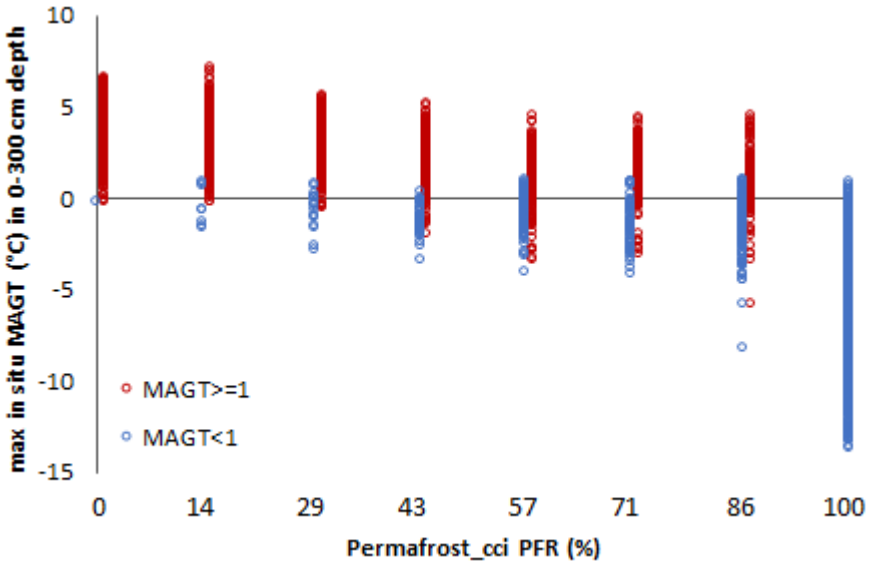

Figure 5.3. max in situ MAGT in 0-300 cm depth per Permafrost_cci PFR percentage.

As a consequence of the cold bias in the warm temperature range, the binary match-up of 'permafrost' versus 'no permafrost' shows that PFR in the grid cell is overestimated compared to in situ-derived 'no permafrost'.

Overall, the majority of match-up pairs (83.89 % for case PFR<=14 % and 87.99 % for case PFR<= 29 %) are in agreement between the in situ proxy and the Permafrost_cci simulation (Figure 5.2 a,b). Notably, the 100 % and the 0 % PFR have a high percentage of agreement, with 98.61 % and 97.88 % match, respectively.

Permafrost_cci PFR and in situ permafrost abundance consensus in temporal trends

We checked for Gleichläufigkeit (glk), by checking the amount of match-up pairs showing changes in the same direction (e.g. from "Permafrost" to "No Permafrost") or no changes. The glk gives the fraction of same-directional changes. The temporal stability was assessed differently to that of MAGT and ALT, as we have only a binary yes/no assessment. We thus checked, in how many cases we get the same result for matches in Permafrost abundance. For ts_all, all matchup-pairs having the same matching result (either a match or no match) from one year to the next get a 1. Different matching results get an 0, ts_all is thus the fraction of no-changes in matching. For ts_pos, only match-up pairs having a true match get a 1 if this matching is stable from one year to the next. Changing matching results as well as pairs with a no-match get an 0 - ts_pos is thus the fraction of no-changes in true matching compared to all match-up pairs.

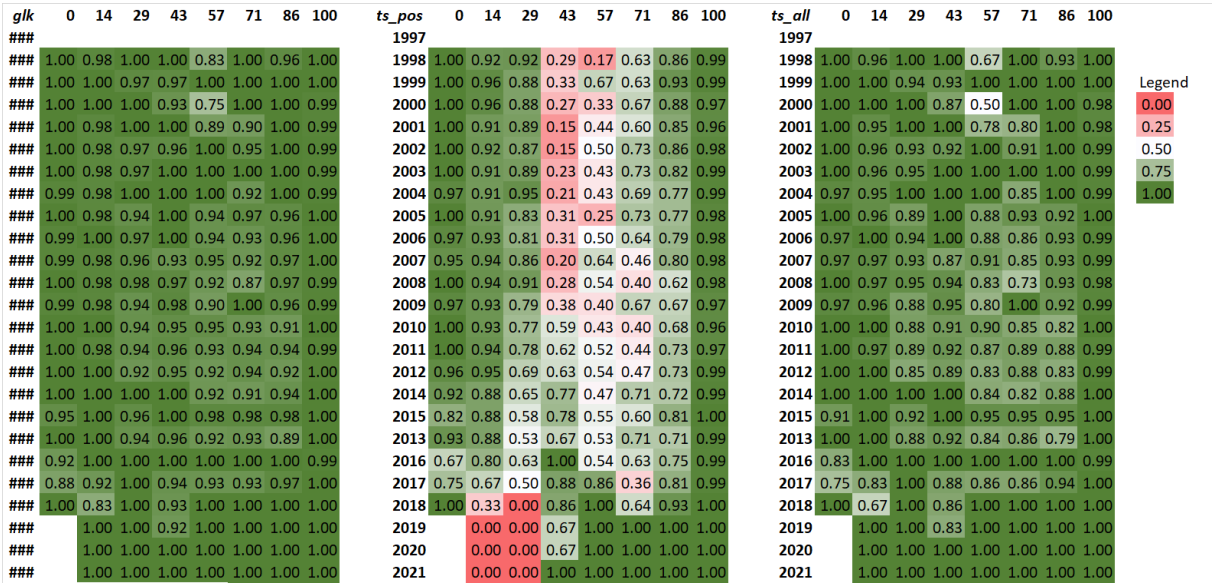

glk	0	14	29	43	57	71	86	100
###								
###	1.00	0.98	1.00	1.00	0.83	1.00	0.96	1.00
###	1.00	1.00	0.97	0.97	1.00	1.00	1.00	1.00
###	1.00	1.00	1.00	0.93	0.75	1.00	1.00	0.99
###	1.00	0.98	1.00	1.00	0.89	0.90	1.00	0.99
###	1.00	0.98	0.97	0.96	1.00	0.95	1.00	0.99
###	1.00	0.98	0.97	1.00	1.00	1.00	1.00	0.99
###	0.99	0.98	1.00	1.00	1.00	0.92	1.00	0.99
###	1.00	0.98	0.94	1.00	0.94	0.97	0.96	1.00
###	0.99	1.00	0.97	1.00	0.94	0.93	0.96	1.00
###	0.99	0.98	0.96	0.93	0.95	0.92	0.97	1.00
###	1.00	0.98	0.98	0.97	0.92	0.87	0.97	0.99
###	0.99	0.98	0.94	0.98	0.90	1.00	0.96	0.99
###	1.00	1.00	0.94	0.95	0.95	0.93	0.91	1.00
###	1.00	0.98	0.94	0.96	0.93	0.94	0.94	0.99
###	1.00	1.00	0.92	0.95	0.92	0.94	0.92	1.00
###	1.00	1.00	1.00	1.00	0.92	0.91	0.94	1.00
###	0.95	1.00	0.96	1.00	0.98	0.98	0.98	1.00
###	1.00	1.00	0.94	0.96	0.92	0.93	0.89	1.00
###	0.92	1.00	1.00	1.00	1.00	1.00	1.00	0.99
###	0.88	0.92	1.00	0.94	0.93	0.93	0.97	1.00
###	1.00	0.83	1.00	0.93	1.00	1.00	1.00	1.00
###		1.00	1.00	0.92	1.00	1.00	1.00	1.00
###		1.00	1.00	1.00	1.00	1.00	1.00	1.00
###		1.00	1.00	1.00	1.00	1.00	1.00	1.00

ts_pos	0	14	29	43	57	71	86	100
1997								
1998	1.00	0.92	0.92	0.29	0.17	0.63	0.86	0.99
1999	1.00	0.96	0.88	0.33	0.67	0.63	0.93	0.99
2000	1.00	0.96	0.88	0.27	0.33	0.67	0.88	0.97
2001	1.00	0.91	0.89	0.15	0.44	0.60	0.85	0.96
2002	1.00	0.92	0.87	0.15	0.50	0.73	0.86	0.98
2003	1.00	0.91	0.89	0.23	0.43	0.73	0.82	0.99
2004	0.97	0.91	0.95	0.21	0.43	0.69	0.77	0.99
2005	1.00	0.91	0.83	0.31	0.25	0.73	0.77	0.98
2006	0.97	0.93	0.81	0.31	0.50	0.64	0.79	0.98
2007	0.95	0.94	0.86	0.20	0.64	0.46	0.80	0.98
2008	1.00	0.94	0.91	0.28	0.54	0.40	0.62	0.98
2009	0.97	0.93	0.79	0.38	0.40	0.67	0.67	0.97
2010	1.00	0.93	0.77	0.59	0.43	0.40	0.68	0.96
2011	1.00	0.94	0.78	0.62	0.52	0.44	0.73	0.97
2012	0.96	0.95	0.69	0.63	0.54	0.47	0.73	0.99
2014	0.92	0.88	0.65	0.77	0.47	0.71	0.72	0.99
2015	0.82	0.88	0.58	0.78	0.55	0.60	0.81	1.00
2013	0.93	0.88	0.53	0.67	0.53	0.71	0.71	0.99
2016	0.67	0.80	0.63	1.00	0.54	0.63	0.75	0.99
2017	0.75	0.67	0.50	0.88	0.86	0.36	0.81	0.99
2018	1.00	0.33	0.00	0.86	1.00	0.64	0.93	1.00
2019		0.00	0.00	0.67	1.00	1.00	1.00	1.00
2020		0.00	0.00	0.67	1.00	1.00	1.00	1.00
2021		0.00	0.00	1.00	1.00	1.00	1.00	1.00

ts_all	0	14	29	43	57	71	86	100
1997								
1998	1.00	0.96	1.00	1.00	0.67	1.00	0.93	1.00
1999	1.00	1.00	0.94	0.93	1.00	1.00	1.00	1.00
2000	1.00	1.00	1.00	0.87	0.50	1.00	1.00	0.98
2001	1.00	0.95	1.00	1.00	0.78	0.80	1.00	0.98
2002	1.00	0.96	0.93	0.92	1.00	0.91	1.00	0.99
2003	1.00	0.96	0.95	1.00	1.00	1.00	1.00	0.99
2004	0.97	0.95	1.00	1.00	1.00	0.85	1.00	0.99
2005	1.00	0.96	0.89	1.00	0.88	0.93	0.92	1.00
2006	0.97	1.00	0.94	1.00	0.88	0.86	0.93	0.99
2007	0.97	0.97	0.93	0.87	0.91	0.85	0.93	0.99
2008	1.00	0.97	0.95	0.94	0.83	0.73	0.93	0.98
2009	0.97	0.96	0.88	0.95	0.80	1.00	0.92	0.99
2010	1.00	1.00	0.88	0.91	0.90	0.85	0.82	1.00
2011	1.00	0.97	0.89	0.92	0.87	0.89	0.88	0.99
2012	1.00	1.00	0.85	0.89	0.83	0.88	0.83	0.99
2014	1.00	1.00	1.00	1.00	0.84	0.82	0.88	1.00
2015	0.91	1.00	0.92	1.00	0.95	0.95	0.95	1.00
2013	1.00	1.00	0.88	0.92	0.84	0.86	0.79	1.00
2016	0.83	1.00	1.00	1.00	1.00	1.00	1.00	0.99
2017	0.75	0.83	1.00	0.88	0.86	0.86	0.94	1.00
2018	1.00	0.67	1.00	0.86	1.00	1.00	1.00	1.00
2019		1.00	1.00	0.83	1.00	1.00	1.00	1.00
2020		1.00	1.00	1.00	1.00	1.00	1.00	1.00
2021		1.00	1.00	1.00	1.00	1.00	1.00	1.00

*Figure 5.4: Match-up summary of Permafrost_cci PFR with in situ MAGT and ALT dataset over years, with Gleichläufikeit (glk) shown in the left panel temporal stability of positive matches (ts_pos) in the middle panel (i.e. for how many of all sites the matchup is constantly TRUE in two consecutive years) and temporal stability of all matches (ts_all) in the right panel (i.e. for how many of all sites the matchup is constantly TRUE OR FALSE in two consecutive years). Permafrost_cci **PFR <= 29 %** is classified as "no permafrost".*

Regional Assessment

Table 5.1 Permafrost abundance matching statistics, Gleichläufigkeit (glk) and temporal stability (ts) of Permafrost_cci PFR time series per region.

	in situ FALSE, Permafrost_cci >29	Match	in situ TRUE, Permafrost_cci ≤29	glk	ts pos	ts all
		Count			Fraction	
US	5	132	2	0.99	0.95	0.99
Canada	37	130	2	0.94	0.71	0.87
Greenland	0	4	0	1.00	1.00	1.00
Svalbard	0	4	0	1.00	1.00	1.00
Scandinavia	6	22	6	1.00	0.91	1.00
Europe	0	2	0	1.00	1.00	1.00
Russia	35	257	6	0.98	0.84	0.97

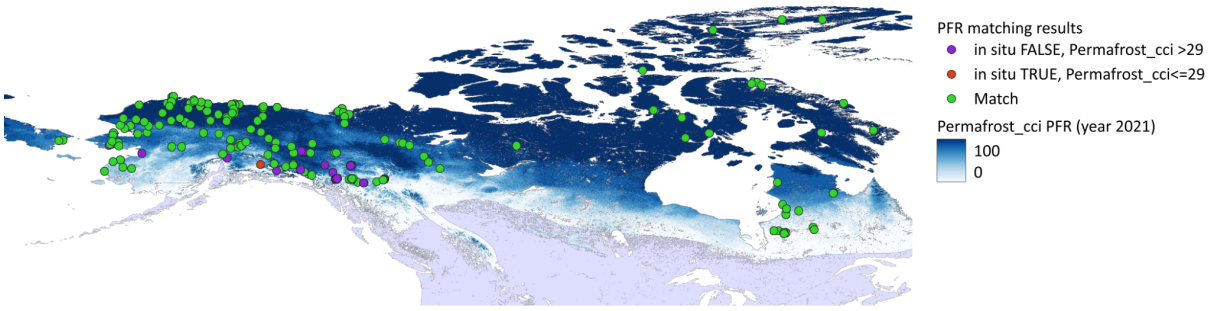

Figure 5.5 Spatial distribution of PFR match-up pairs grouped by matching characteristics over mapped Permafrost_cci PFR 2021 in northern America.

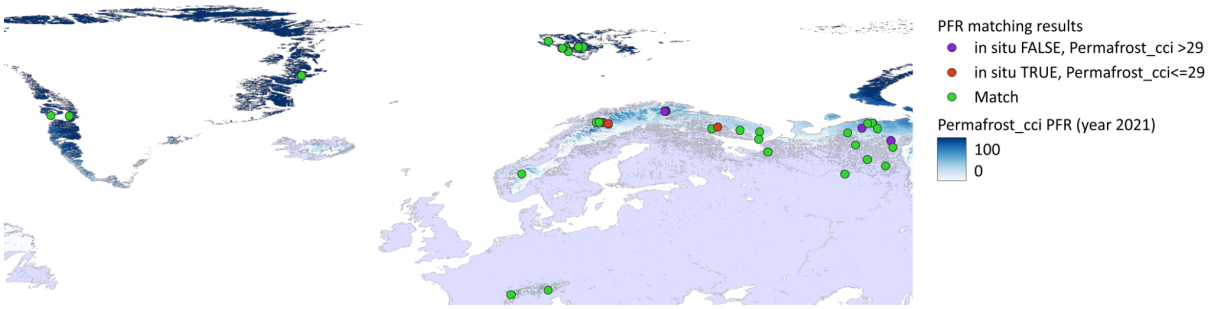

Figure 5.6 Spatial distribution of PFR match-up pairs grouped by matching characteristics over mapped Permafrost_cci PFR 2021 in Greenland and northern Europe.

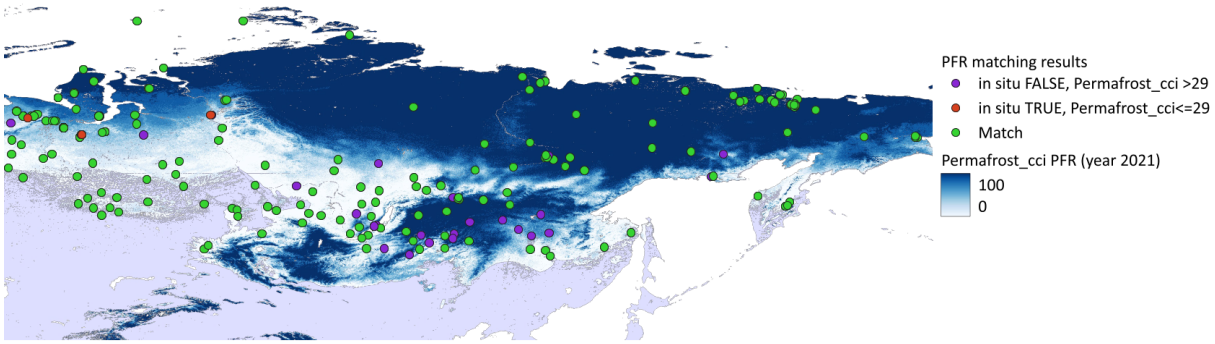

Figure 5.7 Spatial distribution of PFR match-up pairs grouped by matching characteristics over mapped Permafrost_cci PFR 2021 in Siberia.

In summary, Permafrost_cci PFR (1997–2021) shows the following performance characteristics:

- overall, the majority of match-up pairs (83.89 % for case Permafrost_cci PFR <=14 % and 87.99 % for case PFR <= 29 %) are in agreement between the in situ proxy for permafrost abundance yes / no and Permafrost_cci abundance yes / no.
- notably, the 100 % and the 0 % Permafrost_cci PFR show high percentage of agreement, with 98.61 % and 97.88 % match, respectively.
- geographically, most mismatches in permafrost abundance are located in the Eurasian and Canadian southern boundary of the permafrost extent.
- the high agreement in the Permafrost_cci PFR 100 % and 0 % groups is stable across years.
- Permafrost_cci PFR <= 29 % can be regarded as being reliably non-permafrost.

5.2 PERMOS PERMAFROST EXTENT COMPARISONS

There is a considerable enhancement of the Permafrost_cci PFR product performance in high mountain landscapes. Figure 5.8 compares the simulated Permafrost_cci PFR in 2021 in the Bas-Valais region, Alps, with the ESA GlobPermafrost slope movement inventory for the same region (green polygons) and the location of the PERMOS boreholes (yellow dots). Within the GlobPermafrost inventory, we selected only the landforms classified as rock glaciers, push moraines or a complex combination of the two, since they are the ones representative of permafrost occurrence. The blue color represents Permafrost_cci grid cells with PFR > 0 % in 2021. One can clearly see that the permafrost extent in the Permafrost_cci PFR product (i.e. PFR > 0 %) fits well with the GlobePermafrost inventory and the PERMOS boreholes. Only few landforms indicative of permafrost conditions are not included within the Permafrost_cci PFR permafrost extent and all 12 PERMOS boreholes except one are correctly represented.

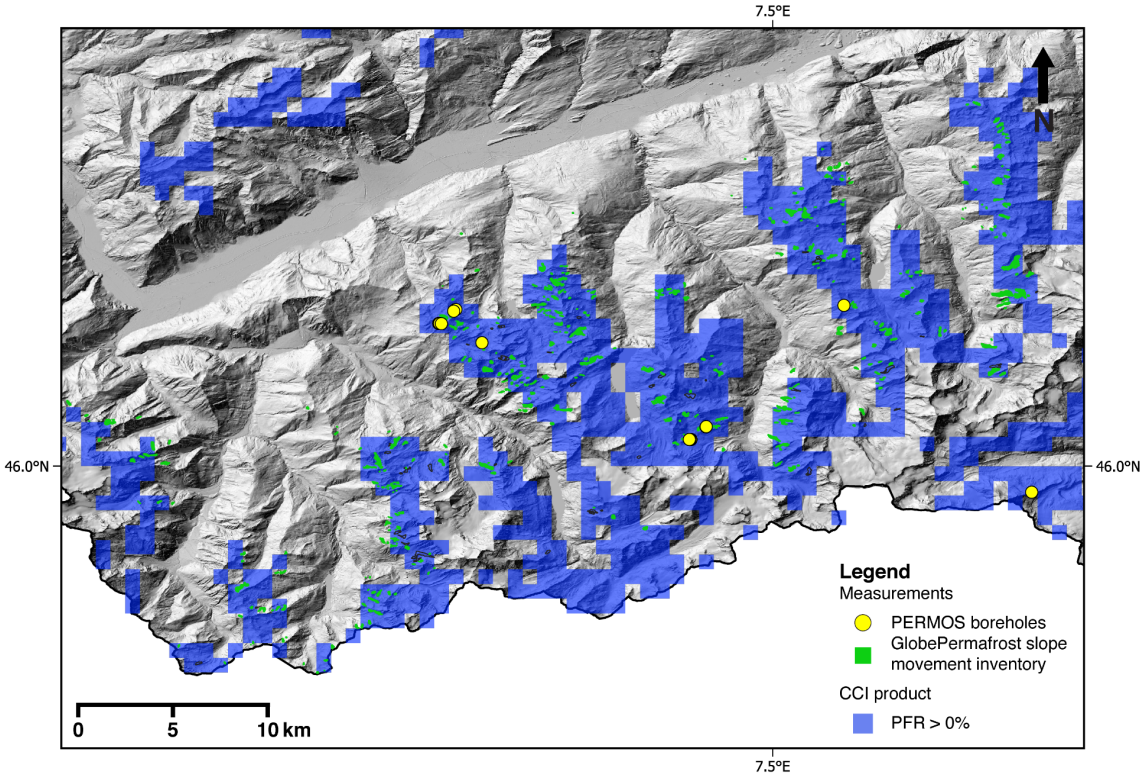

Figure 5.8. Overview of Permafrost_cci PFR in 2021 in Bas-Valais (CH) compared to the ESA GlobPermafrost slope movement inventory and PERMOS permafrost monitoring borehole locations.

Looking at additional regions worldwide (Figure 5.9), one can see that the Permafrost_cci PFR permafrost extent fits well with the Permafrost_cci phase I rock glacier inventory products in general. In detail, in most areas, the 1 km grid cell resolution Permafrost_cci PFR still fails to reproduce the small scale topographical variations and the Permafrost_cci PFR permafrost extent is slightly overestimated in the zones of continuous permafrost. This is true for Disko Island (Western Greenland) and Brooks range (North Alaska), as well as in the discontinuous European permafrost zone of the, Troms area (North Norway) and at mid-latitudes in Central Asia in the Tien Shan area (Khazastan).

In contrast in the high mountain area of the Alps, such as in the Swiss Vanoise area, Permafrost_cci PFR shows slightly underestimated permafrost extent, although the majority of the inventoried landforms indicative for permafrost are well represented. In the mountain area of the Carpathians, no permafrost is present in the Permafrost_cci PFR product which is consistent with the inventory, where only relict landforms have been identified.

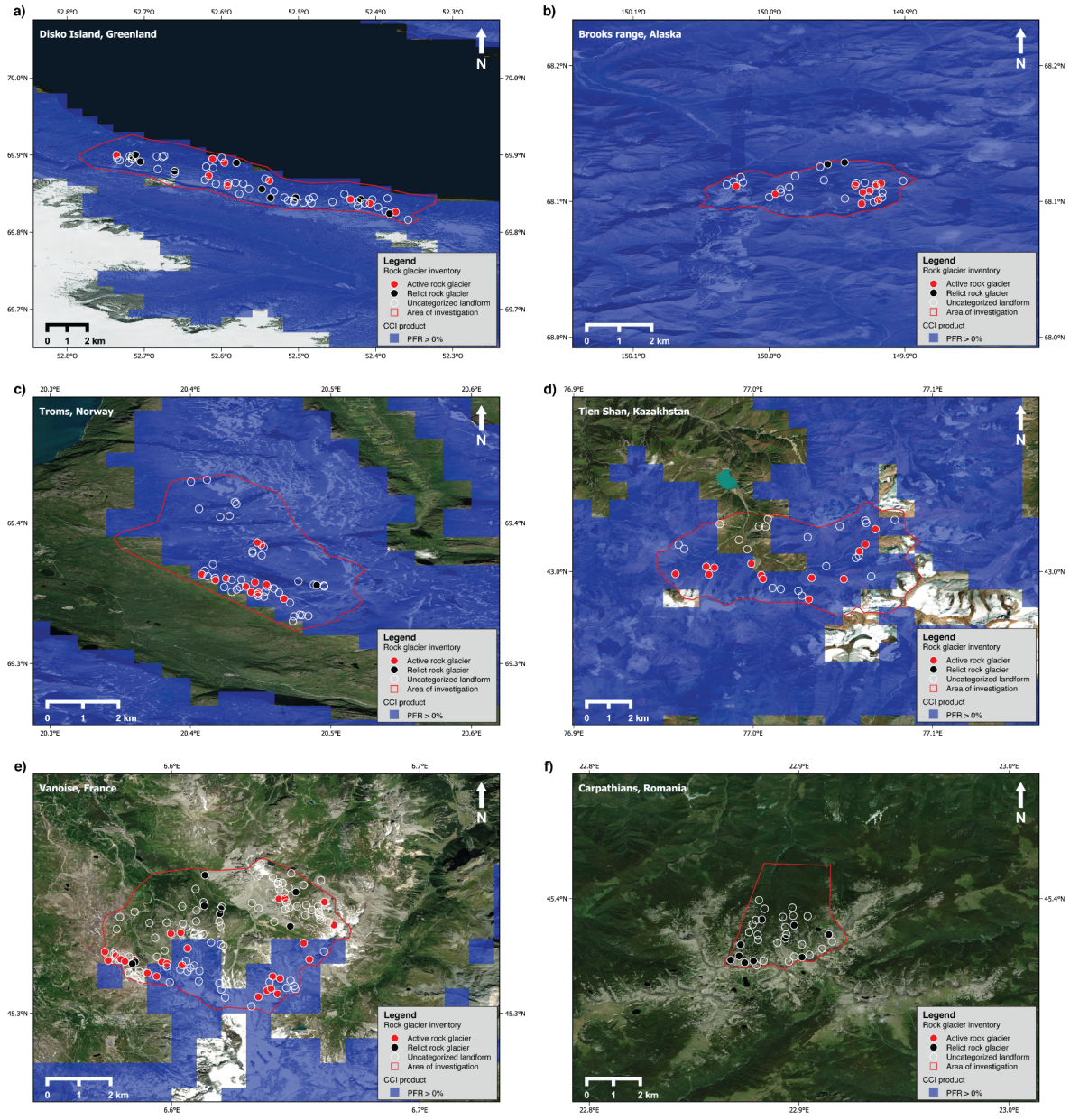

Figure 5.9. Overview of Permafrost_cci PFR permafrost extent in 2021 compared to the Permafrost CCI phase I rock glacier inventories in Disko Island (Western Greenland) (a), Brooks mountain range (North Alaska) (b), Troms area (North Norway) (c), Tien Shan (Khazastan) (d), Vanoise (Swiss Alps) (e) and Carpathians (f). The active rock glaciers (i.e., currently affected by permafrost creep) are indicated in red and the relict rock glaciers (i.e., formerly affected by permafrost creep) are in black. Uncertain and uncategorized landforms are indicated with hollow circles.

6 SUMMARY

Permafrost_cci CRDPv3 provides 1 km pixel resolution ECV products on mean annual ground temperature (MAGT) at discrete depths (product name GTD), Active Layer Thickness (product name ALT) and Permafrost Fraction (product name PFR). All products cover the Northern hemisphere north of 30 °N. Permafrost_cci GTD, ALT and PFR time series from 1997 to 2021 come with an annual resolution. The growing demand for mapped permafrost products needs to accommodate user requirements that span permafrost regions from Scandinavia, Mongolia, China to higher latitude permafrost in North America, Greenland, Siberia and all altitude ranges from lowland to mountain permafrost. This results in high difficulties of assessing how the Permafrost_cci products perform in all regions across a wide range of latitudes, altitudes, climate zones, land cover, and lithologies.

The three Permafrost_cci product groups GTD, ALT, PFR, are evaluated using standard match-up statistical approaches, supported by expert knowledge. The match-ups were executed using a pixel-based approach with the in situ measurement located inside the pixel. The Permafrost_cci GTD maps are provided in 0.0, 1.0, 2.0, 5.0, and 10.0 m depth and depth-interpolated to fit the depths of the extensive in situ dataset. For a match-up analyses in depth, the Permafrost_cci product team also produced GTD time series in 0.0, 0.2, 0.25, 0.4, 0.5, 0.6, 0.75, 0.8, 1.0, 1.2, 1.6, 2.0, 2.4, 2.5, 3, 3.2, 4.0, 5.0 and 10.0 m depth at the sites of the borehole locations. The match-up data is highly standardized, but still contains a large variability of match-up pairs in time, region, and MAGT reference depths. The mountain permafrost monitoring program PERMOS in Switzerland is specifically assessing the Permafrost_cci products for high-mountain permafrost regions, using in situ observations of surface temperature and borehole temperatures and the ESA GlobPermafrost slope movement inventory in the Swiss Alps and the Permafrost_cci rock glacier inventory in the Alps and worldwide at case study sites. In addition, the validation and evaluation efforts innovatively apply the Freeze-Thaw to Temperature (FT2T) product, an EO microwave-derived ground temperature, for comparison with the Permafrost_cci permafrost temperature product.

Permafrost_cci GTD match-up evaluation shows a median bias of -0.89 °C (mean bias -0.73 °C) for the circum-arctic. Geographically, a relatively large proportion of residuals >95% & <5% quantile of the bulk dataset is located in the mountainous regions of southern Alaska and western Canada, while a large share of <5% residuals is found in northern Alaska and eastern Russia. The Permafrost_cci GTD < 1 °C group shows a much better performance than the bulk dataset, with a median bias of 0.38 °C (mean bias 0.15 °C) for all depths, and a median bias of 0.32 °C (mean bias 0.08 °C) for all depths excluding the surface temperature at 0 m depth.

Overall, the majority of match-up pairs (83.89 % for case PFR <= 14 % and 87.99 % for case PFR <=29 %) is in agreement between the in situ proxy for permafrost abundance yes / no and Permafrost_cci abundance yes / no. Notably, the 100 % and the 0 % PFR show high percentage of agreement, with 98.61 % and 97.88 % match, respectively. Geographically, most mismatches are located in the Eurasian and Canadian southern boundary of the permafrost extent. The high agreement in the 100 % and 0 % Permafrost_cci PFR groups is stable across years.

For the Permafrost_cci ALT match-up analyses, we restricted the analysis on high-latitude to mid-latitude permafrost regions related to the Permafrost_cci model parameterization, excluding all sites in Mongolia, Central Asia, on the Tibetan Plateau (China) due to their different snow and subground regimes. Permafrost_cci ALT performance with match-up pairs from China and Mongolia excluded is characterised by a median bias of -13 cm (95 % CI: -90 to 48 cm).

A large bias > 1 m (deep Permafrost_cci ALT versus shallow in situ ALT) occurs only in a few match-up pairs in Alaska, Canada and Russia and < -1.5 m mainly occurs in Svalbard in rocky and pebble terrain (shallow Permafrost_cci ALT versus deep in situ ALT). The mean temporal stability (ts, year-year change in magnitude of the bias*)* shows stable ranges around -0.2 cm, with variation mainly in the range of +/- 50 cm and gleichläufigkeit (glk, fraction of same-directional year-to-year changes) shows a robust temporal stability around 60 %.

PERMOS investigations in the Swiss Alps show that the performance of Permafrost_cci GTD and Permafrost_cci PFR highly improved for mountain regions. Permafrost_cci GTD shows a slight cold bias of -0.265 °C only. At larger depth, Permafrost_cci GTD shows a slight warm bias of +0.275 °C at 10 m depth. Permafrost_cci GTD fits best with the in situ observations near the surface with the bias increasing with depth at all sites. Although the absolute values are different, both the in situ measurements and Permafrost_cci GTD show the consistent warming trend over the period 1997-2021. Permafrost_cci GTD matches some of the inter-annual variability (i.e. warmer GTD due to the extreme warm years in 2003 and 2015) but not the cooling events due to snow effects. At depth, measured in situ MAGT in 2017 shows a more or less marked cooling effect due to the extremely snow-poor winter 2016/17 in the Swiss Alps, which enabled the cold winter air temperature to cool the ground more efficiently. This effect is not matched in Permafrost_cci GTD, illustrating the difficulty to include the winter snow effects in mountain regions.

However, due to the major improvement in Permafrost_cci GTD, also the Permafrost_cci PFR product matches now the large majority of inventoried ESA GlobPermafrost slope movement products are located within Permafrost_cci PFR permafrost extent, as well as 11 amongst the 12 PERMOS permafrost borehole sites in the Alps are located within Permafrost_cci PFR permafrost extent. The majority of inventoried ESA GlobPermafrost slope movement products and Permafrost_cci rock glacier products that were located outside of the Permafrost_cci PFR in phase I before. Permafrost_cci PFR also performs well in the 10 regions where Permafrost_cci rock glacier inventory products are available for the Northern hemisphere.

Ground temperatures based on satellite-derived freeze/thaw agree (FT2T) at selected cold sites for the overlap period 2008-2018 (CRDPv1). Deviations occur in the permafrost transition zone. In the presented cases, only one product (either CRDPv1 or FT2T) agrees with in situ measurements. A bias of about 1.5°C can be observed for Alaska as well as Greenland (CRDPv2).

In summary, the Permafrost_cci permafrost temperature (that we define as GTD < 1°C) shows good performance with a median bias of 0.35 °C for all depth layers and is well usable by the climate research community. Users of Permafrost_cci GTD products should consider that Permafrost_cci GTD > 1 °C outside of the permafrost zones is characterised by a cold median MAGT bias of -1.17 °C (mean bias -1.11 °C). This leads in turn to and an overestimation of the areal extent of permafrost (especially in the Permafrost_cci PFR= 29 % class) at the southern boundaries of Permafrost in discontinuous, and sporadic permafrost regions.

We consider Permafrost_cci GTD and PFR products for the Northern hemisphere to be most reliable in the permafrost temperature range with GTD < 1 °C and in PFR > 50% as well as PFR <= 29% is reliable as non-permafrost.

7 REFERENCES

7.1 BIBLIOGRAPHY

Allard, M., Sarrazin, D. and L'Hérault, E. (2020). Borehole and near-surface ground temperatures in northeastern Canada, v.1.5 (1988-2019). Nordicana D8. https://doi.org/10.5885/45291SL-34F28A9491014AFD.

Bartsch, A., Pointner, G., Leibman, M.O., Dvornikov, Y., Khomutov, A.V., and Trofaier A.M. (2017). Circumpolar ground-fast lake ice fraction by lake from ENVISAT ASAR late winter 2008, links to Shapefiles. PANGAEA, https://doi.org/10.1594/PANGAEA.873674

Bartsch, A ., Pointner, G., Leibman, M.O., Dvornikov, Y., Khomutov, A.V., and Trofaier A.M.. (2017). Circumpolar Mapping of Ground-Fast Lake Ice. Frontiers in Earth Science, 5(12), 16 pp. https://doi.org/10.3389/feart.2017.00012

Bergstedt, H. and Bartsch, A. (2020a). Near surface ground temperature, soil moisture and snow depth measurements in the Kaldoaivi Wilderness Area, for 2016-2018. PANGAEA, https://doi.org/10.1594/PANGAEA.912482

Bergstedt, H., Bartsch, A., Duguay, C and Jones, B. (2020b). Influence of surface water on coarse resolution C-band backscatter: Implications for freeze/thaw retrieval from scatterometer data. Remote Sensing of Environment, 247. https://doi.org/10.1016/j.rse.2020.111911.

Bergstedt, H., Bartsch, A., Neureiter, A., Hofler, A., Widhalm, B., Pepin, N. and Hjort, J. (2020c). Deriving a frozen area fraction from Metop ASCAT backscatter based on Sentinel-1. IEEE Transactions On Geoscience And Remote Sensing, 58(9), 6008-6019. https://doi.org/10.1109/tgrs.2020.2967364

Biskaborn, B.K., Smith, S.L., Noetzli, J., Matthes, H., Vieira, G., Streletskiy, D.A., Schoeneich, P., Romanovsky, V.E., Lewkowicz, A.G., Abramov, A., Allard, M., Boike, J., Cable, W.L., Christiansen, H.H., Delaloye, R., Diekmann, B., Drozdov, D., Etzelmüller, B., Grosse, G., Guglielmin, M., Ingeman-Nielsen, T., Isaksen, K., Ishikawa, M., Johansson, M., Johannsson, H., Joo, A., Kaverin, D., Kholodov, A., Konstantinov, P., Kröger, T., Lambiel, C., Lanckman, J.-P., Luo, D., Malkova, G., Meiklejohn, I., Moskalenko, N., Oliva, M., Phillips, M., Ramos, M., Sannel, A. B. K., Sergeev, D., Seybold, C., Skryabin, P., Vasiliev, A., Wu, Q., Yoshikawa, K., Zheleznyak, M. and Lantuit, H. (2019). Permafrost is warming at a global scale. Nature Communications, 10, 264. https://doi.org/10.1038/s41467-018-08240-4

Biskaborn, B.K., Lanckman, J.-P., Lantuit, H., Elger, K., Streletskiy, D.A., Cable, W.L., and Romanovsky, V.E. (2015): The new database of the Global Terrestrial Network for Permafrost (GTN-P), Earth Syst. Sci. Data, 7, 245–259.

Boike, J., Nitzbon, J., Anders, K., Grigoriev, M.N., Bolshiyanov, D.Y., Langer, M., Lange, S., Bornemann, N., Morgenstern, A., Schreiber, P., Wille, C., Chadburn, S., Gouttevin, I., and Kutzbach,

L. (2018). Soil data at station Samoylov (2002-2018, level 1, version 1), link to archive. PANGAEA, https://doi.org/10.1594/PANGAEA.891140

Brown, J., Ferrians Jr., O.J., Heginbottom, J.A. and Melnikov, E.S. (1997). Circum-Arctic Map. of Permafrost and Ground-Ice Conditions. US Geological Survey Reston.

Bryant, R.N., Robinson, J.E., Taylor, M.D., Harper, W., DeMasi, A., Kyker-Snowman, E., Veremeeva, A., Schirrmeister, L., Harden, J. and Grosse, G. (2017). Digital Database and Maps of Quaternary Deposits in East and Central Siberia: U.S. Geological Survey data release, https://doi.org/10.5066/F7VT1Q89

CEN 2020a. Climate station data from Nikku Island in Nunavut, Canada, v. 1.0 (2010-2016). Nordicana D64, https://doi.org/10.5885/45505SL-528A7C505494428A.

CEN 2020b. Climate station data from the Biscarat river region in Nunavik, Quebec, Canada, v. 1.0 (2005-2019). Nordicana D62, https://doi.org/10.5885/45495SL-78FA5A95C5FB4D21.

CEN 2020c. Climate station data from the Clearwater lake region in Nunavik, Quebec, Canada, v. 1.1 (1986-2019). Nordicana D57, https://doi.org/10.5885/45475SL-5A33FE09B0494D92.

CEN 2020d. Climate station data from the Laforge Reservoir region, Quebec, Canada, v. 1.0 (1995-2013). Nordicana D66, https://doi.org/10.5885/45515SL-CFC7E8137E8B4323.

CEN 2020e. Climate station data from the Little Whale River region in Nunavik, Quebec, Canada, v. 1.1 (1993-2019). Nordicana D58, https://doi.org/10.5885/45485SL-78F4F9C368364100.

CEN 2020f. Climate station data from the Robert-Bourassa Reservoir region, Quebec, Canada, v. 1.1 (1996-2019). Nordicana D60, https://doi.org/10.5885/45470SL-7BD92481E2CF4DC0.

CEN 2020g. Climate station data from the Sheldrake river region in Nunavik, Quebec, Canada, v. 1.1 (1986-2019). Nordicana D61, https://doi.org/10.5885/45480SL-C89DEB92A4FE4536.

Clow, G.D., 2014, Temperature data acquired from the GTN-P Deep Borehole Array on the Arctic Slope of Alaska, 1973–2013, Earth System Science Data, 6, 201-218. https://doi.org/10.5194/essd-6-201-2014

Fortier, D., Sliger, M., Gagnon, S. and Rioux, K. (2021). Ground temperature in natural conditions along the Alaska Highway at the Beaver Creek Road Experimental Site, Yukon, Canada, v.1.0 (2008-2020). Nordicana D94, https://doi.org/10.5885/45738CE-D75F3C9342D34C83.

GTN-P, 2021, Long-term mean annual ground temperature data for permafrost. PANGAEA, https://doi.org/10.1594/PANGAEA.930669

GTN-P, 2018, GTN-P global mean annual ground temperature data for permafrost near the depth of zero annual amplitude (2007-2016). PANGAEA, https://doi.org/10.1594/PANGAEA.884711

Kroisleitner, C., Bartsch, A., and Bergstedt, H. (2018): Circumpolar patterns of potential mean annual ground temperature based on surface state obtained from microwave satellite data, The Cryosphere, 12, 2349-2370, https://doi.org/10.5194/tc-12-2349-2018.

Naeimi, V., Bartalis, Z., Hasenauer, S., and Wagner, W. (2009). An improved soil moisture retrieval algorithm for ERS and METOP scatterometer observations. IEEE Transactions on Geoscience and Remote Sensing, 47(7), 1999-2013. https://doi.org/10.1109/TGRS.2008.2011617

Paulik, C, Melzer.,T., Hahn, S., Bartsch, A., Heim, B., Elger, K. and Wagner, W. (2014). Circumpolar surface soil moisture and freeze/thaw surface status remote sensing products (version 4) with links to geotiff images and NetCDF files (2007-01 to 2013-12). Department of Geodesy and Geoinformatics, TU Vienna, PANGAEA, https://doi.org/10.1594/PANGAEA.832153

RGIK (2023). Guidelines for inventorying rock glaciers: baseline and practical concepts (version 1.0). IPA Action Group Rock glacier inventories and kinematics, 25 pp, https://doi.org/10.51363/unifr.srr.2023.002

Wang, K. (2018): A synthesis dataset of near-surface permafrost conditions for Alaska, 1997-2016. Arctic Data Center, https://doi.org/10.18739/A2KG55.

7.2 ACRONYMS

ALT	Active Layer Thickness
AWI	Alfred Wegener Institute Helmholtz Centre for Polar and Marine Research
B.GEOS	b.geos GmbH
CALM	Circumpolar Active Layer Monitoring
CC3	Permafrost_cci CryoGrid 3
CEN	Center for Northern Studies in Canada
CCI	Climate Change Initiative
CRDP	Climate Research Data Package
ECV	Essential Climate Variable
EO	Earth Observation
ESA	European Space Agency
FT2T	Freeze-Thaw to Temperature
GAMMA	Gamma Remote Sensing AG
GCOS	Global Climate Observing System
GCW	Global Cryosphere Watch
GST	Ground Surface Temperature
GT	Ground Temperature
GTD	Ground Temperature per Depth
GTN-P	Global Terrestrial Network for Permafrost
GTOS	Global Terrestrial Observing System
GUIO	Department of Geosciences University of Oslo
IASC	International Arctic Science Committee
IPA	International Permafrost Association
IPCC	Intergovernmental Panel on Climate Change
MAGT	Mean Annual Ground Temperature
NSIDC	National Snow and Ice Data Center
PE	Permafrost Extent
PERMOS	Swiss Permafrost Monitoring Network
PFR	Permafrost FRaction
RD	Reference Document
TSP	Thermal State of Permafrost
UNIFR	Department of Geosciences University of Fribourg
URD	Users Requirement Document
WMO	World Meteorological Organisation